IMPROVING THE CONTRACTILE PERFORMANCE OF HUMAN PLURIPOTENT STEM CELL-DERIVED CARDIOMYOCYTES FOR CARDIAC CELL THERAPY

Scott David Lundy

A dissertation submitted in partial fulfillment of the requirements for the degree of

Doctor of Philosophy

University of Washington

2013

Reading Committee:

Michael Regnier, Chair

Michael A. Laflamme

Luis F. Santana

Program Authorized to Offer Degree:

Bioengineering

University of Washington

Abstract

Improving the Contractile Performance of Human Pluripotent Stem Cell-Derived Cardiomyocytes for Cardiac Cell Therapy

Scott Lundy

Chair of the Supervisory Committee

Professor Michael Regnier

Department of Bioengineering

Heart disease is the leading cause of death worldwide, and each year over 1 million Americans suffer from a myocardial infarction, with many subsequently developing heart failure. Our labs have worked extensively to develop next-generation therapies for heart failure based upon remuscularizing the scar with stem cell-derived cardiomyocytes. While promising, these immature cells fail to recapitulate the adult cardiomyocyte phenotype and lack the ability to generate meaningful force, which may explain the relatively modest gains in cardiac function seen in most studies to date. Motivated by this challenge, I hypothesized that developing novel strategies to improve the contractile performance of human pluripotent stem cell-derived cardiomyocytes will improve the efficacy of cardiac cell therapy.

My thesis work has focused on developing two independent strategies to improve the contractile capabilities of these cells. First, I developed a novel maturation process

whereby immature cardiomyocytes begin to recapitulate key structural and functional characteristics of mature adult cardiomyocytes. These cells become larger and more directional, exhibit highly organized intracellular contractile machinery, and demonstrate improved contractility, Ca^{2+}-handling, and action potential characteristics.

I then worked to develop a second approach based on the small molecule dATP, which our lab has shown dramatically increases cardiac function by substituting for ATP as the energy substrate for cardiac myosin. Based upon preliminary studies, I hypothesized that like other small metabolites, dATP is capable of crossing gap junctions and diffusing between neighboring cells. Using several independent techniques, I confirmed this phenomenon and subsequently showed that transplanting stem cell-derived cardiomyocytes overexpressing ribonucleotide reductase, the enzyme that synthesizes dATP, dramatically improves global heart function via gap junction-mediated dATP transfer.

Based upon these studies, our lab is currently testing both approaches in models of myocardial infarction, with hopes of one day translating these approaches to a future clinical therapy for heart failure.

TABLE OF CONTENTS

LIST OF FIGURES

LIST OF TABLES

LIST OF SUPPLEMENTAL FIGURES

GLOSSARY

AFM	Atomic Force Microscopy
AV	Adenovirus
cAMP	Cyclic Adenosine Monophosphate
CK	Creatine Kinase
CM	Cardiomyocyte
cTnT	Cardiac Troponin T
Cx43	Connexin 43
dADP	2'Deoxyadenosine Diphosphate
dATP	2'Deoxyadenosine Triphosphate
EB	Embryoid Body
EHT	Engineered Heart Tissue
FS	Fractional Shortening
GCaMP3	Genetically Encoded Calcium Sensor
GFP	Green Fluorescent Protein
GJIC	Gap Junction Intercellular Communication
H&E	Hematoxylin and Eosin
hESC	Human Embryonic Stem Cell
hiPSC	Human Induced Pluripotent Stem Cell
hMSC	Human Mesenchymal Stem Cell
HNDF	Human Neonatal Dermal Fibroblast
hPSC	Human Pluripotent Stem Cell
ISO	Isoproterenol
LVEDD	Left Ventricular End Diastolic Dimension
LVESD	Left Ventricular End Systolic Dimension
MEF-CM	Mouse Embryonic Fibroblast-Conditioned Medium
MI	Myocardial Infarction
mPAD	Microfabricated Post-Array Detector
MYH7	β-Myosin Heavy Chain
MYH7	α-Myosin Heavy Chain
Pi	Inorganic Phosphate
R1	R1R2 Regulatory Subunit
R1R2	Ribonucleotide Reductase
R2	R1R2 Catalytic Subunit
SERCA2a	Sarco-Endoplasmic Reticulum ATPase
SICM	Scanning Ion Conductance Microscopy
TEM	Transmission Electron Microscopy
WT	Wild Type

ACKNOWLEDGEMENTS

I must first express my sincerest gratitude to my co-mentors, Mike Regnier and Mike Laflamme, for their guidance and support throughout my tenure as a graduate student. Many students never have the luxury of working for a thoughtful, kind, and scientifically rigorous advisor, and I was fortunate enough to find two advisors who both equally fit this description.

In addition to having fantastic mentors, I was blessed to work with a number of extremely talented and selfless research scientists. Ben Van Biber was truly irreplaceable as both a tissue culture expert and as a friend. Wei Zhong Zhu always seemed to have a smile on his face as he provided critical scientific expertise on numerous occasions. The senior scientists of the Regnier lab -- Masha Razumova, Galina Flint, Charles Luo, Jin Dai, and An-Yue Tu – were extremely helpful in mentoring me from a young naive graduate student towards the path to independence. Additionally, I want to particularly thank Steve Korte for providing daily mentorship, scientific discussions, and friendship during our combined time in the Regnier lab.

I would also like to thank all of my fellow graduate students from the Regnier and Laflamme labs. In particular, I would like to thank Kara White Moyes, Jay Gantz, Kassandra Thomson, Erik Feest, Dan Wang, Sarah Nowakowski, and Dominic Filice for their willingness to always grab a cup of coffee or lunch (or beer) and talk science (or anything but science). I cannot think of a better group of people to have shared this

experience with. A number of undergraduates also worked hard to make much of this work possible – thank you Sean Murphy, Robin Wilson, Michael McNamara, Willi Obenza, Cody Horst, and Beth Gay for all of your hard work.

I would like to sincerely thank our friends and colleagues in the Department of Physiology at the University of Firenze – in particular, I must acknowledge Corrado Poggesi and Chiara Tesi for their scientific guidance and hospitality, and Cecilia Ferrantini and Raffaele Coppini for truly making me feel at home during my time in Italy.

A number of other key faculty and staff provided critical resources and fruitful scientific discussion as well. Thank you to Lil Pabon, Marta Scatena, Ron Seifert, Sarah Dupras, Veronica Muskheli, Martha Lee, Hans Reinecke, Bill Mahoney, Dorian Varga, Kareen Kreutziger, and Al Gordon for all of your help and support.

Finally, I must thank my friends and family for their unyielding support throughout this process. My wife Brittany is one of the most supportive, patient, and inspiring people I have ever met, and without her I could never have succeeded in graduate school. My parents Dave and Cindy Lundy have supported me every step of the way not just in graduate school but also in life, and I thank them from the bottom of my heart for being such outstanding role models and constant sources of inspiration.

DEDICATION

I dedicate this work to my wife Brittany and my son Jacob. Brittany you are my soul mate and my best friend, and it was your support along this journey that made this work possible. Jacob, it is my hope that you will be blessed with the same love, support, and encouragement to pursue your dreams that my mother and father gave me.

Chapter 1. Introduction

Myocardial Infarction and Heart Failure

The heart is a remarkable organ capable of pumping over 225 million liters of blood and maintaining adequate tissue oxygenation for over 3 billion beats. From young age to old and exercise to rest, the heart is capable of continuously adjusting its performance to meet physiological demands. One of the primary mechanisms underlying this performance modulation is the Frank-Starling law of the heart, first described by Otto Frank and Ernest Starling over 100 years ago[1-3]. This law describes the ability of the heart to increase output (stroke volume) in response to an increase in diastolic filling (preload), and while the exact molecular mechanisms are still incompletely understood, this relationship is critical in maintaining normal cardiac function and adequate end-organ perfusion.

Despite these extraordinary abilities, the loss of adequate myocardial oxygenation due to occlusion of a coronary artery rapidly results in a myocardial infarction (MI), characterized by irreversible widespread tissue destruction and death of a billion or more cardiomyocytes[4]. The consequences of this and other related cardiovascular diseases are staggering; cardiovascular disease is the number one killer worldwide and costs the US over $300 billion dollars annually, and every minute an American dies of an heart attack[5].

Heart Failure

Following infarction, the damaged heart attempts to preserve existing end-organ perfusion by forming a noncontractile fibrotic scar and dilating in attempt to take advantage of the Frank-Starling effect. If the damage is too severe, however, these efforts instead trigger a feed-forward relationship between increasing chamber size and decreasing pump function in a condition termed heart failure, characterized by fluid accumulation, exercise intolerance, shortness of breath, and ultimately death. Once this vicious cycle commences, modern medicine has very little in the way of treatment options to offer patients. On one end of the treatment spectrum, pharmacologic therapies such as inotropic agents (discussed in detail below), β-adrenergic blockers, or angiotensin-converting enzyme inhibitors merely attempt to prevent disease progression and fail to treat the underlying pathology. On the other end of the spectrum, heart transplants and left ventricular assist devices can effectively replace the damaged heart with a new pump, but these therapies are extremely expensive and require concomitant therapy for life (immunosuppression and/or anticoagulation, respectively). It is clear that next-generation treatment options designed to treat the root cause of the disease are necessary to ameliorate the epidemic of heart disease.

Inotropic drugs – the paradox of Ca^{2+}, contractility, and mortality

Over 200 years ago, Dr. William Withering published his seminal report on the use of foxglove extracts for the treatment of “dropsy” (heart failure)[6]. One hundred years later, the active compound – digoxin – was isolated and subsequently shown to inhibit the Na^{+}-K^{+} ATPase pump, indirectly modulating the Na^{+}-Ca^{2+} exchanger and exerting its

inotropic effect via increased $[Ca^{2+}]_i$ stores[7]. In the century that followed this discovery, the manipulation of Ca^{2+} has become the primary underlying mechanism of action of nearly all therapeutically available inotropic agents. Milrinone, for example, is a phosphodiesterase-3 inhibitor that increases PKA-mediated phosphorylation of myofilament and Ca^{2+}-handling proteins including L-type Ca^{2+} channels, thereby increasing contractility[8]. Dobutamine is a sympathomimetic developed to activate cardiac β_1 adrenergic receptors and increase contractility without significant off-target β_2 adrenergic receptor activation[9]. Calcium sensitizers, including levosimendan, have also been developed to increase the myofilament sensitivity to Ca^{2+} and provide inotropic support in acute decompensation[10]. Despite the unquestionable ability of these compounds to exert increases in cardiac output, none of these compounds have shown to definitively reduce all-cause mortality in heart failure patients[11], and several clinical trials have even shown an increase in mortality in the treatment groups[12-14]. Investigating new approaches capable of modulating contractility independent of Ca^{2+} may overcome this clinical challenge and offer truly functional inotropic therapy for patients in end-stage heart failure.

Next generation cardiac therapies

Inotropic Compounds

Omecantiv Mecarbil. One next-generation investigational drug is omecantiv mecarbil, a small molecule agent capable of modulating contractility via direct interaction with cardiac myosin[15]. This interaction with the catalytic domain of myosin appears to

enhance the transition to the strongly actin-bound state[16]. Preliminary studies with the drug have suggested a potent effect on contractility independent of $[Ca^{2+}]_i$, but there is a question about whether these increases in systolic function will come at the sacrifice of diastolic function, which could impair filling and exacerbate the hypoxia and tissue damage found in infarcted hearts[16]. Initial clinical results, however, are favorable[17,18], and further preclinical studies and clinical trials are necessary before FDA approval and widespread clinical adoption occurs.

dATP. 2'-deoxyadenosine triphosphate, or dATP, is a nucleotide used ubiquitously for DNA synthesis. In 1998, Regnier *et al* published the unexpected result that unlike other ATP nucleotide analogs evaluated, dATP was unique in demonstrating increased hydrolysis rates and unloaded shortening velocities over ATP in skeletal myosin[19-21]. Subsequent studies with α- and β- cardiac myosin demonstrated even more dramatic improvements (**Table 1.1**), including an increase of >40% in maximum isometric force generation in demembranated cardiac trabeculae at all levels of $[Ca^{2+}]_i$[22]. A series of follow-up experiments demonstrated that dATP enhances the kinetics of strong crossbridge binding and the rate of Pi and ADP release, but importantly these increases in function did not compromise the Frank-Starling Effect. Furthermore, following hydrolysis by cardiac myosin, dADP has been shown to be rapidly rephosphorylated by creatine kinase and other kinases with kinetics similar to ADP, suggesting that small amounts of nucleotide can be used as an energy substrate for comparatively large numbers of hydrolysis events. Work by Schoffstall *et al* demonstrated that these effects persist even with small amounts of dATP relative to ATP. These suggest that, even in

Table 1.1 Summary of dATP effects on striated muscle

small quantities, dATP acts directly at the myofilament to enhance contractility of cardiac muscle[19,22].

(data compiled from Regnier et al[19])

Parameter	Fast Skeletal Muscle	Cardiac Muscle (α-MHC)	Cardiac Muscle (β-MHC)
cto-HMM NTPase Actin Sliding Speed (*In Vitro* Motility) (V_f) aximal Unloaded Shortening Velocity (V_u)	+25-30%	+50-75%	+70-100%
aximal Ca^{2+} Activated Force (F_{max})	No Change	+35-45%	+35-45%
aximal Rate of Force Redevelopment (K_{tr})	+10%	+30-60%	+30-50%
a^{2+} Sensitivity of Force (pCa_{50})	+0.15 pCa	+0.13 pCa	+0.26 pCa

Mechanistically, the work conducted to date supports the hypothesis that dATP works to enhance the crossbridge cycle in three specific steps of the eight stage chemomechanical cycle (**Fig. 1.1**)[23]. Briefly, this cycle begins when ATP binds myosin (step 1), facilitating the detachment of actin from the complex (step 2). ATP is then rapidly hydrolyzed (step 3), and a weak attachment to actin reforms (step 4). In the presence of Ca^{2+}, this weak bond is converted to a strongly bound state (step 5), which facilitates a transition to the force producing state in myosin and the release of Pi (step 6). Following the power stroke and a rate-limiting isometric step (step 7), ADP is released (step 8) and the cycle repeats. Data collected in demembranated muscle preparations with dATP found an increase in the Ca^{2+} sensitivity of force, which correlates with the Ca^{2+}-regulated strong attachment step (step 5). Increases in unloaded shortening velocity (V_u) and f-actin sliding velocity (V_f) suggest an increase in the relatively slow ADP release step (step 8)[22]. Finally, an increase in the rate of force

redevelopment following release and restretch, a maneuver termed k_{tr}, suggests an increase in the kinetics of the power stroke as well (step 6). Taken collectively, these alterations suggest that dATP works to enhance both the rate of crossbridge idge detachment

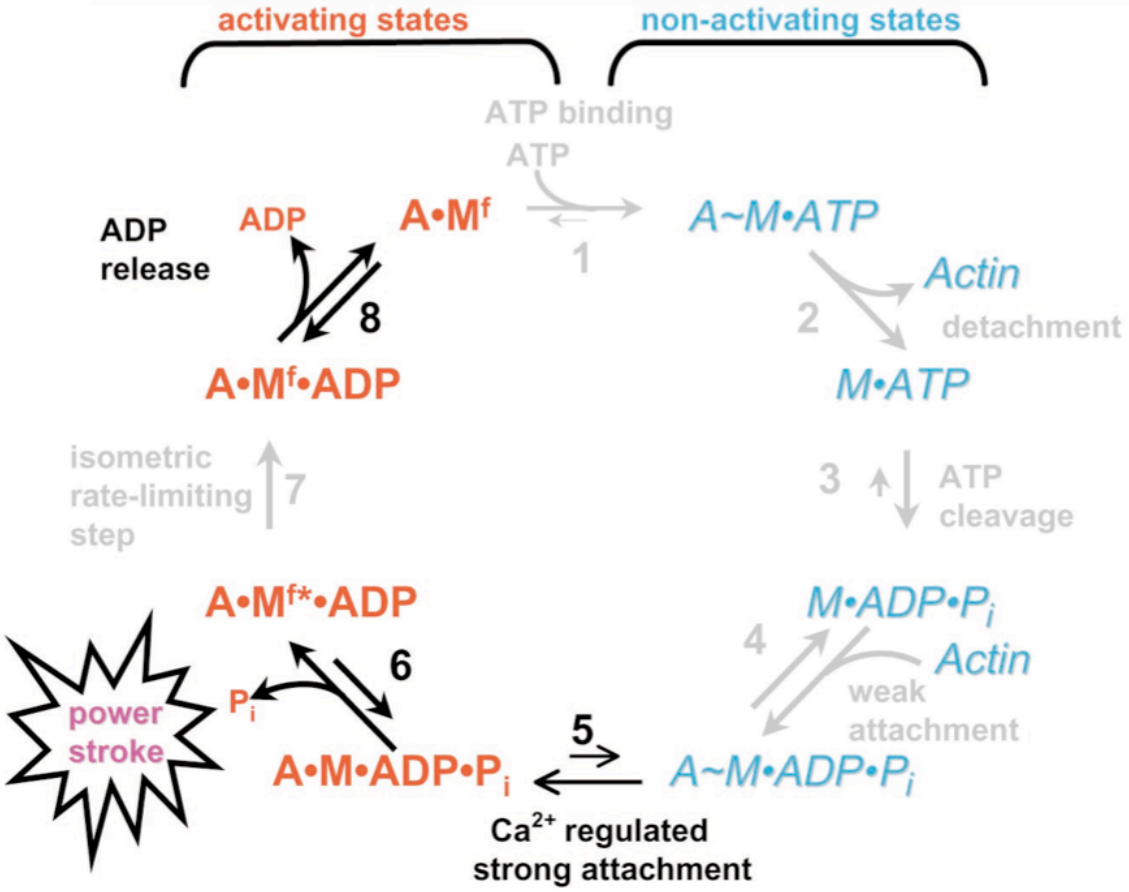

Figure 1.1 Effects of dATP on myosin chemomechanical cycle

(Adopted from Gordon et al[23])

dATP is naturally produced in the cytoplasm by the highly conserved enzyme ribonucleotide reductase (R1R2), which converts ADP to dADP for subsequent

rephosphorylation by creatine phosphokinase[21]. Ribonucleotide reductase is a heterotetrameric enzyme composed of two R1 regulatory subunits and two R2 catalytic subunits and catalyzes formation of the deoxynucleotide via a tyrosyl free-radical mechanism[24]. The expression and function of R1R2 is tightly controlled *in vivo* at the transcriptional and translational levels, and dATP inhibits enzymatic activity via allosteric feedback inhibition[24]. Our lab has recently investigated the cardiac consequences of a global R1R2 overexpressing transgenic mouse and found sustained increases in systolic cardiac function without accompanying fibrosis or hypertrophy[25]. Investigation into the metabolic consequences of dATP overexpression found normal levels of ATP and only slightly decreased levels of phosphocreatine[25]. Importantly, these hearts retained their rate responsiveness to dobutamine challenge[25]. Finally, dATP appeared to have no apparent untoward effects on smooth muscle function[25]. Taken together, these findings suggest that long-term dATP overproduction in the heart may be a viable therapeutic approach.

Recent work in our lab has taken advantage of R1R2 to apply dATP overproduction to intact WT cardiomyocytes[26]. Using adenoviral transduction to overexpress the dATP-producing enzyme subunits R1 and R2 under control of the CMV promoter, we demonstrated ~50% improvements in contractile magnitude of adult rat cardiomyocytes with no corresponding increase in Ca^{2+} transient magnitude[26]. Western blots demonstrated increases in both R1 and R2 proteins, and HPLC analysis demonstrated a 10-fold increase in dATP content[26]. This increase, while dramatic, still only constitutes

~1% of the total cellular adenine nucleotide pool[46]. In summary, the data collected thus far further supports a potential role for dATP as a therapeutic inotropic agent.

Cardiac Gene Therapy

The premise of gene therapy is a deceptively simple idea that overexpressing a key gene in a diseased tissue can reverse disease progression and/or restore baseline functionality. Delivery of genes modulating these effects has been accomplished using viral (adenovirus, adeno-associated virus, or lentivirus) or nonviral (naked plasmid, polymer, or lipid-based) delivery strategies[27]. While viral strategies often achieve transduction efficiencies of 50% or greater, they pose the potential hurdles of transient expression, immune response, and/or oncogenesis[28]. Nonviral delivery strategies are thought to be safer, but unfortunately they exhibit far lower transfection efficiencies and transient expression profiles[29].

Using this knowledge and primarily relying on viral transduction strategies, a number of recent publications have demonstrated that overexpression of key genes can improve cardiac function following MI. Much like inotropic drugs, the majority of these efforts have focused on modulating genes associated with Ca^{2+} handling, including the small molecule Ca^{2+} binder S100A1[30], phospholamban[31], and SERCA2a[32]. The latter has recently completed phase 2 clinical trials with promising results[33]. With larger studies ongoing, it remains to be seen if these exciting early results will be recapitulated.

Cardiac Cell Therapy

Cell types. Motivated by the insufficient treatment options for patients suffering from heart failure, researchers first began investigating the delivery of exogenous cell to remuscularize the myocardium in the early 1990s. The first experiments were conducted using autologous skeletal myoblasts as a cell source[34-36], primarily due to their ischemic resistance and lack of significant immunogenicity. Despite initial excitement demonstrating improvement in cardiac function in early clinical trials[37,38], subsequent trials disappointingly revealed increased arrhythmogenesis[39-42], and a randomized placebo-controlled double-blind study demonstrated no long-term benefit in echocardiographic function[43]. It is now thought that any functional benefit is likely due to paracrine signaling or passive mechanical buttressing effects, as these cells are incapable of electrically coupling with host myocardium[44,45]

The second primary cell type investigated in clinical trials is the bone marrow cell, which was initially reported to give rise to de novo cardiomyocytes upon transplantation[46]. In sharp contrast, subsequent studies with extremely sensitive fate mapping experiments could not replicate these findings[47] and instead suggested rare cell fusion events as the potential underlying phenomenon. Nevertheless, a number of clinical trials were undertaken to test the ability of these cells to improve cardiac function by indirect mechanisms. While a detailed discussion of the results from these trials is beyond the scope of this discussion and has been discussed extensively in other reviews[48], the majority of findings thus far suggest that while transplantation of these cells is safe, the

benefit on long-term cardiac function following transplantation is negligible or modest at best[49-51].

Finally, the use of human mesenchymal stem cells (hMSCs), a multipotent stromal cell population derived from bone marrow with unique immunogenic characteristics, has gained popularity recently as a potential cell source for cardiac repair. Based upon an extensive body of literature from the hematopoietic field, preclinical studies for cardiac repair began in earnest roughly a decade ago[52-55], and clinical trials followed soon thereafter[56]. Most recently, results from the POSEIDON trial demonstrated improvements in several cardiac indices following transplantation of hMSCs, but neither allogeneic or autologous populations statistically increased the ejection fraction (EF)[57]. Most studies to date now concur that long-term survival of hMSCs is extremely low, and questions remain about the ability of these cells to permanently improve cardiac function following injection.

Pluripotent Stem Cell-Derived Cardiomyocytes

Historical Perspective

Perhaps the ideal cell source for regenerating lost myocardium is the human cardiomyocyte itself. With the discovery of human embryonic stem cells (hESCs) by Thomson and colleagues in 1998[58], the dream of producing de novo human cardiomyocytes for therapeutic applications became a reality. Derived from the inner cell mass of excess blastocysts from in vitro fertilization clinics, hESCs are pluripotent

cells capable of giving rise to all three germ layers (endoderm, ectoderm, and mesoderm) and forming any type of cell found in the adult human[58]. Phenotypically, undifferentiated hESCs form compact colonies with a high nuclear-to-cytoplasmic ratio. They express high levels of alkaline phosphatase and pluripotency transcription factors including Oct4, Sox2, and Nanog[58,59], and they are capable of expanding indefinitely *in vitro* without loss of pluripotency.

Less than a decade after the first report of hESCs by Thomson *et al*, the Yamanaka group detailed the successful generation of human induced pluripotent stem cells (hiPSCs) via retrovirally-mediated overexpression of Oct4, Sox2, Klf4, and c-Myc in human foreskin fibroblasts[60]. While these cells are virtually indistinguishable from hESCs on the basis of morphology and ability to differentiate into any adult terminal cell population[60], it remains to be seen whether subtle differences in epigenetic status and/or gene expression will be clinically relevant[61,62].

PSC-CM Phenotype

Differentiation. Inspired by the work of Doetschmann *et al* in the mouse ESC field[63], cardiomyocytes (CMs) were first generated from hESCs and/or iPSCs via spontaneous embryoid body (EB) differentiation, which typically results in a cardiac purity of <1%. Subsequent work established a number of guided differentiation protocols, many of which took cues from the developmental biology literature, to guide cells from pluripotency through mesoderm and mesendoderm specification towards a definitive cardiac lineage[64-66]. While the details of these protocols are beyond the scope of this

work, the reader is directed towards several excellent reviews discussing these protocols in detail[67,68]. Recent advances to these protocols have included elucidating the importance of using insulin-free media during early differentiation[69], the addition of a matrigel overlayer to enhance purity and yield[70], and the use of small molecules to manipulate Wnt signaling[71]. Using these next-generation protocols, we and others routinely achieve >80% cardiac purity, and in exceptionally good examples reach >95% cardiomyocytes without the use of genetic selection[72].

Phenotype. By light microscopy, early PSC-CMs appear as small, nondescript, mononucleated cells with variable size and shape[65,73-76]. They express sarcomeric proteins including α-actinin, cardiac troponins I and T, α- and β-myosin heavy chains (MHCs), atrial- and ventricular- myosin light chains (MLC2v and MLC2a), desmin, and tropomyosin[65,75-81]. Ultrastructurally, they show poorly organized sarcomeres and intercalated discs[72,74,77,82]. Interestingly, PSC-CMs show robust proliferative activity characteristic of early chamber myocardium, with cell cycle activity slowly tapering off over several weeks of in vitro maturation[82-84] Somewhat surprisingly, they also possess the ability to migrate in response to haptotactic molecules such as fibronectin or chemotactic molecules such as Wnt5a[85].

From an electrical standpoint, PSC-CMs exhibit spontaneous rhythmic cardiac action potentials (APs) that can be stratified into nodal and working cardiomyocyte subtype populations[65,80]. Early hESC-CMs show immature AP properties (i.e. automaticity, a slow AP upstroke, and a depolarized maximum diastolic potential), but these improve

somewhat with prolonged duration in culture[80,86]. In voltage-clamp studies, hESC-CMs exhibit most of the major cardiac ion currents, including fast sodium, L- and T-type calcium, pacemaker, as well as transient outward and inward rectifier potassium currents[65,86-88]. Depolarization in these cells is dominated by sodium influx via the $Na_V1.5$ channel, and this current is at least partially responsible for their spontaneous electrical activity[88]. As in adult cardiomyocytes, depolarization activates L-type calcium channels in hESC-CMs, which results in a calcium influx that is amplified by release from sarcoplasmic reticulum calcium stores[87,89,90]. Recent data from our group indicates that this calcium-induced-calcium release process operates via a tight "local control" mechanism, similar to that of adult myocardium[87].

Preclinical experience with PSC-CM cell therapy

Motivated by reports that mESC-CMs readily engraft and form stable grafts in mouse hearts[91], several groups embarked on transplanting hESC-CMs into animal models of myocardial infarction[77,92-99]. These studies showed that human cardiomyocytes survive and proliferate in host myocardium[93], readily form gap junctions with the host and conduct electrical impulses[77,92], and mature to a degree *in vivo*[95]. Recent work by our group has shown that in addition to the potential for electrical coupling with the host heart, hESC-CM transplantation actually decreases the incidence of arrhythmias in a guinea pig cryoinjury model[100]

Despite the numerous preclinical studies conducted with hESC-CMs and hiPSC-CMs in animal models of heart failure, there is exceedingly little data on whether these grafts

truly contribute meaningful pumping capacity *in vivo.* Indirect evidence has been provided by changes in global cardiac function as measured by echocardiographic imaging[94,97,98,101], but these increases can also be explained by indirect paracrine or mechanical buttressing effects. Magnetic resonance imaging studies have provided slightly more quantitative data by demonstrating increased regional wall motion in regions receiving grafts[94,102]. To our knowledge, the only study published to date that quantitatively examines this issue is by our group using neonatal rat cardiomyocytes (NRCs) as a model of cell transplantation[103]. Moreno-Gonzalez *et al* transplanted these cells into infarcted hearts and measured graft and remote tissue force production in demembranated wall strips[103]. The study convincingly showed that engrafted cells, but not scar, produced active force in the presence of Ca^{2+}, and that compared to the sham group, the Ca^{2+} sensitivity of force was higher in both graft tissue and in the remote myocardium of hearts receiving grafts. Taken together, this evidence suggests that the increase in global cardiac function following cell transplantation may be multifocal in nature, but whether these findings will directly translate to studies with human PSC-CMs remains to be seen.

Given the lack of information regarding *in vivo* PSC-CM contractile force production, it is necessary to reorient and first evaluate what is known about PSC-CM contractility *in vitro*, both as it relates to single cells and engineered myocardial constructs.

Measuring Cardiac Cell and Tissue Contractility

Traditional Approaches

The field of cardiac physiology has developed a number of elegant techniques to measure the contractility and force production of the heart at hierarchical levels ranging from individual actomyosin interactions to the entire organ (**Fig. 1.2**). Individual crossbridge dynamics have been assessed using optical laser traps[104], single thin filament kinetics measured using the *in vitro* motility assay[105,106], and small bundles (~1000 thick filaments) of cardiac muscle lattice probed using the myofibril assay pioneered by Iwazumi and Poggessi groups[107-111]. Single cardiomyocyte contractility

cent advances

[14] and intact

a single adult

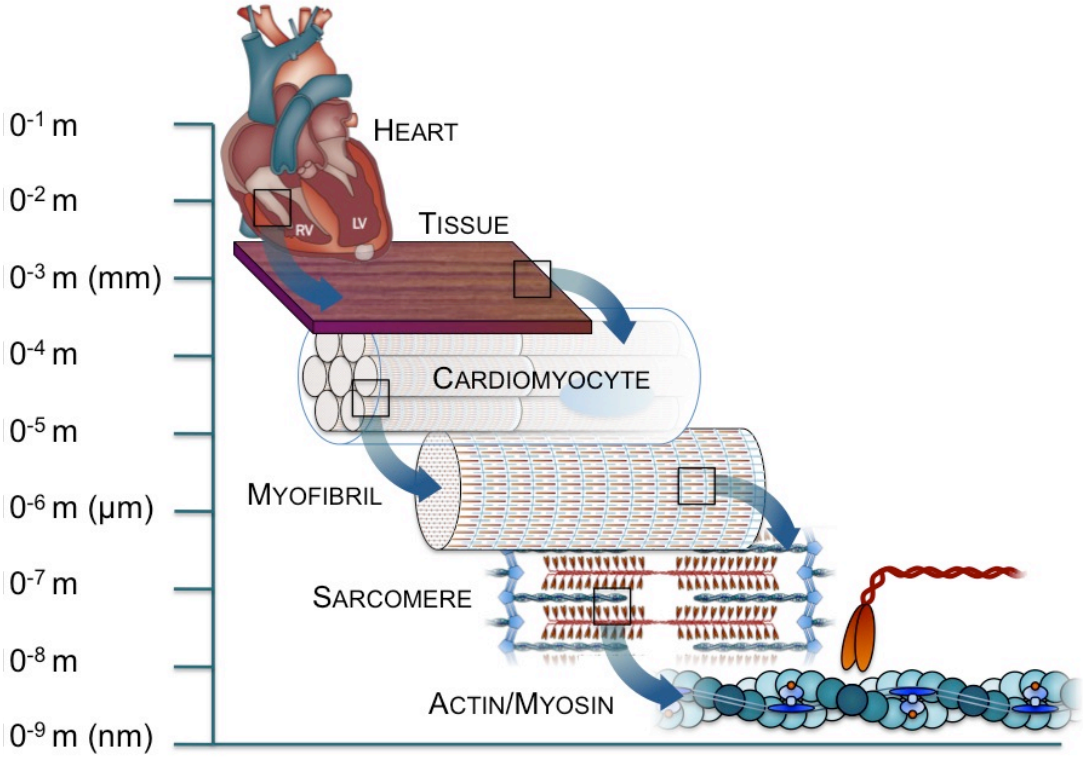

Figure 1.2 Hierarchical nature of cardiac muscle

cardiomyocyte produces on the order of 1-10 μN of force. On a larger scale, isolated trabeculae and wall strip measurements can be made using a force transducer and a length controller[22,117-119]. Finally, *ex vivo* intact heart function has been extensively studied using the experimental setup pioneered by James Neely[120-122].

Despite the immense progress made over the past half-century in these areas, the measurement of contractility and force production in stem cell-derived cardiomyocytes has lagged behind, likely due to (1) small cell sizes and irregular cell shapes associated with immature cardiomyocytes, (2) difficulty in producing tissue-size constructs with defined geometry mimicking human myocardium, and/or (3) difficulty in obtaining large quantities of purified preparations. These challenges render many of the traditional techniques incapable of quantitating force generation in immature cardiomyocytes, which has necessitated the development of a host of new assays. Despite these challenges, a number of studies have succeeded in addressing these challenges, and a growing body of literature has investigated the contractile capabilities of hPSC-CMs.

Initial Contractility Studies in PSC-CMs

Embryoid body measurements. The first measurements of hESC-CM contractility were performed on videomicroscopic contraction analysis of embryoid bodies (EBs)[123-125]. This technique allows for rapid measurement of beating EBs using arbitrary contraction units. Primary strengths of this approach include its simplicity – the technique only requires a microscope and a high-speed camera – and the ability to track acute changes following administration of various pharmacologic treatments. Dolnikov *et al*

used this technique to demonstrate intact excitation-contraction coupling by simultaneously measuring $[Ca^{2+}]_i$ using the ratiometric dye fura-2[124,125]. The group also showed that unlike adult cardiomyocytes, hESC-CMs possess a negative force-frequency relationship but do indeed respond to pharmacologic stimuli such as angiotensin-II administration[125]. More recently, this technique has been utilized to demonstrate that beating hiPSC EBs also demonstrate a negative force-frequency relationship[126]. While useful as a proof-of-principle assay, this technique suffers challenges associated with EB heterogeneity, including variable/low (typically below 5%) cardiac purity and inconsistent EB size and orientation. These limitations make it difficult to gather any quantitative data beyond relative changes in contractility over a short period of time.

Single Cell Measurements

Optical contractility assessment. Due to the limitations associated with EBs, several groups have instead investigated contraction analysis on single cells, which alleviate concerns with purity by instead focusing on a single spontaneously beating cardiomyocyte. These measurements, however, are more technically challenging due to the small size (~20 μm) and even smaller contraction magnitudes (~1 μm) of immature cardiomyocytes. Our group used the commercially-available Ionoptix videomicroscopy system to quantify both the magnitude and kinetics of spontaneous contractions[72] of immature PSC-CMs, and we found that typical early stage cardiomyocytes from both hESCs and iPSCs demonstrate a ~5% contraction magnitude. Shinozawa *et al* used a similar technique to calculate the average

contraction velocity for single cells at various time points during differentiation[127]. Despite the advantages with single cell optical measurements, however, this assay measures contractility as a surrogate for force production, which is likely a more relevant parameter for cell therapy applications.

Scanning Ion Conductance Microscopy. Developed in 1989 by Hansma *et al*, the scanning ion conductance microscope (SICM) allows the user to track changes in the z-axis topography of cells in culture by measuring differences in current flow between an electrically charged pipette and the surrounding electrolytic solution as the tip is rastered over the surface (or the cells contract)[128]. SICM has been successfully applied to PSC-CMs in two reports to date; the first in 2006 described the protocol and demonstrated changes in height following administration of pharmacologic agents[129], and the second to investigate the arrhythmogenic consequences of bile acids as a model for fetal arrhythmias[130]. While rapid and noninvasive, this technique is only capable of measuring displacements and to date cannot convert these measurements into forces. Nevertheless, as a tool to rapidly assess changes in beat frequency or relative changes in contractility, SICM remains a viable approach.

Traction Force Microscopy. Motivated by the lack of information regarding force production in hPSC-CMs, several groups developed protocols to seed deformable gels containing fluorescent beads with hESC-CMs and measure the corresponding deformation that occurred with each contraction. By producing a vector map and using bulk properties, the groups were able to calculate a theoretical net force production

vector and magnitude for a single cell. Using this technique with a 4kPa polyacrylamide gel substrate, Kita-Matsuo[131] reported a maximum force of 350 nN, which is approximately two orders of magnitude less than that of an adult cardiomyocyte.

Hazeltine *et al* greatly expanded on this initial work by investigating force production across a range of substrate stiffnesses (4-100 kPa) and developmental stages (D30-D60). In contrast with previous reports from the neonatal cardiomyocyte literature[132,133], the group found that both hESC-CMs and hiPSC-CMs cultured on stiffer substrates (~100kPa) exerted increased average contraction stress (~25-50 mN/mm^2) compared to softer substrates. The discrepancy in these values underlies several of the primary challenges associated with traction force microscopy; data analysis can be challenging and requires several theoretical assumptions, and extrapolating real-world anisotropic force production is not always straightforward.

Microfabricated Platforms. The field of microfabrication has provided powerful tools to assist in the organization and measurement of cardiomyocytes and cardiac tissue. This technology relies on soft lithography techniques pioneered in the semiconductor industry to produce a three-dimensional culture substrate, typically of polydimethylsiloxane (PDMS), with defined architecture capable of supporting cell adhesion and integration. Serena *et al* used these principles to develop a high-throughput functional assay to screen cardiomyocyte functionality *in vitro*[134]. This approach eliminates many of the challenges associated with measuring contractility in traditional EB clusters (including concerns with purity and cluster size hetereogeneity),

but nevertheless contractility must still be measured using arbitrary units.

An elegant technique was recently developed by Sniadecki *et al*, who used soft lithography to produce microfabricated post array detectors (mPADs) resembling a "bed of nails" and allowed cells to adhere and subsequently exert forces on individual discrete posts[135]. By applying beam theory to posts of known height and thickness, an exact force value can be calculated for each post and these vectors summed to produce a net force vector per cell. This technique was initially applied to cells exerting static stresses such as fibroblasts and endothelial cells[136], but more recent studies have examined the dynamic force production of neonatal rat cardiomyocytes[137]. More recently, this technique was modified and applied to hESC-CMs by seeding cells onto a flat hybrid NIPAAm/PDMS surface and selectively dissolving the NIPAAm away, leaving cells adherent to the remaining PDMS mPADs. By applying a known calibration from a piezoresistive cantilever, the group was able to calculate forces approaching 100nN for single hESC-CMs[138]. Benefits of this assay include the ability to survey many cells quickly and noninvasively, as well as the ability to measure changes in contractility over time. Drawbacks include a complicated substrate production process and specialized experience and equipment (lithography equipment, a microcantilever device for calibration, and high-resolution imaging capabilities).

Optical Traps. Perhaps the most technically demanding approach undertaken thus far is the use of optical tweezers to measure the passive mechanical properties of hESC-CMs. Briefly, a highly focused beam of laser light can "trap" two dielectric beads in

space and exert a force on an object in between by gradually spreading the beads apart. Using this technique Tan *et al*[139] succeeded in calculating the elastic modulus of hESC-CMs at 14 Pa, which is approximately 2.5 fold higher than the corresponding value for undifferentiated hESCs but still 3 orders of magnitude lower than adult cardiomyocytes[140-142]. While technically demanding and currently unable to resolve dynamic contractile properties, optical trapping has provided valuable insight into the passive mechanical properties of hESC-CMs.

Atomic Force Microscopy. Arguably the most sensitive single cell contractile assay applied to date to hESC-CMs is atomic force microscopy (AFM). This technique, based upon placing a sharp cantilever tip on the surface of a beating cell and measuring the resulting deflections using laser light, is capable of resolving contractions with excellent sensitivity kinetics, even in immature cardiomyocytes. While several studies utilized AFM to probe the static ultrastructural characteristics of immature and adult cardiomyocytes[143,144], the first reports of AFM applied to dynamic beating cardiomyocytes were in 1999[145] for embryonic chick cardiomyocytes and in 2004[142] for adult rat cardiomyocytes. Lieu *et al*[143] and Wang *et al*[146] simultaneously published reports detailing AFM measurements in PSC-CMs in 2012[143], and both reported values of approximately 0.2nN per cell, well below the values predicted by previous methods. Follow up studies by the same group reported a similar value for hiPSC-CMs derived from dilated cardiomyopathy (DCM) patients, but interestingly the control cell force in this study was approximately an order of magnitude higher (~2-3nN)[147]. Interestingly, values obtained for passive stiffness (~300Pa) were also much higher than values

obtained from optical trapping. Whether these discrepancies reflect differences in AFM technique or cell preparation is unclear, but nevertheless it is clear that this technique as a whole appears to report force production values significantly lower than the techniques described above.

Lessons Learned From Single Cell Studies

Taken together, two primary lessons can be learned from the PSC-CM contractility data published thus far. First, there appears to be approximately three orders of magnitude in variation when results across techniques are compared and summarized (**Table 1.2**). This may reflect a difference in underlying the underlying cell population or over/underestimations used in calibration factors, but the more likely explanation is rooted in the artificial nature of culturing 3-dimensional cells in a 2-dimensional environment. PSC-CMs cultured on flat substrates such as tissue culture plastic offer very little relief in the third dimension, and the majority of their contractile apparatus is found in close opposition to the underlying substrate and the corresponding adhesion points. Practically speaking, this means that techniques such as traction force microscopy will capture the entire contractile force being produced by these cells, whereas techniques such as AFM and SICM will only capture the perpendicular movement of the cell membrane and likely very little of the myofibillar force being generated and transmitted orthogonally to the probe. Future studies aimed at culturing these cells in a truly three-dimensional environment may overcome this limitation and offer a more physiologically relevant cell population on which to base these types of measurements.

Table 1.2 Contractile parameters for single hPSC-CMs

l traction force microscopy **SICM** scanning ion conductance microscopy **AFM** atomic e microscopy **mPAD** microfabricated post array detectors **VM** videomicroscopy

mary Author	Year	Cell Source	Stage	Assay	Shortening	Force	Notes
ta-Matsuo[131]	2009	hESC	Early	TFM		50nN	4kPa substrate stiffness
Kadir[130]	2009	hESC	Early	SICM	8μm		
			Mid		7μm		
Wang[146]	2012	hESC	Early	AFM		0.1nN	
Liu[172]	2012	hESC	Early	AFM		0.49nN	Single cell
		hiPSC	Early			0.23nN	Single cell
			Early			2.37nN	Single cell within cluster
lazeltine[173]	2012	hESC	Early	TFM		40nN/mm²	Max force obtained with 100 kPa substrate
			Mid			50nN/mm²	
		hiPSC	Early	TFM		25nN/mm²	
Sun[147]	2012	hiPSC	Early	AFM		4nN	
Taylor[138]	2012	hESC	Early	mPAD		75nN	
Lundy[72]	2013	hESC	Early	VM	5%		
			Late		10%		
		hiPSC	Early	VM	5%		
			Late		9%		

The second primary lesson that can be gleaned is that despite the variability in values reported thus far, forces generated by immature PSC-CMs are miniscule in comparison to mature adult cardiomyocytes. Even in the most conservative measurements, adult cardiomyocytes still produce roughly 10-fold higher force on per-cell basis. If PSC-CMs are ever to succeed in regenerating myocardium following MI, then they must be made to exert forces comparable to the tissue they are attempting to replace. One approach to accomplishing this is to develop techniques to produce *in vitro* engineered

myocardium capable of mimicking the key parameters (cellular organization and maturation, construct anisotropy, and electrical conduction) found in the heart.

Myocardial Construct Force Measurements

Devitalized native myocardial constructs. One approach developed by the Hescheler group is to seed hESC-CMs into myocardial slices devitalized by oxygen/glucose deprivation and measure the resulting force production following integration[148-151]. Using this approach, Pillekamp *et al* reported active force values of approximately 5 μN per tissue section[151], which is less than the value reported for a single adult cardiomyocyte[152]. Follow-up work directly comparing native murine heart tissue to slices seeded with mESC-CMs or miPSC-CMs found that these produce roughly 1/50th the force of native mouse heart in similar preparations[153], underscoring the need to develop a more robust population of cardiomyocytes for future transplantation. Despite the lack of significant force production, this assay provides a novel approach to studying integration of transplanted cells into the myocardial niche. This model may prove to be especially useful if a local region of hypoxia can be generated to mimic a localized infarction, which can then be reseeded with cells in an *in vitro* model of cell therapy.

De novo myocardial construct force measurements. Since the first seminal reports of engineered heart tissue (EHT) by the Eschenhagen group over a decade ago [154,155], a number of groups have actively pursued the development and refinement of de novo cardiac tissue constructs. Such constructs are valuable not only as *in vitro* models for drug development and cardiac toxicity studies, but they may also ultimately provide

valuable insight into cardiac development. Finally, transplantation of de novo engineered cardiac tissue may represent a viable clinical alternative to direct cell injection, which often results in low cell retention and poor engraftment. The Eschenhagen group has continued to innovate in this area, publishing a number of reports on EHT using various cell types and functional endpoints. Beginning with embryonic chick cardiomyocytes and neonatal rat cardiomyocytes, the group has shown that EHT produces active force and chronic stretch increases this force[155,156], that EHT robustly engrafts into host myocardium[157,158], and that complex geometries of tissue can be generated for *in vivo* therapeutic applications[159]. Most recently, the group produced fibrin-based human EHTs using hESC-CMs capable of producing >60μN of force and then showed that they respond appropriately when subjected to hERG-modifying arrhythmogenic compounds[160].

Several other groups have also successfully produced cardiac tissue engineered constructs using PSC-CMs. Shimko *et al* reported the development of a collagen/fibronectin scaffold seeded with mESC-CMs and subjected to cyclic stretch; compared to controls, the stretched constructs showed increased organization and expression of key structural cardiac genes[161], but active force production was not assessed. In contrast, Stevens *et al* reported the development of a scaffold-free cardiac patch composed of cardiomyocytes, endothelial cells, and fibroblasts that spontaneously aggregate and organize *in vitro*[162]. These “tricell” constructs exert passive stiffness values approaching that of neonatal pig myocardium and survive upon transplantation into damaged myocardium[162].

Taking cues from the biophysical literature, Tulloch *et al* published a highly relevant report on collagen-based scaffolds seeded with hESC-CMs or hiPSC-CMs[163]. Most notably, the group performed detailed mechanical analyses using a setup originally built to test skinned cardiac trabeculae and found that constructs subjected to static conditioning exerted forces exceeding 80μN/mm^2. Even more excitingly, these constructs appeared to exhibit length-dependence of force analogous to the Frank-Starling law of the heart.

The Bursac group published an interesting report on the development of a mESC-based construct with an emphasis on recapitulating the physiological characteristics of adult myocardium[164]. The group used soft lithography to pattern cocultures of mESC-CMs and fibroblasts into a cohesive 2-dimensional tissue and then demonstrated conduction velocities approaching 20 cm/s and forces exceeding 2mN[164]. Again, as with work by the Murry group[163], these PSC-CM based constructs exhibited a positive length-tension relationship.

Perhaps the most comprehensive evaluation of PSC-CM construct contractility undertaken thus far was recently published by Kensah *et al* in 2012[165]. This group produced EHT constructs using collagen and matrigel seeded with either miPSC-CMs or hiPSC/hESC-CMs and subjected them to static or cyclic stress in a custom bioreactor[165]. The group showed progressive increases over 21 days in key cardiac

transcripts (MLC2v and Kir2.1), conduction velocities approaching 5cm/s, and positive force-length relationships, with maximum active forces exceeding 1mN per construct[165].

Finally, an innovative recent study by Didié *et al* reported the creation of mouse parthenogenetic stem cells are capable of giving rise to cardiomyocytes for allogeneic heart repair[166]. Notably, the group used these cells to generate engineered heart tissue and found that active force production (170μN per construct) is comparable that of native murine myocardium[166]. Interestingly, these constructs exhibited dramatically higher Ca^{2+} sensitivity than the native tissue, a finding which is consistent with previous reports of engineered heart tissue containing immature cardiomyocytes[167,168].

Lessons Learned from Construct Force Measurements

A number of insightful conclusions can be drawn from the growing number of reports involving hPSC-CM myocardial tissue constructs that now exist (**Table 1.3**). First, these studies complement the literature on single cell contractility discussed above, and both approaches provide unique and valuable insight into very different aspects of future cardiac cell therapy strategies. Second, while this process can be guided by geometric cues or variations on input cell population (including the addition of fibroblasts or endothelial cells), it appears that cardiomyocytes spontaneously aggregate and form functional, synchronized, beating tissue with little or no external effort required. The remaining challenges moving forward are centered on developing strategies to induce structural and functional maturation towards the ideal goal of recapitulating myocardium in the dish. Third, it is becoming increasingly apparent that critical components of

cardiac physiology, including the Frank-Starling length-tension relationship, are intrinsic and conserved throughout multiple species, even in immature cardiomyocytes derived from PSCs. Researchers in the field should find this very reassuring, as the biophysics underlying this phenomenon are still not yet completely understood and thus would be impossible to recapitulate using current knowledge.

Finally, while it is easy to directly compare force values from these studies in a head-to-head fashion, caution must be exercised when interpreting these values as subtle

Table 1.3 Contractile properties of human engineered myocardial constructs

Primary Author	Year	Construct Design	Cell Source	Max Force	Positive Length-Tension Relationship?	Notes
Pillekamp[148]	2007	Devitalized murine myocardium	hESC-CMs	4.9μN	yes	
Schaaf[160]	2011	Engineered heart tissue	hESC-CMs	61μN		
Tulloch[163]	2011	De novo collagen construct	hESC-CMs	~70μN	yes	Examined static/cyclic stress
Streckfuss-Bömeke[167]	2012	Engineered heart tissue	hESC-CMs	240μN	yes	
Didié[166]	2013	Engineered heart tissue	pSC-CMs	~125μN		Increased Calcium sensitivity

ctrical pacing,

differences in $[Ca^{2+}]_e$, and subtle changes in instrumentation) may have disproportionately large effects on the results. What can be generalized, however, is that despite the advances made in the previous decade, engineered heart tissue still fails to recapitulate the highly structural, organized nature of adult myocardium. It is likely that further incremental improvements in cell maturity, construct material

properties, and tissue geometry will be needed before a fully functional tissue-based therapy will be realized.

Efforts to Improve PSC-CM contractility

Motivated by the lackluster performance of hPSC-CMs in their current form, several groups have investigated methods to improve cell functionality from a mechanical perspective, with the goal of subsequently improving performance upon transplantation. Broadly speaking, these efforts can be categorized as either short-term acute changes in contractility (e.g. pharmacologic treatments), or long-term modulations in contractile capabilities.

Acute increases in contractility. Perhaps the most utilized and physiological method of rapidly increasing cardiac function is activation of the *β*-adrenergic pathway by endogenous agonists such as epinephrine or synthetic agonists such as isoproterenol. Activation of these receptors results in increased production of cAMP by the enzyme adenylate cyclase, which in turn alters the phosphorylation of key cardiac proteins. In adult cardiomyocytes, the consequences of these changes include increased inotropy, chronotropy, and lusitropy. Despite being extremely well characterized in the adult system, the response of hESC-CMs and hiPSC-CMs to adrenergic stimulation remains controversial. Most reports agree that administration of *β* agonists such as isoproterenol results in an increase in spontaneous rate of contraction in both hESC-CMs and hiPSC-CMs[76,82,92,125,127,147,151,169-171]. A number of these reports report a corresponding

increase in contraction magnitude[80,126,172], but several others report no such increase in inotropy[72,151,173]. Whether this discrepancy reflects differences in underlying cell physiology remains to be seen.

Aside from traditional adrenergic stimulation, other pharmacologic approaches have also been tested. Administration of angiotensin II, the active peptide hormone in the renin-angiotensin axis, resulted in a small increase in contraction magnitude in hESC-CM contractions[174]. Increasing extracellular [Ca^{2+}] has also been shown to increase contractile magnitude[124]. Finally, post-rest contractions have also been shown to increase the amplitude of contraction in hPSC-CMs[126]. These approaches, while providing fundamental information about the fundamental physiology of hPSC-CMs, are nevertheless unlikely be therapeutically relevant in a cell therapy setting, where long-term enhancement of contractility is necessary.

Long-term enhancements in contractility. In contrast to acute changes with inotropic drug treatment, the prospect of permanently increasing the contractile performance of immature cardiomyocytes is far loftier goal. A number of studies have proposed mechanisms to facilitate this maturation, with mixed success to date. Many of these approaches take their inspiration from the dynamic environment of the heart itself, which provides continuous electrical and mechanical cues. Kensah systematically tested the effect of cyclic stretch, adrenergic stimulation, or combined stretch/adrenergic stimulation on neonatal rat cardiomyocyte construct force production. Their results suggested that the adrenergic stimulation alone enhanced force to the greatest degree.

Other studies have examined static versus cyclic stretch and found that cyclic stretch promotes the greatest increases in cardiac gene expression and cellular alignment[163]. One relatively logical approach is to transplant immature cardiomyocytes into adult myocardium and test whether they spontaneously mature due to intrinsic biophysical or biochemical cues. Results from several groups[95,103,175] suggest that to an extent this does indeed occur, but despite engraftment over several weeks the cells still remained smaller than native cardiomyocytes in nearly all cases.

Wang et al examined the role of apelin, a peptide known to play a role in mesodermal migration by binding the APJ receptor, in hESC-based cardiac differentiation[146]. The group found that the addition of apelin resulted in a doubling of contractile force by AFM. While the exact mechanism of this increase remains to be elucidated, the effect appears to be independent of a number of candidate inotropic pathways[176].

Sun *et al* elegantly demonstrated using AFM that overexpression of SERCA2a in hiPSC-CMs derived from patients with dilated cardiomyopathy could rescue depressed contractility to healthy levels. While the group did not perform a similar experiment in healthy cells to see if contractility could be increased above baseline, the study provides compelling evidence that diseased cell function may be manipulated by gene therapy strategies.

Work by our lab (**Chapter 2**) has shown that prolonged culture on stiff (glass) culture substrates induces structural and functional maturation of hESC-CMs and hiPSC-CMs

to levels approaching adult cardiomyocytes. While we did not directly measure force generation, the late stage cells exhibited a doubling in shortening magnitude over their early stage counterparts. These changes in contractility were accompanied by improvements in the maturity of Ca^{2+}-handling kinetics and action potential phenotype, suggesting that immature hPSC-derived cardiomyocytes are indeed capable of recapitulating the adult phenotype, albeit slowly.

Closing perspectives and thesis introduction

In 1999 researchers promised that with adequate funding and 10 years, the research community could successfully grow a complete heart in the lab. The field of stem cell-based cardiac cell and tissue engineering has made monumental progress in the past decade, and while the promise of producing an *ex vivo* heart for therapeutic applications remains a distant target, the much more tractable goal of using stem cells to repair a damaged heart seems now within reach. A number of preclinical trials are now being planned and conducted to test the efficacy of stem cell-derived cardiomyocytes as a therapy for myocardial infarction, with promises of phase I trials to follow soon after in the next 3-5 years. One of the biggest series of questions directly applicable to these efforts is whether hPSC-CM grafts contribute meaningful active force generating units and pumping capacity, and if not how can they be engineered to do so. Developing new assays to directly assess *in vivo* graft-specific contractility is a critical area moving forward. Recent work has developed a novel strain sensor capable of directly visualizing actomyosin interactions[177]. While this technology is not yet directly

applicable to human cardiomyocytes, perhaps future generations of this technology can be combined with cell therapy to better understand the role of transplanted cells in active force generation. A second critical question that remains to be addressed is identifying the ideal maturation state of hPSC-CMs for cell therapy. While mature cells may produce more force, it remains to be seen whether these cells are capable of engrafting without significant cell death. Furthermore, these cells are likely less proliferative than their immature counterparts. Finding the proper balance between proliferation, survival, and functionality will be a critical step in moving forward towards a successful translational cell therapy.

Before these goals can be accomplished, however, we must first identify the intrinsic capabilities of hPSC-CMs to mature. Furthermore, it would be beneficial to also develop in parallel strategies to improve force generation independent of cellular maturity, so that even if the cardiac regenerative medicine is forced to use immature cells for survival and engraftment reasons, the force production capabilities of these cells can be maximized.

In the work presented in this dissertation, I present novel data to address these two critical points. First, in Chapter 2 I will describe the work I have completed in facilitating and evaluating the intrinsic maturation capabilities of hESC-CMs and hiPSC-CMs. This data suggests that hPSC-CMs from both hESC and hiPSC lineages can indeed recapitulate many key features of the adult cardiomyocyte phenotype, and it provides proof-of-principle for future studies aimed at streamlining this process for therapeutic

applications. Next, in Chapter 3 I describe the validation of a novel cardiac cell-based therapeutic approach that takes advantage of the intrinsic cardiac communication system – gap junctions – to deliver a biological inotropic agent throughout the myocardium. Taken together, this work represents two unique and complementary approaches to improving the functionality of future cardiac cell therapies and may one day aid in treating the devastating disease of heart failure.

Chapter 2. Structural and Functional Maturation of Cardiomyocytes Derived From Human Pluripotent Stem Cells

Summary

Despite preclinical studies demonstrating the functional benefit of transplanting human pluripotent stem cell-derived cardiomyocytes (PSC-CMs) into damaged myocardium, the ability of these immature cells to adopt a more adult-like cardiomyocyte phenotype remains uncertain. To address this issue, we tested the hypothesis that prolonged in vitro culture of human embryonic (hESC) and human induced pluripotent (hiPSC) stem cell-derived cardiomyocytes would result in the maturation of their structural and contractile properties to a more adult-like phenotype. Compared to their early stage counterparts (PSC-CMs after 20-40 days of in vitro differentiation and culture), late stage hESC-CMs and hiPSC-CMs (80-120 days) showed dramatic differences in morphology, including increased cell size and anisotropy, greater myofibril density and alignment, sarcomeres visible by brightfield microscopy, and a 10-fold increase in the fraction of multinucleated cardiomyocytes. Ultrastructural analysis confirmed improvements in myofibrillar density, alignment, and morphology. We measured the contractile performance of late stage hESC-CMs and hiPSC-CMs and found a doubling in shortening magnitude with slowed contraction kinetics compared to early stage cells. We then examined changes in the calcium handling properties of these matured

cardiomyocytes and found an increase in calcium release and reuptake rates with no change in maximum amplitude. Finally, we performed electrophysiological assessments in hESC-CMs and found late-stage myocytes have hyperpolarized maximum diastolic potentials, increased action potential amplitudes, and faster upstroke velocities. To correlate these functional changes with gene expression, we performed qPCR and found a robust induction of key cardiac structural genes including β-MHC and Cx43 in late stage hESC-CMs and hiPSC-CMs. These findings suggest that pluripotent stem cell-derived cardiomyocytes are capable of slowly maturing to more closely resemble the phenotype of adult cardiomyocytes and may eventually possess the potential to regenerate lost myocardium with robust de novo force-producing tissue.

Introduction

The loss of viable myocardium due to ischemic or other pathologic insult often leads to insufficient cardiac performance to maintain end-organ perfusion, a condition known as heart failure. Cell therapy represents a promising strategy to halt or reverse the progression of this disease, and a number of candidate cell types have been investigated in both pre-clinical and clinical studies with mixed success [178-181]. Pluripotent stem cell-derived cardiomyocytes (PSC-CMs), including human embryonic stem cell-derived (hESC-) and human induced pluripotent (hiPSC-) derived cardiomyocytes (CMs), offer a number of advantages for cell-based cardiac repair, but most *in vivo* studies to date have shown only partial or transient restoration of contractile function [94,98,182,183]. One potential explanation is the underdeveloped

contractile properties of PSC-CMs, which lack the robust contractile machinery found in mature adult cardiomyocytes and instead resemble primitive cardiomyocytes [73,74,89,124,125,184]. Even if PSC-CMs successfully engraft in the infarcted heart, it seems unlikely that in their current form, they possess the ability to replace the force-generating capacity of the mature myocardium lost during the initial insult. On the other hand, it is possible that enhancing the force production capabilities of PSC-CMs could result in a more robust and permanent improvement in cardiac function following cell transplantation.

A number of recent studies have examined the maturation of pluripotent stem cell-derived cardiomyocytes towards the adult phenotype [86,184-186], but the majority of these studies have focused primarily on electrophysiological endpoints. While these reports have demonstrated that hESC-CMs are capable of some degree of phenotypic maturation, it remains to be seen whether comparable improvements in structural and contractile properties are possible. Additionally, while some initial efforts to characterize hESC-CM contractility have been performed, they have primarily focused on aggregate properties of embryoid bodies or tissue engineered constructs containing variable cell numbers and densities [123,148]. To the best of our knowledge no studies to date have examined the effects of prolonged in vitro culture on the contractile and structural maturation of either hESC- or hiPSC-CMs. To resolve these uncertainties, we tested the hypothesis that both hESC- and hiPSC-CMs would show enhanced structural organization and functional performance over time, and that these changes are readily apparent at the resolution of the single cell. To accomplish this, we developed a long-

term culture protocol capable of supporting highly purified PSC-CM development for over 150 days in vitro. Compared to early stage hESC-CMs, these late stage hESC-CMs exhibit increased functional performance as measured by contractile, calcium transient, and electrophysiological endpoints. hiPSC-CMs subjected to the same protocol demonstrated similar levels of morphological maturation and identical improvements in contractile performance. Finally, both hESC-CMs and hiPSC-CMs displayed a remarkable upregulation in expression of key cardiac structural genes, most notably β-myosin heavy chain, to similar levels found in adult human heart. To our knowledge, this represents the first study to measure and demonstrate meaningful long-term enhancement in the contractile and structural properties of individual hESC-CMs and hiPSC-CMs to levels approaching those found in adult cardiomyocytes. Our results suggest that these cells may possess the capability to generate new force producing units and perhaps prevent heart failure upon transplantation.

Methods

PSC Maintenance and Guided Cardiac Differentiation. All experiments were approved by the University of Washington Embryonic Stem Cell Research Oversight Committee (ESCRO) and conducted using the H7 (NIHhESC-10-0061) and RuES-2 (NIHhESC-09-0013) hESC lines and the iMR90 hiPSC (WiCell) line. PSCs were maintained and differentiated as previously described [94]. Briefly, PSCs were cultured in feeder free conditions on Matrigel-coated plates (BD Biosciences) and fed with mouse embryonic fibroblast-conditioned medium (MEF-CM) supplemented with 4ng/mL basic fibroblast

growth factor (bFGF). Prior to cardiac differentiation, cells were passaged using versene-EDTA and replated at a density of 175,000 cells/cm^2. To induce cardiogenesis, we replaced the MEF-CM with RPMI-B27 (Gibco) supplemented with L-glutamine, Matrigel, and 10μg/mL recombinant human activin A (R&D Systems). After 24 hours the media was switched to RPMI-B27 supplemented with L-glutamine and 100ng/mL recombinant human bone morphogenetic protein-4 (BMP-4, R&D Systems). Four days later, the media was aspirated and cells were subsequently fed every 3-5 days with RPMI-B27 containing L-glutamine. Cells typically began beating spontaneously on approximately day 14 post-induction.

hESC-CM Maturation. Glass coverslips (Corning) were prepared by overnight treatment with 0.1% polyethyleneimine (PEI)(Sigma) at 4C, rinsed thoroughly with PBS, and incubated with 0.67% gelatin (Sigma) overnight at 4C. After 20 days of in vitro differentiation, PSC-CMs were dispersed using 0.05% trypsin-EDTA and replated at 30,000 cells/cm^2 onto the PEI-gelatin glass coverslips. Cultures were fed every other day thereafter with serum-free RPMI-B27 plus L-glutamine. Only cell preparations containing >75% cardiac troponin T+ (cTnT+) cardiomyocytes (by flow cytometry) were used for these experiments, and any cultures exhibiting non-cardiac cell overgrowth were excluded from analysis. Cultures were monitored daily for signs of contractile structure organization and the emergence of sarcomere banding.

Optical contraction analysis. Cells were visualized using a Nikon TS100 inverted microscope coupled to an Ionoptix videomicroscopy system (Ionoptix). Only isolated

contracting hESC-CMs were chosen for analysis. Prior to measurement, cells were placed in a stimulus chamber containing HEPES-buffered Tyrode's solution and maintained at 25C for the duration of the experiment unless otherwise specified. Experiments requiring administration of pharmacological agents employed a rapid solution stepper setup with temperature control to keep perfusates at 37C. Traces were collected and analyzed using Ionwizard software, and a minimum of five traces were analyzed and averaged for each cell.

Electrophysiology. Electrophysiological endpoints were acquired as previously reported in detail [187]. All experiments were conducted using a HEKA EPC-10 patch clamp amplifier (HEKA Instruments) in current clamp mode. We recorded from isolated spontaneously beating hESC-CMs using pipettes with resistance of 2-4MΩ by establishing a gigaohm seal and recording using the traditional ruptured patch approach. All recordings were performed at 37C, and all data was analyzed using Patchmaster and IgorPro software.

Calcium Imaging. Intracellular calcium content was measured using the ratiometric indicator dye fura2-AM as described previously [26]. In brief, cells were incubated in 1μM fura2-AM dye for 20 minutes at 37° C and washed with PBS. Spontaneous Ca^{2+} transients were then monitored with the Ionoptix Stepper Switch system coupled to a Nikon inverted fluorescence microscope. The fluorescence signal was acquired using a 40x Olympus objective and passed through a 510 nm filter, and the signal was quantified using a photomultiplier tube.

Immunocytochemistry. Cells were fixed in 4% paraformaldehyde for 10 minutes and permeabilized using 0.25% Triton X-100 for 6 minutes. Fixed cells were blocked with 1.5% normal goat serum for one hour at room temperature and incubated overnight at 4C with primary antibody at 1:500. Antibodies used in this study include mouse anti-α-actinin (Sigma), mouse anti-cTnT (Abcam), rabbit anti-Cx43 (Thermo), rabbit anti-smooth muscle actin (Abcam), mouse anti-cytokeratin (Dako). Samples receiving actin staining were incubated with 1:50 FITC-labeled phalloidin (Sigma) for 5 minutes at RT. The samples were rinsed with PBS and incubated with secondary antibody (Alexa Fluor 488 or 594) at 1:500 for one hour at RT, rinsed, and cover-slipped using Vectashield containing DAPI (Vector Labs).

Imaging and Morphological Analysis. Brightfield and fluorescent images were acquired using a Zeiss AxioCam mounted to a Zeiss AxioObserver microscope, and confocal images were acquired using a Nikon A1R confocal microscope. Images were processed and exported using Adobe Photoshop, and image quantification was performed in ImageJ software using standard analysis plugins. Each cell was analyzed for average sarcomere length, cell area, cell perimeter, and cell circularity index.

Flow Cytometry. Cells were fixed in 4% paraformaldehyde for 10 minutes and incubated with 1:100 anti-cTnT or isotype control mouse IgG (eBioscience) in 0.75% saponin followed by visualization with goat anti-mouse conjugated to phycoethryin. Samples

were run on a BD Sciences FACS Canto flow cytometer and analyzed using FlowJo software.

Quantitative PCR. Total RNA was isolated using the Qiagen RNeasy kit, and mRNA was reverse transcribed using the Superscript III first-strand cDNA synthesis kit (Invitrogen). All primers were purchased from Real Time Primers, and qPCR was performed using SYBR green chemistry and an ABI 7900HT instrument. Samples were normalized using GAPDH as a housekeeping gene.

Transmission Electron Microscopy. Cells were fixed overnight in ½ strength Karnovsky's (2% Paraformaldehyde/2.5% glutaraldehyde buffered with 0.2M cacodylate) and post-fixed in 2% OsO_4 buffered in 0.2M cacodylate buffer. Following dehydration, cells were embedded in Epon 812 (Electron Microscopy Sciences), thin sectioned (70nm), and stained with uranyl acetate for 2 hours and lead citrate for 5 min. Samples were imaged using a JEOL 1230 transmission electron microscope set to 80kV and images were captured using a Gatan digital imaging system.

Statistical Analysis. All data is presented as mean ± S.E.M. All data was compiled in Microsoft Excel and normal parameter distributions were confirmed using the Shapiro-Wilk test for normality. All statistical tests were performed using a 2-tailed Student's t-Test with unequal sample variance or Fisher's exact test for proportions.

Results

hESC-CMs can be differentiated with high purity and grown in long term culture

hESCs were maintained and differentiated as previously described (**Fig. 2.1A**) [94]. Approximately 14 days after induction, cultures began displaying a contractile phenotype, and flow cytometry analysis of representative cultures at the time of replating on day 20 indicated a cardiomyocyte purity of 86.6 ± 6.14% as measured by cardiac Troponin T (cTnT+) staining (**Fig. 2.1B**). At this point, the cells were enzymatically dispersed and replated at low density onto coverslips coated with PEI and gelatin and maintained for up to six months. This PEI/gelatin substrate appeared to improve cardiomyocyte purity by favoring their initial adhesion at the day 20 replating step, and 99.6±0.1% of cells exhibited cTnT+ immunostaining by the late stage time point (**Supplemental Fig. 2.1C**). 10.1±1% of cells also co-stained for smooth muscle α-actin in either fibril or sarcomere staining patterns (**Supplemental Fig. 2.1A-B**). We also stained for cytokeratin, an epithelial marker. Interestingly, while we found only exceedingly rare cytokeratin+ cells, the latter also co-expressed cTnT in the typical striated sarcomere pattern (**Supplemental Fig. 2.1D-F**).

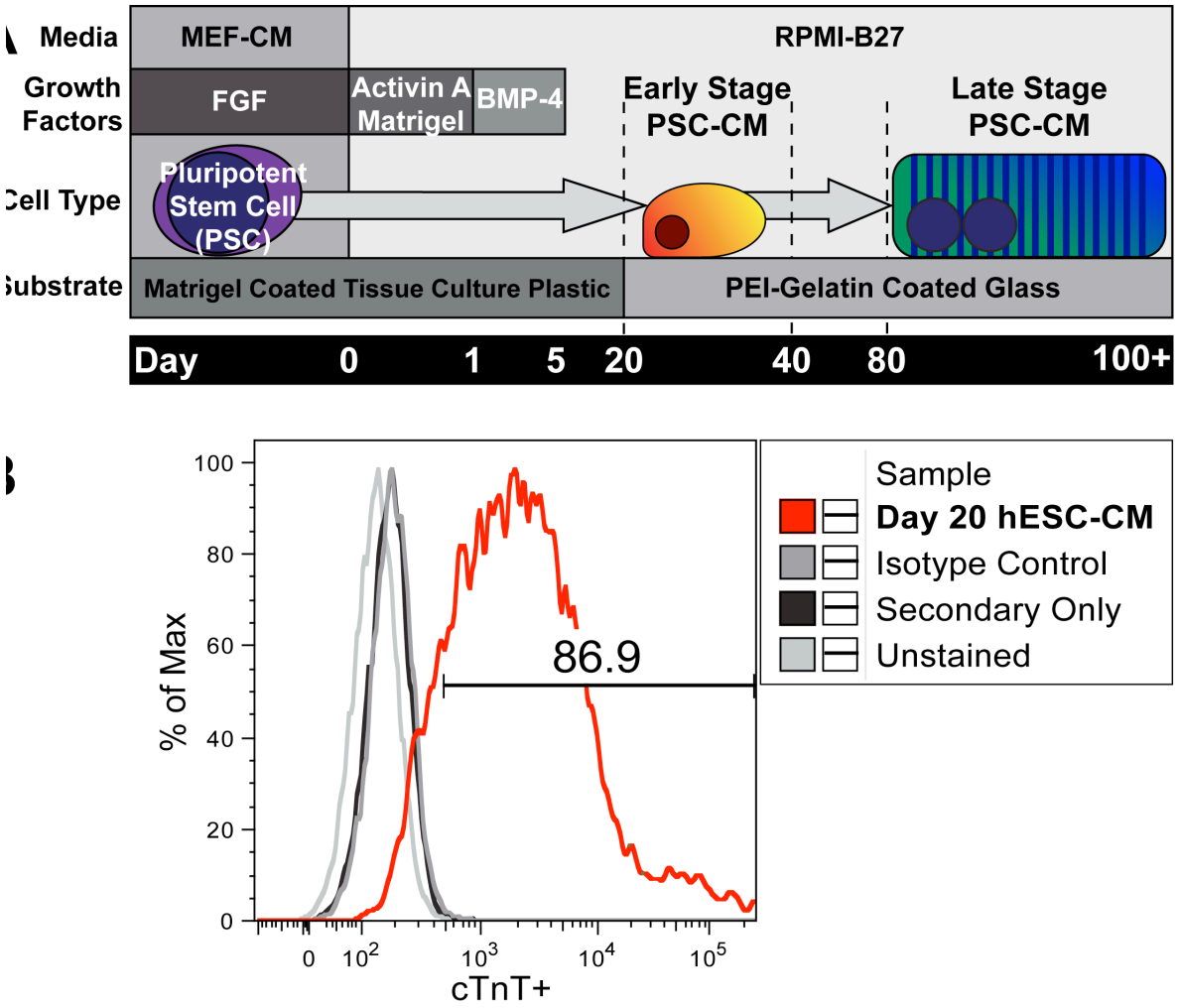

Figure 2.1 Differentiation and maturation scheme for early and late stage cardiomyocytes from pluripotent stem cells.

.) hESC and iPSCs were maintained in mouse-embryonic fibroblast conditioned medium **IEF-CM**) supplemented with fibroblast growth factor (**FGF**) and differentiated into rdiomyocytes by serial treatment with Activin A and BMP-4. Spontaneous beating activity pically commenced by day 14. On day 20, PSC-CMs were replated onto glass coverslips ated with PEI-gelatin and then maintained for up to 6 months in culture. We classified lls between days 20-40 as "early stage" PSC-CMs and cells between days 80-100 as "late age" PSC-CMs. **(B)** Representative flow cytometry analysis of hESC-CMs at day 20

hESC-CMs slowly grow in size and contractile apparatus organization

Following replating, cultures were examined at regular intervals for changes in morphology. hESC-CMs and hiPSC-CMs between 20 and 40 days post-induction were

categorized as “early stage.” While typically exhibiting spontaneous contractile activity, early stage myocytes appeared as small, rounded cells lacking any discernible organized cardiac structure when viewed by phase contrast microscopy (**Fig. 2.2A**).

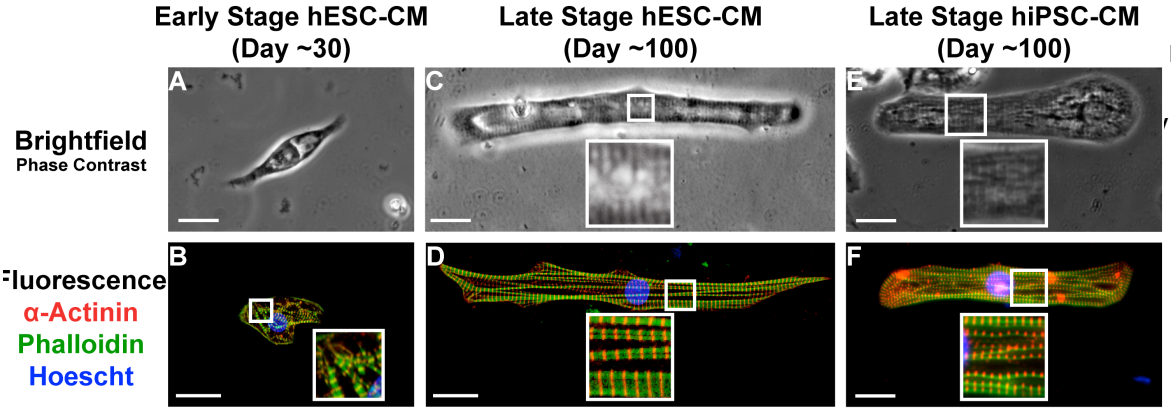

igure 2.2 Long-term culture induces significant changes in hESC-CM and hiPSC-CM morphology

.) By phase contrast microscopy, early stage hESC-CMs were round and lacked any scernable sarcomeric elements. (**B**) Cells at this stage were fixed and stained for α-tinin+phalloidin and showed irregular subcellular organization and low myofibril density.) In contrast, late stage hESC-CMs demonstrated sarcomeres clearly visible by phase ntrast microscopy and (**D**) a high degree of myofibril density, alignment, and z-disk gistration. (**E**) Late stage iPSC-CMs demonstrated similar enhancements by phase ntrast imaging and (**F**) immunocytochemistry. Scale bar 25 μm

revealed poorly

and orientation

and variable z-disc alignment (**Fig. 2.2B**). Over the course of the next 2 months, PSC-CMs slowly altered their appearance by becoming larger, more elongated, and less circular. Between day 80-100, cells began exhibiting signs of contractile machinery organization along their entire length under phase contrast microscopy. These cells demonstrated repetitive banding patterns characteristic of organized sarcomeres with good registration across the entire width of the cell. hESC-CMs and hiPSC-CMs between days 80 to 120 of in vitro development were termed “late stage” cells (**Fig. 2.2C-F**). Quantitative immunocytochemical analysis of late stage hESC-CMs

demonstrated dramatic maturation in their morphology and immunophenotype (**Fig. 2.3A**). The percentage of multinucleated cardiomyocytes, which ranges from 25% to 57% in adult myocardium [188,189], increased from 4.2% in early stage hESC-CMs to 35.3% in late stage hESC-CMs (**Fig. 2.3B**) ($p<0.001$). Compared to their early stage counterparts, late stage hESC-CMs showed increased cell area (480 ± 32μm^2 vs. 1716 ± 150μm^2, $p<0.001$) and perimeter (131 ± 32μm vs. 284 ± 15μm, $p<0.001$), as well as a decrease in circularity index (0.38 ± 0.02 vs. 0.28 ± 0.02, $p<0.01$)(**Fig. 2.3D-F**). In addition, late stage hESC-CMs demonstrated a dramatic increase in the density and alignment of myofibrils throughout the cytoplasm of the cell. Importantly, these cells had a far greater number of aligned myofibrils in register, as evidenced by an increase in the width of continuous Z-bands in both brightfield and confocal microscopy. Finally, the resting sarcomere length (measured by the distance between z-disks) increased from 1.65 ± 0.02μm in early stage hESC-CMs to 1.81 ± 0.01μm ($P<0.001$) in late stage hESC-CMs (**Fig. 2.3C**). Despite these dramatic phenotypic changes, however, we failed to identify any clear t-tubule formation by Di-8-ANEPPS or wheat germ agglutinin membrane staining (data not shown). We did, however, see robust expression in late stage cells of the gap junction protein connexin-43, which localized to the perinuclear region and to the periphery of the cell (**Supplementary Fig. 2.2**).

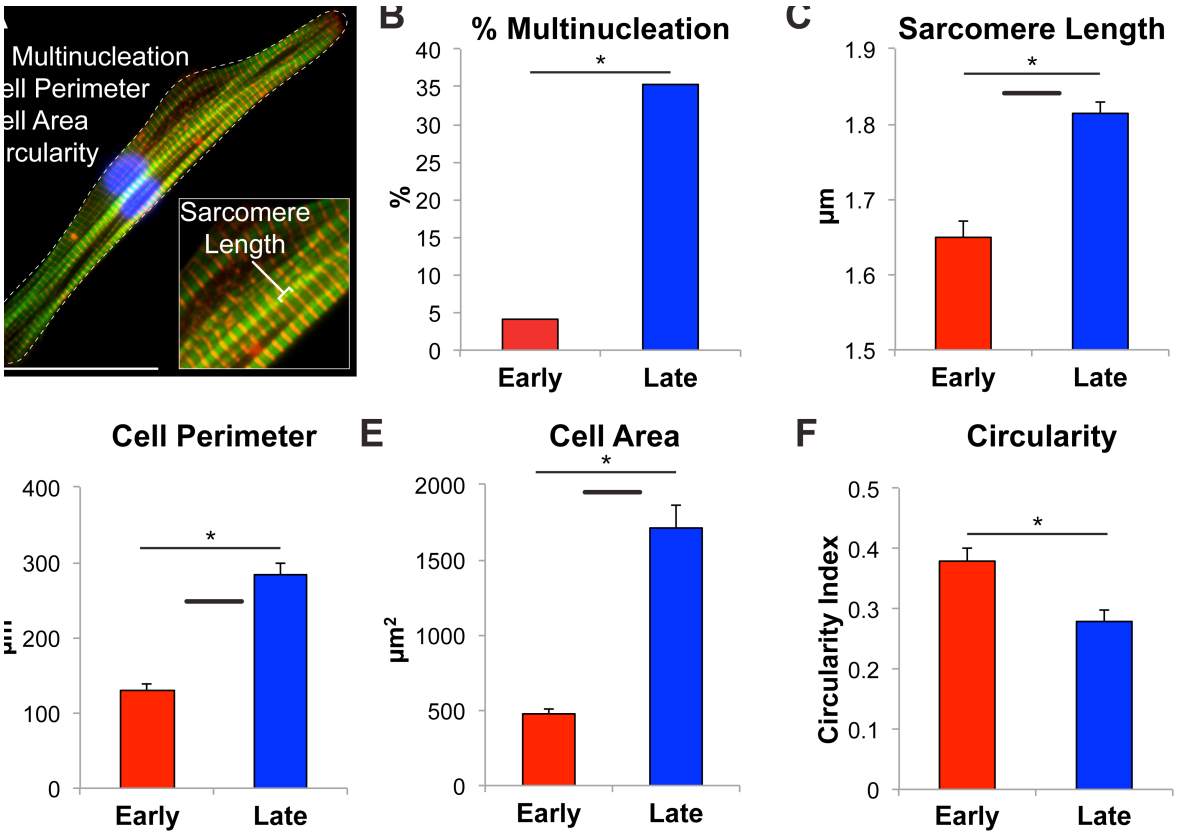

Figure 2.3 Late stage hESC-CMs recapitulate many features of adult human cardiomyocyte morphology

.) Fixed and stained cells were imaged using fluorescence microscopy and quantitatively alyzed. Scale bar 50 µm. (**B**) Compared to early stage hESC-CMs, late stage hESC-CMs monstrated significant changes in multinucleated cell fraction, **(C)** sarcomere length **(D)** ll perimeter, (**E**) cell area, and (**F**) circularity index**.** These numbers compare favorably with eviously reported values for these parameters in adult human ventricular cardiomyocytes[27], dicated graphically by the solid black reference lines. n=24-34 per condition. *p<0.05 vs. rly stage hESC-CMs.

Ultrastructural analysis shows increased organization in late stage hESC-CMs

The ultrastructural elements underlying these morphological changes were analyzed by transmission electron microscopy (TEM). Images obtained from early stage hESC-CMs suggest highly underdeveloped contractile machinery composed of misaligned myofibrils at low density (**Fig. 2.4A**). Higher magnification of these myofibril bundles

demonstrated punctate electron-dense aggregates previously described as “Z-bodies” [190,191] rather than the more mature, linear z-disks found in adult cardiomyocytes (**Fig. 2.4B**). Spanning between these structures were thick filaments composed of myosin at relatively low density. In contrast, late stage hESC-CMs showed significant improvements in myofibril alignment, density, and morphology (**Fig. 2.4C**). Highly aligned myofibrils ran parallel to the long axis of the cell and were interspersed with larger quantities of mitochondria. Investigation of single sarcomeres in late stage cells (**Fig. 2.4D**) showed an adult-like appearance of Z-disks in register, A- and I-bands, and H-zones but no clear M-band. Ultrastructural studies revealed additional evidence of greater structural maturation in the late-stage myocytes, including the presence of fascia adherens (**Supplementary Fig. 2.3A**), gap junctions (**Supplementary Fig. 2.3B**), and mitochondria with prominent cristae located adjacent to myofibril bundles (**Supplementary Fig. 2.3C**). On the other hand, we found no clear examples of t-tubule formation at the ultrastructural level, though the cells did show scalloping of the sarcolemma in register with the z-disks (**Supplementary Fig. 2.3D**).

PSC-CM contractile performance improves during long term culture

We next used optical video microscopy to track developmental changes in the contractile properties of hESC-CMs and hiPSC-CMs (**Fig. 2.5**). Early stage PSC-CMs lack visible sarcomeres, so we quantified contractile performance by monitoring changes in cell length. Similar cell length measurements were also made in late stage hESC-CMs (**Supplementary Fig. 2.4**), but a better measure of contractile performance is to monitor sarcomere length changes during contraction, which has been shown

previously to correlate well with whole cell contractility [192]. The magnitude of contraction

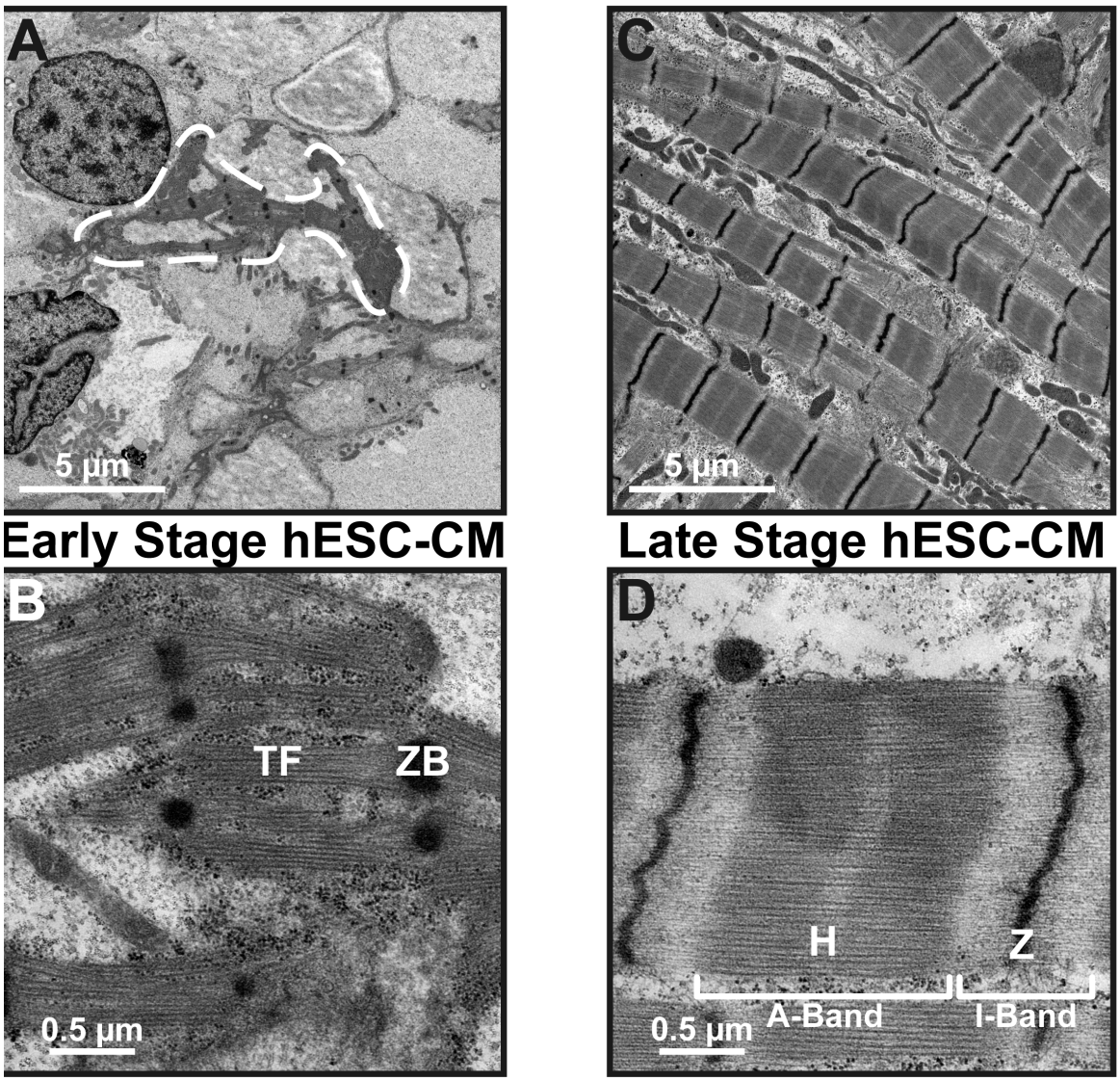

4.95 ± 0.68%

p<0.0001) and

Figure 2.4 Late stage hESC-CMs demonstrate dramatically increased ultrastructural organization

A) Transmission electron microscopy images of early stage hESC-CMs at low magnification ow fragmented myofibrils at low density (outlined by the white dashed line). (**B**) Higher agnification images reveal fragmented Z-disks called Z-Bodies (**ZB**) and irregularly-spaced ick filaments (**TF**). (**C**) In contrast, late stage hESC-CMs at low magnification show high ensity of organized and aligned myofibrils. (**D**) Sarcomeres under high magnification show ear aligned Z-disks (**Z**) and organized A- and I-bands with a clear H zone (**H**).

10.17 ± 1.35% (p<0.01) of resting sarcomere length for late stage cells (**Fig. 2.5B**). Additionally, late stage hESC-CMs and hiPSC-CMs exhibited slightly slower contractile kinetics, including time to 50% peak contraction (p<0.05) and time to peak contraction (p<0.05) (**Fig. 2.5C**). There was no difference in rate of spontaneous contraction between early and late stage hESC-CMs. To confirm these results in an independent hESC population, we also performed contractility analysis experiments in a second line

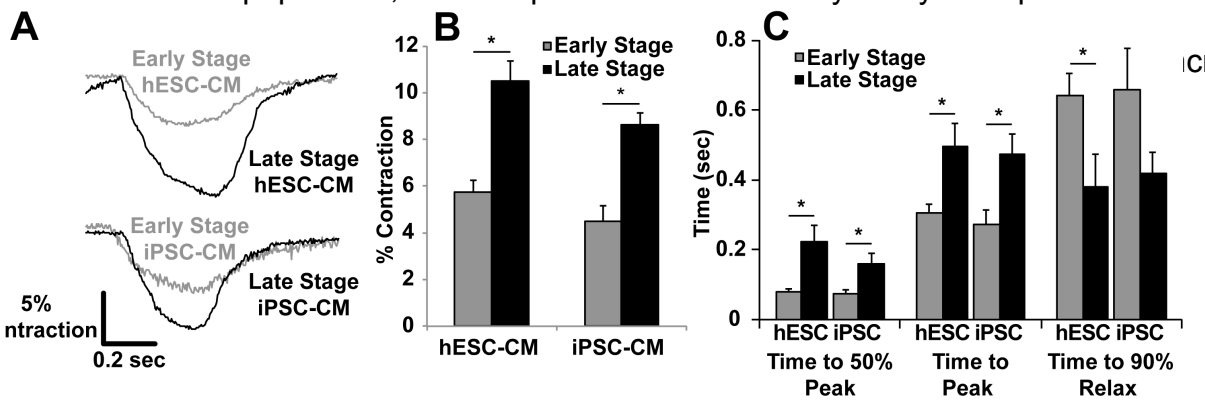

creases in late

Figure 2.5 Late stage hESC-CMs and hiPSC-CMs demonstrate increased contractile performance with slowed kinetics

.) Spontaneous contractions of early stage cells and late stage cells were obtained using ıtical videomicroscopy. (**B**) Quantitative analysis revealed that early stage hESC-CMs and SC-CMs contract approximately 5% of their resting length, while late stage hESC-CMs and SC-CMs exhibit contractions roughly twice as large in magnitude. (**C**) In addition to creased contractile magnitude, late stage hESC-CMs and iPSC-CMs also contracted with owed kinetics compared to their early stage counterparts. Direct comparison between SC-CMs and hESC-CMs at early stage or late stage showed no statistical differences in ıy parameter. n=9-31 per condition *p<0.05

Late stage hESC-CMs demonstrate faster Ca^{2+} transient kinetics

To further investigate the mechanism underlying changes in the kinetics of contractility over time, we compared the $[Ca^{2+}]_i$ transient characteristics of early versus late stage

hESC-CMs (**Fig. 2.6**) using the ratiometric dye fura-2. While peak transient amplitude remained unchanged between early vs. late stage cells (0.22 ± 0.02 vs. 0.24 ± 0.02 F/F_0, p=0.47) (**Fig. 2.6B**), the maximal upstroke and decay velocities were significantly higher in late stage hESC-CMs (**Fig. 2.6C-D**), and the time to peak $[Ca^{2+}]_i$ was significantly shorter (342 ± 2ms vs. 102 ± 1ms, p<0.0001) for late stage cells (**Fig. 2.6E**). The kinetics of Ca^{2+} reuptake also changed over time in culture with late stage hESC-CMs, which demonstrated a faster Ca^{2+} transient decay as measured by the time to 50% relaxation (446 ± 3ms vs. 227 ± 2ms, p<0.001) (**Fig. 2.6F**).

Late stage hESC-CMs exhibit mature action potential characteristics

To assess whether the changes in structure and contractile function were accompanied by changes in action potential properties, we obtained current clamp recordings of early versus late stage hESC-CMs (**Fig. 2.7**). These studies demonstrated a dramatic increase in the maximal upstroke velocity (dV/dt max) from 44 ± 10.8 V/s in early stage hESC-CMs to 188.7 ± 12.6 V/s in late stage hESC-CMs (p<0.05) (**Fig. 2.7C**). Furthermore, when compared to early stage cells, late stage cells had more hyperpolarized maximum diastolic potentials (MDP, -57.3 ± 1.9 mV vs. -68.2 ± 2.1 mV respectively, p<0.05) and larger action potential amplitudes (APA, 94.1 ± 3.4 mV vs. 113.2 ± 2.8 mV, respectively, p<0.05) (**Fig. 2.7C**). There were no significant differences noted in action potential duration (measured at 50% and 90% of repolarization) parameters.

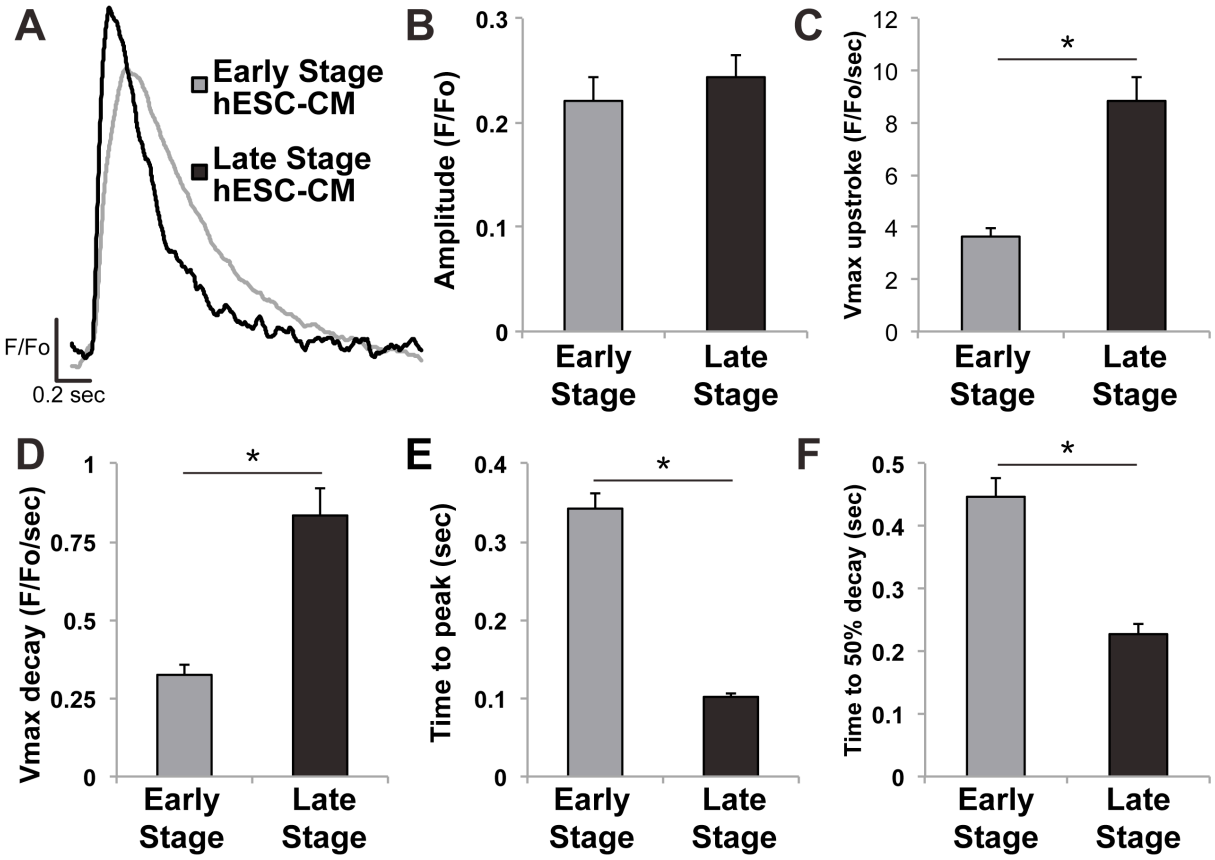

Figure 2.6 Late stage hESC-CMs exhibit increased calcium transient kinetics but no change in magnitude

Calcium transients were assessed in hESC-CMs loaded with the ratiometric indicator fura-2. (**A**) Representative fluorescence transients from early and late stage hESC-CMs. (**B**) Although transient amplitude magnitudes were similar, the kinetics were significantly different in late stage cells, as indicated by increases in maximal transient (**C**) upstroke and (**D**) decay velocities, reduced (**E**) time to peak $[Ca^{2+}]_i$, and (**F**) reduced time to 50% decay. n=6-7 per condition *p<0.05 vs. early stage hESC-CMs.

Late stage hESC-CMs retain adrenergic responsiveness

Previous reports have demonstrated that early stage hESC-CMs respond to adrenergic stimulation [82,151]. Therefore we tested whether late stage hESC-CMs retain this pharmacologic sensitivity by applying 10μM isoproterenol (ISO) and measuring changes in spontaneous frequency and contractility (**Supplemental Fig. 2.6**). ISO treatment

increased the spontaneous beating frequency of late-stage hESC-CM from 35.3 ± 4.4 bpm to 49.3 ± 3.5 bpm ($p<0.05$). ISO also elicited a 34.4 ± 2.7% reduction in contraction magnitude ($p<0.05$) with no change in the kinetics of contraction (time to peak contraction or time to 50% relaxation). The lack of positive inotropy is consistent

: in myofilament

-ate stage cells.

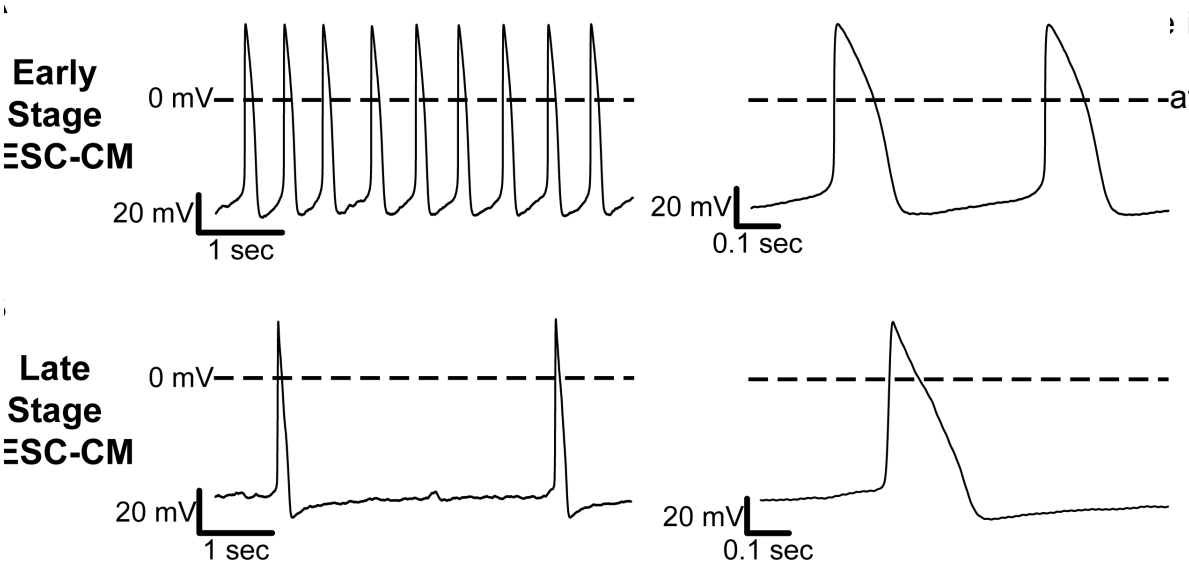

	dV/dt max (V/s)	APA (mV)	MDP (mV)	APD50 (ms)	APD90 (ms)	Rate (bpm)
arly Stage hESC-CM	44.0±10.8	94.1±3.4	-57.3±1.9	88.3±5.0	146.4±10.5	102.2±11.8
ate Stage hESC-CM	188.7±12.6*	113.2±2.8*	-68.2±2.1*	87.0±9.7	188.9±35.8	9.3±3.1*

Figure 2.7 Late stage hESC-CMs show significantly enhanced action potential upstroke and a hyperpolarized maximum diastolic potential

A) Representative recording of early stage hESC-CM action potentials demonstrates a latively high spontaneous beat rate. (**B**) Compared to early stage cells, late stage hESC-Ms demonstrated a slower rate and higher maximum upstroke velocity (**dV/dt**). (**C**) ompared to their early-stage counterparts, late stage hESC-CMs showed a hyperpolarized aximum diastolic potential (**MDP**) and a larger action potential amplitude (**APA**). There as no statistical change in either the time to 50% or 90% action potential duration (**APD50** **APD90**, respectively). n=5-11 per condition *$p<0.05$

Late stage PSC-CMs demonstrate changes in cardiac gene expression profile

We compared gene expression in early versus late stage PSC-CMs by quantitative RT-PCR for a panel of cardiac markers, and we also examined these same markers in adult human myocardium as a benchmark with a known level of maturation (**Fig. 2.8**). Consistent with the previously described changes in structural and functional endpoints, we observed substantial increases in the expression of cardiac genes in the late-stage myocytes, which in some cases approached levels observed in adult myocardium. For example, β-myosin heavy chain (MYH7) showed an 18-fold increase in expression in late stage hESC-CMs and 14-fold increase in late stage hiPSC-CMs over their respective early stage counterparts ($p<0.05$). In addition, there was a 15-fold and 8-fold increase in α-myosin heavy chain (MYH6) transcripts in late stage hESC-CMs and hiPSC-CMs, respectively ($p<0.05$). We also found significant increases in other genes, including connexin-43 (GJA1), HCN4 (If channel), and the Sarco-Endoplasmic Reticulum ATPase (SERCA2A) ($p<0.05$). Conversely, the expression of the fast Na^+ ion channel (SCN5A) and the K+ Inward Rectifier (KCNJ2) showed no difference in expression between early and late stages in either population.

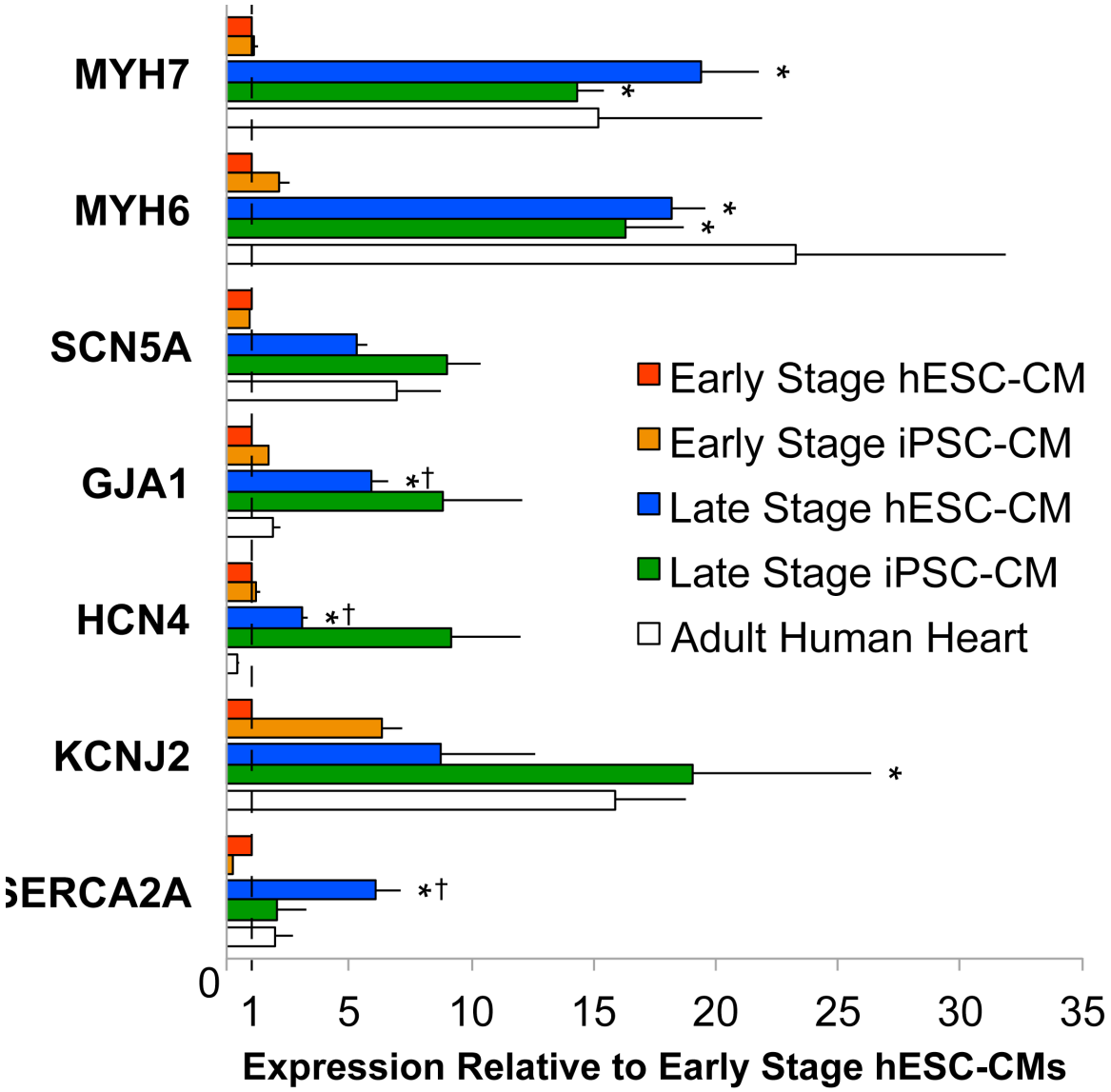

Figure 2.8 Late stage hESC-CMs and hiPSC-CMs robustly upregulate key cardiac structural and functional genes

ene expression levels for key cardiac genes were measured via qPCR and normalized to lues obtained for early stage hESC-CMs. Late stage hESC-CMs and iPSC-CMs (dark ay bars) demonstrated increased expression of **MYH7** (β-myosin heavy chain), **MYH6** (α-yosin heavy chain), **GJA1** (connexin-43), **HCN4** (hyperpolarization-activated K+ channel), id **SERCA** (sarco-endoplasmic reticulum ATPase). The majority of these transcript levels atch reasonably well to values observed in healthy adult human myocardium. n=3 per ndition *p<0.05 vs. corresponding early stage PSC-CMs. †p<0.05 vs. adult human heart.

Discussion

The production of large quantities of PSC-CMs offers an attractive option for regenerating *bona fide* human myocardium lost during myocardial infarction. However, for this strategy to provide maximal therapeutic benefit, the graft cells must recapitulate the structure and contractile performance of adult ventricular cardiomyocytes. Before this challenge can be fully addressed, it is important to assess the baseline time-course and maturation potential of PSC-CMs in vitro. We reasoned that prolonged duration in culture may be required to approach the maturation normally achieved by human heart, which develops over a gestational period of ~40 weeks and continues to mature for several years after birth[178]. To test this hypothesis, we developed a cell culture protocol capable of generating and maintaining highly purified hESC- and hiPSC-CMs for several months in vitro (**Fig. 2.1**). Our analysis was restricted to two time points, both to facilitate the examination of comprehensive structural and functional endpoints and because all preclinical transplantation work to date has employed cell preparations comparable to the early stage hESC-CMs and hiPSC-CMs (day 20-40) in this study [77,93-95,97]. While the late stage cultures described here showed dramatically altered phenotypic properties, it would also be of interest to examine even later time-points in future work. This, however, would be challenging in terms of experimental throughput.

In agreement with previously published reports[73-75], early stage hESC-CMs demonstrated poor subcellular organization and structural alignment, weak contractile performance, and relatively slow calcium release and reuptake kinetics. Over the subsequent weeks, however, these cells grew in size and elongated in shape.

Sarcomeres aligned along the long axis of the cell, and z-disks became regular and in register with neighboring myofibrils (**Fig. 2.2**). After 3-4 months in culture, essentially all cardiomyocytes exhibited an organized sarcomeric structure and approximately one-third were multinucleated (**Fig. 2.3**). Interestingly, these late-stage cardiomyocytes showed many morphological parameters (e.g. cell length, cell area, sarcomere length, etc) approaching values previously reported for adult human cardiomyocytes in culture [188,193]. Ultrastructural analysis confirmed the preceding findings made at the light microscopic level and revealed a highly ordered contractile apparatus with signs of mature cardiomyocyte structures, including dense myofibrils with clear A- and I- bands, fascia adherens, and gap junctions (**Fig. 2.4**). These cells can be stably cultured for at least six months, and they survive passaging (albeit with a transient loss of structural organization). To our knowledge, no one has previously described hESC-CMs or hiPSC-CMs with such a dramatic degree of structural maturation, even when exogenous pro-maturation stimuli (e.g. electromechanical conditioning) have been applied[184,194].

In addition to examining morphology and ultrastructure, we investigated the functional performance of late stage hESC-CMs and hiPSC-CMs and saw a robust increase in spontaneous contraction magnitude (**Fig. 2.5**). Interestingly, this increase in magnitude was accompanied by a slowing of contraction kinetics, a finding compatible with a switch in relative expression from the faster α isoform to the slower β isoform of myosin heavy chain. This hypothesis was supported by the robust induction of the gene encoding for β-MHC (MYH7) over early stage hESC-CMs. This finding could also be

explained by a shift down the force-velocity curve, as these late stage cells are more adherent and must contract against a greater perceived load than the comparatively unrestrained early stage cells. One limitation of the current study is the lack of true force production metrics, which could provide evidence for the latter possibility. Future studies would benefit from the development of a reliable method to accomplish force measurements that is compatible with the long-term culture of PSC-CMs on rigid substrates.

The changes in cell contractility were also accompanied by changes in Ca^{2+} handling properties. We found an increase in the kinetics of Ca^{2+} release and sequestration but no change in transient magnitude, suggesting a modest improvement in the calcium handling capabilities of late stage cells (**Fig. 2.6**). In prior work, our group has shown that hESC-CM populations equivalent to the early stage cells in this study have surprisingly mature mechanisms of excitation-contraction coupling and Ca^{2+} handling[87]. While we have shown that early stage cells do have intact SR Ca^{2+} cycling, the present finding of enhanced $[Ca^{2+}]_i$ transient kinetics in late stage cardiomyocytes proves there is still room for functional maturation in SR Ca^{2+} reuptake[87]. However, neither electron microscopy nor membrane staining using Wheat Germ Agglutinin or Di-8-ANNEPPS demonstrated definitive t-tubules in any developmental stage of hESC-CMs, which is consistent with previous reports[143,195].

In agreement with previously published work[86], late stage hESC-CMs in the present study showed significant changes to key electrophysiological parameters (**Fig. 2.7**).

The increased maximum diastolic potential may reflect the increased expression of KCNJ2, which underlies the I_{k1} current responsible for hyperpolarization. Prior work by Satin et al suggests that even early stage hESC-CMs have abundant voltage-dependent fast sodium current I_{Na}[88]. Given this and our finding of no significant change in SCNA5 expression, we speculate that the enhanced action potential upstroke in late-stage cardiomyocytes may result from the hyperpolarized maximum diastolic potential and a greater quantity of available Na^+ channels, rather than a direct increase in sodium channel content. Despite expectations to the contrary, late-stage cultures showed an increase in the expression of the HCN4, which underlies the I_f current of pacemaker cell types (**Fig. 2.8**). It is still unclear, however, whether the increase HCN4 is present in all cardiomyocytes or is restricted to a subset of the population.

While our late stage hESC-CMs exhibited a degree of structural and functional maturation exceeding levels previously reported, the exact identity of the mechanistic signals driving this maturation remains unknown. A previous study implicated undefined cues derived from "contaminating" non-cardiac cells in hESC-CM cultures, but these authors focused primarily on the maturation of electrophysiological parameters[185]. In contrast, we used highly enriched populations of cardiomyocytes cultured in a basal serum-free medium, indicating that PSC-CMs are capable of a substantial degree of structural and functional maturation in the absence of exogenous pro-maturation signals or significant numbers of non-cardiac cells. This apparent discrepancy may reflect other differences in culture conditions between the latter study and our own (e.g. serum-free versus serum-containing media) or the nature of the maturation endpoints examined.

A second candidate factor potentially driving PSC-CM maturation is the culture substrate itself. We were intrigued to observe such dramatic changes in cell shape and circularity index, given that the substrate chosen for these studies (PEI-gelatin coated glass) contained no anisotropic or directional cues. While others have previously demonstrated the ability of immature cardiomyocytes to align in response to patterned substrates[196-198] or nano-topographical cues[199,200], our data proves that immature cardiomyocytes possess the ability to self-organize and polarize in the absence of extrinsic directional cues. Again, the mechanisms underlying this phenomenon remain unidentified, but we speculate that mechanical mismatch between cell and substrate[201] and/or local changes in extracellular matrix[1-3] may act as potential driving factors for myofibrillogenesis. Indeed, a number of reports have demonstrated the importance of substrate stiffness on cardiomyocyte function and myofibrillogenesis. Kita-Matsuo et al demonstrated that immature cardiomyocytes, including hESC-CMs, respond favorably to softer physiological (kPa) substrates, while stiffer substrates (e.g. glass) caused the formation of stress fibers and inhibited myofibril formation[131,202]. Recent work by Rodriguez *et al* (2011), however, showed that neonatal rat cardiomyocytes exert greater twitch power when cultured on microposts of increased stiffness[137]. Moreover, Hazeltine *et al* (2012) found that when cultured on flexible substrates, early stage hESC-CM contractility increased as substrate stiffness increased[173]. The latter two reports correlate well with our findings in the present study, in which we observed an unprecedented degree of structural organization by hESC-CMs and hiPSC-CMs cultured on non-deformable glass coverslips with gPa range stiffness. Hence, while the

kinetics of myofibrillogenesis may be accelerated by the use of substrates of physiological stiffness, long-term culture on non-physiological, stiffer substrates clearly also supports morphological maturation, perhaps eventually to an even greater degree. Interestingly, the observations from developmental biology suggest that myofibrillogenesis is a dynamic process that begins with the formation of pre-myofibrils, which form at the periphery of cells at pro-costameres and resemble actin stress fibers in morphology and composition[203]. We speculate that while stiff substrates may initially result in the formation of stress fibers, long-term culture may allow these structures to convert to mature myofibrils to a greater degree. We have attempted to directly test this hypothesis, but so far have not been successful in culturing hESC-CMs on flexible substrates for long periods of time due to cell death and hESC-CM migration off of the flexible substrate. Hence, while driving structural maturation with culture on "infinitely" stiff substrates may be less physiological, this condition may still be exploitable as a practical approach for enhancing the structural and mechanical maturation of PSC-CMs.

In summary, we have developed a stable platform to study the morphological and functional changes in pluripotent stem cell-derived cardiomyocytes, and we have shown that hESC-CMs and hiPSC-CMs are capable of maturing to a phenotype that more closely resembles adult cardiomyocytes in both structure and function. The remarkable similarity in contractile performance maturation parameters between two independent hESC lines and one hiPSC line suggests that this is phenomenon is robust and cell line-independent. This study provides proof-of-concept and useful baseline data for future work aimed at elucidating the mechanisms underlying these morphological changes,

and we have described a platform that should serve as a useful tool for evaluating the effects of candidate hypertrophic or pharmacologic treatments. Finally, the results of this study provide hope that cell-based therapeutics may possess, at least in principle, the ability produce anisotropic force-producing muscle and perhaps one day can regenerate the contractile function of adult myocardium lost during the initial pathological insult.

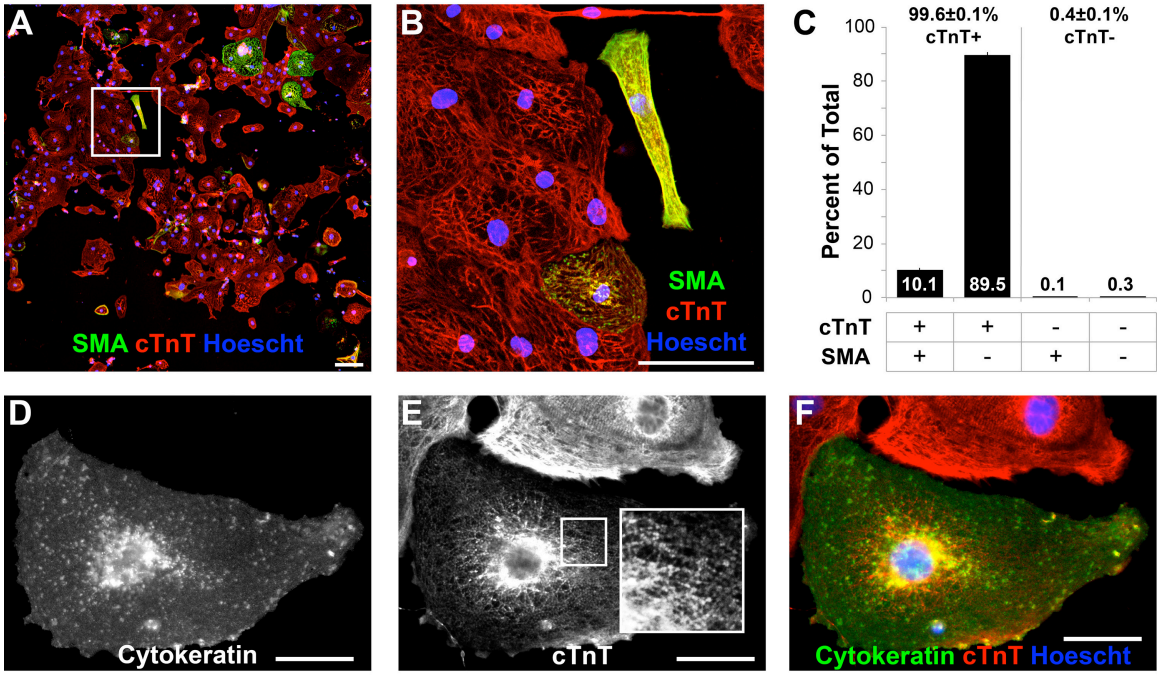

Supplemental Figure 2.1 Late stage hESC-CM preparations are highly enriched for cardiac markers, and a subset express other non-muscle markers

(**A**) Late stage hESC-CM preparations were stained for cardiac troponin T (**cTnT**) and smooth muscle α-actin (**SMA**). (**B**) SMA appeared in cells as either fibrillar or as punctate regions associated with myofibrils. (**C**) Quantification of these samples demonstrated >99% cTnT+ cells, 10% of which co-expressed SMA. (**D-F**) Cytokeratin staining demonstrated exceedingly rare positive cells, all of which co-expressed cTnT in the characteristic myofibrillar morphology. n=3. Scale bar 50μm

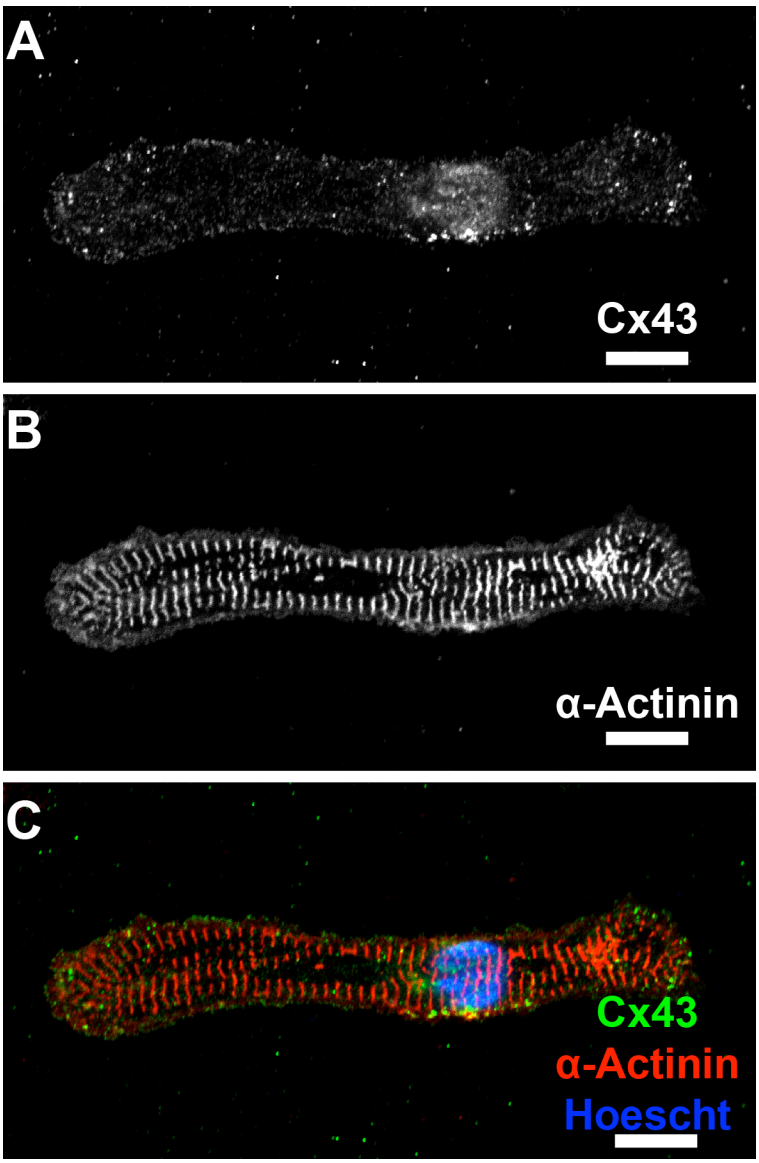

Supplemental Figure 2.2 Late Stage hESC-CMs demonstrate localized peripheral Cx43 expression.

(**A-C**) Late stage hESC-CMs stained positively for Cx43, which localized primarily to the perinuclear region and lateral long axis margins. Scale bar 25μm.

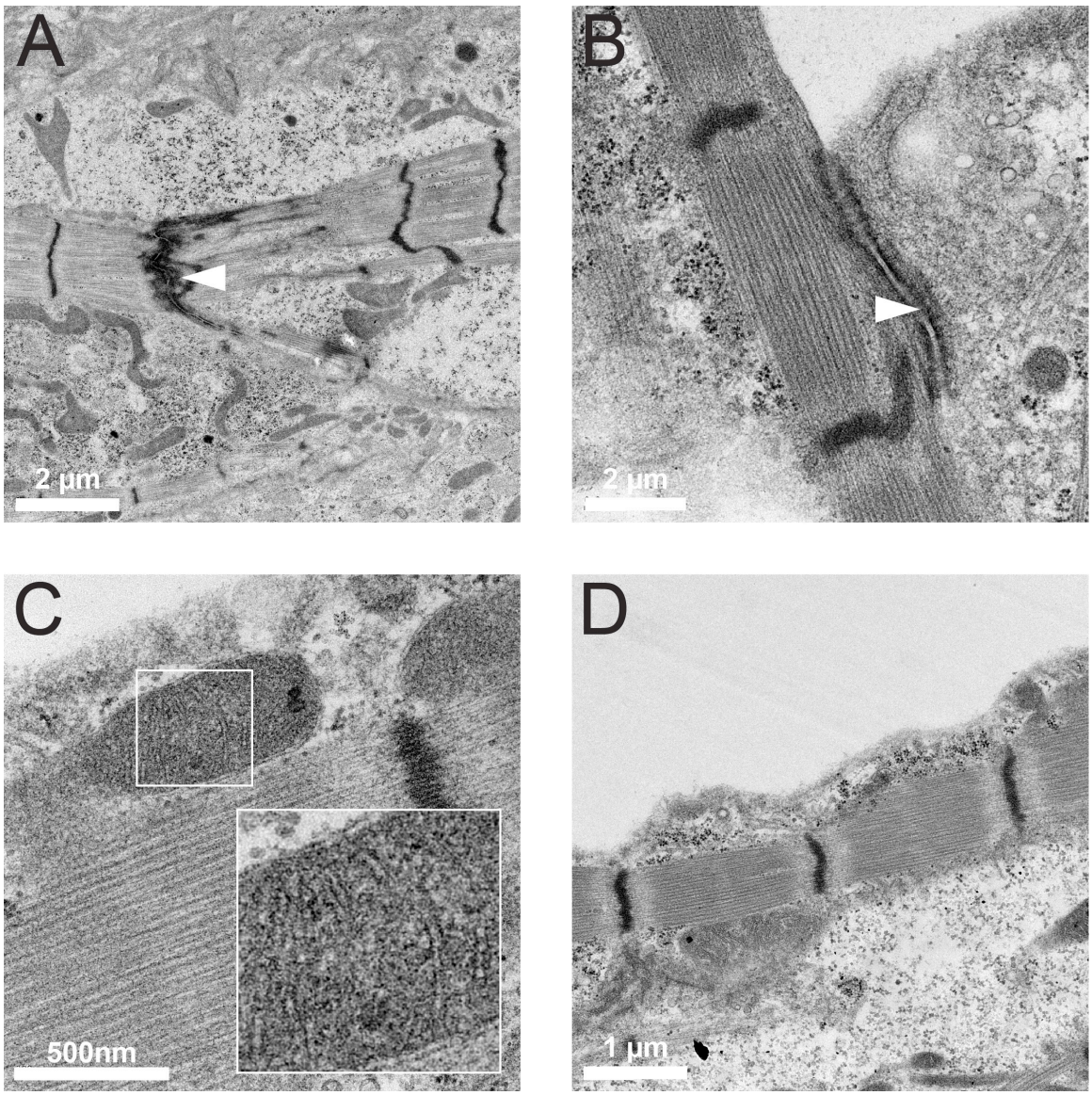

Supplemental Figure 2.3 Late Stage hESC-CM ultrastructural characteristics.

(**A**) Detailed ultrastructural analysis of Late Stage hESC-CMs demonstrated fascia adherens between myofibrils in series, (**B)** transverse gap junctions between neighboring cells**, (C)** mitochondria with numerous cristae located adjacent to sarcomeric structures, and (**D**) repetitive membrane scalloping in register with z-disks.

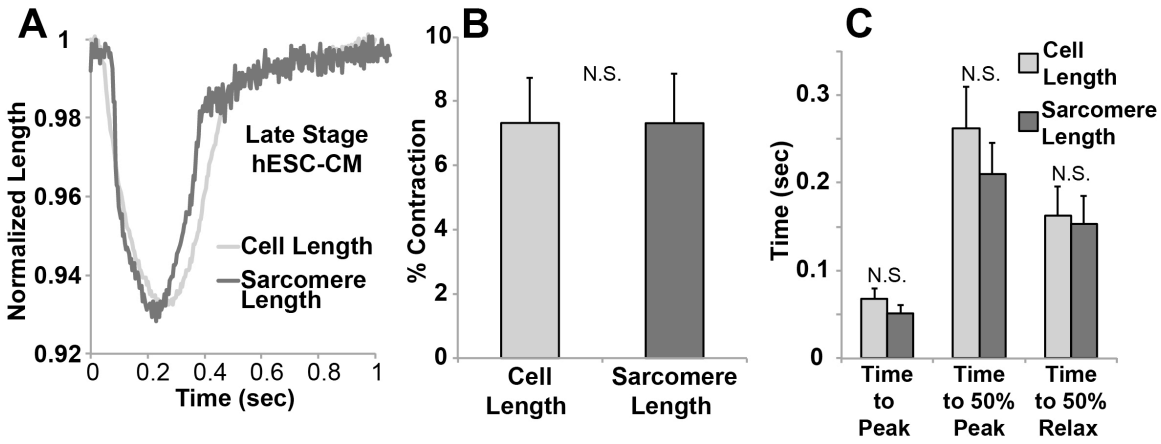

Supplemental Figure 2.4 Late Stage hESC-CM cell and sarcomere contractility comparison shows no apparent differences.

Both sarcomere and cell length contractility measurements were performed on a subset of late stage hESC-CMs at 37C. (**A**) Representative traces demonstrated similar waveform morphology, and quantification of these traces yielded no statistical differences in (**B**) the magnitude or (**C**) the kinetics of contraction. n=7 per condition.

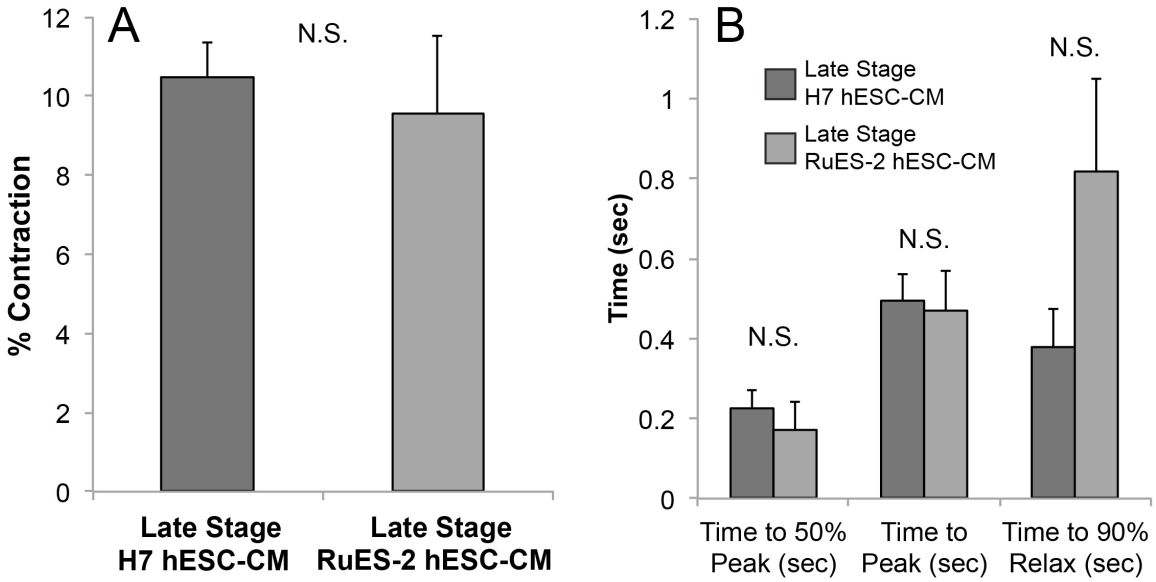

Supplemental Figure 2.5 Contractile maturation is similar between two independent hESC lines.

RuES-2 cells were differentiated and matured, and the contractile performance of late stage CMs from H7 and RuES2 hESC-CMs were compared. No statistical differences were found in contraction (**A**) magnitude or (**B**) kinetics. n=5-20 per condition.

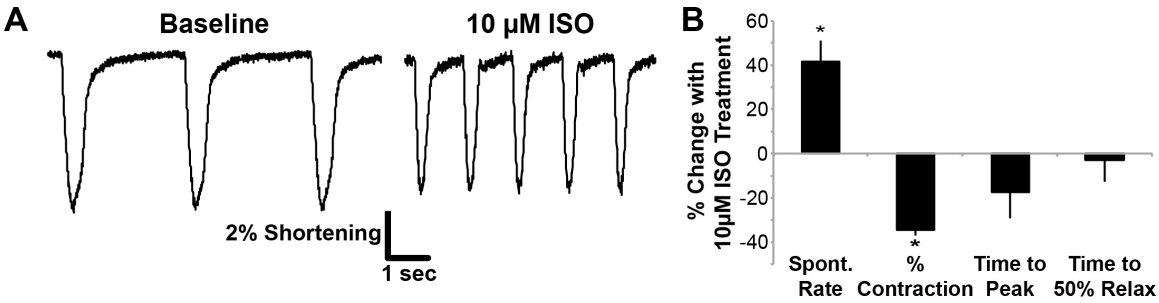

Supplemental Figure 2.6 Late Stage hESC-CMs respond to adrenergic stimulation with positive chronotropy and negative inotropy.

Late stage hESC-CMs were placed in a temperature-controlled perfusion system and subjected to pharmacologic treatments. (**A**) Administration of 10μM isoproterenol (ISO) resulted in a positive chronotropic and negative inotropic response. (**B**) Quantification of these parameters demonstrated a 40% increase in spontaneous rate and a 30% decrease in contraction magnitude, with no change in the kinetics of contraction as measured by the time to peak contraction or to 50% relaxation. n=3

Chapter 3. Engineered Pluripotent Stem Cells as a Novel Inotropic Cardiac Therapy

Summary

The transplantation of pluripotent stem cell-derived cardiomyocytes is a promising strategy to treat myocardial infarction and reverse heart failure, but to date most studies have failed to demonstrate meaningful long-term improvements in cardiac function. The Regnier lab (UW Bioengineering) has previously shown that 2-deoxyadenosine triphosphate (dATP), the ubiquitous nucleotide used in DNA synthesis, can replace ATP as an energy substrate for cardiac myosin and can increase maximal shortening velocity, maximal force, and Ca^{2+} sensitivity of force. When [dATP] is increased in adult cardiomyocytes via overexpression of the enzyme ribonucleotide reductase (R1R2), contractile performance is increased with no change in Ca^{2+} transient magnitude. Importantly, these effects occurred with [dATP] accounting for only 1.5% of the total cellular adenine nucleotide content, suggesting that small amounts of dATP can facilitate large enhancements in contractility via the cooperative nature of muscle.

In preliminary *in vivo* R1R2 overexpression studies, we noted that cardiac performance was enhanced disproportionately compared to the relatively modest number of successfully transduced cardiomyocytes. As ATP and other small metabolites are known to diffuse between cells via gap junctions[204,205], we hypothesized that dATP also

diffuses between cells via gap junctions, and that transplantation of a small population of dATP overproducing cells would improve global cardiac performance via the delivery of dATP throughout the host myocardium.

To test this hypothesis, we performed collaborative studies with the goals of (1) validating gap junction-mediated dATP transfer and (2) investigating the use of R1R2-overexpressing human embryonic stem cell-derived cardiomyocytes (hESC-CMs) as a novel cardiac therapeutic strategy. We first performed intracellular dye transfer studies using dATP conjugated to fluorescein and demonstrated rapid gap junction-mediated transfer between cardiomyocytes. We then used coculture assays to demonstrate enhanced contractile performance in WT cardiomyocytes coupled to cells overproducing dATP. Finally, we transplanted hESC-CMs overexpressing R1R2 into healthy uninjured rat hearts and noted an increase in fractional shortening from 41±4% to 53±5% five days after cell transplantation. These findings suggest that transplantation of dATP-producing stem cell-derived cardiomyocytes may provide a novel strategy to directly enhance cardiac function.

Introduction

Cardiovascular disease is the leading cause of death worldwide[206], and current treatments to address the growing problem of heart failure are limited to drugs to slow disease progression or pump replacement. New approaches, including new pharmacologic agents and cell- or gene-based strategies, have generated substantial

scientific interest for their potential to halt or reverse the deleterious effects of heart failure, but each of these strategies is also associated with potential challenges to clinical translation. New pharmacologic compounds such as Ca^{2+} sensitizers provide potent inotropic benefits, but clinical trials thus far have failed to definitively show a decrease in all-cause mortality in patients with acute heart failure[11]. Myosin activators such as omecamtiv mecarbil offer the opportunity to improve cardiac function directly at the myofilament and without changes in $[Ca^{2+}]_i$, but these agents are still in the experimental stage, and concerns of enhancing systolic function at the expense of causing diastolic dysfunction remain[16]. Similarly, a number of studies have explored the therapeutic potential of cell transplantation therapy using human embryonic stem cell-derived cardiomyocytes (hESC-CMs) to remuscularize the scar with bonafide human myocardium, but most to date have reported low engraftment efficiency and only a modest benefit at best in cardiac function[94,98,183]. Finally, gene therapy approaches have demonstrated efficacy in preclinical and phase I/II clinical trials, but concerns regarding the ideal delivery strategy to maximize efficacy and minimize risk still remain[207]. We hypothesized that a number of these limitations could potentially be alleviated by the development of a novel hybrid therapeutic strategy to exploit the strengths of each of the above approaches while minimizing the accompanying limitations.

We[19-22,25,26,208-210] and others[211,212] have extensively studied the effects of 2-deoxyadenosine triphosphate (dATP), a novel inotropic agent that enhances cardiac contractility by acting as an energy substrate for striated muscle. These studies have

shown that when compared to ATP, dATP increases the maximum rate of shortening, Ca^{2+} sensitivity of force, and maximally Ca^{2+}-activated force production in demembranated cardiac trabeculae[22]. Importantly, these effects occur with cardiac tissue containing either α- and β-cardiac myosin isoforms and persist with dATP accounting for as little as 1% of the total adenosine nucleotide pool[26,211,212]. These effects are presumably due to the highly cooperative nature of cardiac muscle and the rapid rephosphorylation of dADP by creatine kinase, which allows single molecules of dATP to be hydrolyzed and rephosphorylated repeatedly before degradation[213]. More recent work by our group has investigated the effect of overexpressing the enzyme ribonucleotide reductase (R1R2), the enzyme responsible for conversion of ADP to dADP and rate-limiting step in dATP production, in intact cardiomyocytes[26]. These studies showed that overexpression of the subunits encoding for R1R2 (Rrm1 and Rrm2) resulted in a 40% increase in shortening magnitude and 80% increase in the shortening rate in cultured adult rat cardiomyocytes[26]. Importantly, these effects were noted in the absence of any increase in $[Ca^{2+}]_I$, suggesting that dATP exerts its effects on contractility primarily by acting on the myofilament. Furthermore, we recently reported that transgenic mice overexpressing R1R2 maintain a hypercontractile state without detrimental effects on metabolism or adverse remodeling[25]. Taken together, these findings suggest that dATP may represent a next-generation inotropic therapy for the treatment of heart failure. Despite these promising results attained thus far, the efficient and safe delivery of dATP remains a challenge. The half-life of free triphosphate nucleotides in the bloodstream is exceptionally low [214], making systemic delivery untenable, and in order for the nucleotide to exert its inotropic effects, it must

be localized specifically to the cytoplasm of cardiomyocytes.

Our group has previously shown that human embryonic stem cell-derived cardiomyocytes (hESC-CMs) efficiently engraft in both healthy and damaged rodent myocardium[93,94,100]. These cells are capable of electrically coupling with host myocardium via the formation of host-graft gap junctions, which facilitate electrical propagation and allow graft cells to beat synchronously with the host[100]. In addition to the ions necessarily for electrical communication, gap junctions have also been shown to allow the efficient intercellular transfer of other small metabolites such as cAMP or ATP between cells in a process termed gap junction intercellular communication (GJIC)[204]. Work by Goldberg et al showed that connexin-43 (Cx43), the predominate connexin isoform comprising cardiac gap junctions, exhibited a ~300 fold higher conductance of ATP compared to other neural connexins such as Cx32[205].

Based upon these findings, our long term goal is to determine if a small population of engrafted hESC-CMs overexpressing the genes encoding for R1R2 will produce and diffuse the small molecule dATP throughout coupled host myocardium, increasing global cardiac function and slowing or reversing the deleterious cardiac remodeling and subsequent heart failure following infarction. In the present work, we take the first step towards this goal by demonstrating that (1) dATP is capable of efficiently crossing gap junctions between both cardiomyocytes and fibroblasts, (2) cardiomyocytes coupled to cells that overexpress R1R2 show increased contractility, and (3) transplantation of R1R2-overexpressing hESC-CMs can dramatically increase cardiac performance above

healthy baseline levels. While other groups have postulated that GJIC can be utilized as a therapeutic approach[215], to our knowledge this represents the first study to successfully demonstrate a functional benefit of GJIC in a therapeutic setting. Taken together, this work proposes a new paradigm in cardiac therapy; rather than attempting complete scar remuscularization, cells could instead be genetically engineered to exert positive inotropic support via intracellular small molecule delivery in a targeted, cardiac-specific fashion and with minimal systemic side effects. Furthermore, these cells can be exhaustively characterized prior to transplantation, limiting the risk of oncogenesis typically associated with gene manipulation, and placed into healthy myocardium rather than the hostile scar zone, improving engraftment efficiency compared to traditional cell therapy approaches.

Methods

Neonatal rat cardiomyocyte isolation and culture. Neonatal rat ventricular cardiomyocytes (NRCs) were isolated and cultured as previously described[216]. Briefly, neonatal hearts were hearts rapidly excised and placed into cold buffer (in mmol/L: NaCl 116.4, HEPES 20, NaH2PO4 1, glucose 5.5, KCl 5.4, MgSO4 0.8; pH 7.4). The ventricles were trimmed, minced, and incubated for 5 cycles of 25 min at 37C in collagenase type II (95 U/mL, Worthington) and pancreatin (0.6 mg/mL, Gibco BRL). After each incubation, cells were pelleted and resuspended in DMEM/M199 (4:1) supplemented with 10% horse serum (ICN Flow), 5% fetal bovine serum (HyClone), penicillin G (100 U/mL), and streptomycin (100 μg/mL, Gibco) and preplated for 30

minutes to reduce contaminating nonmyocytes. The cells were then plated in media onto sterile, gel-coated 6-well dishes at a concentration of $2x10^5$ cells per well for culturing and infection. After 2-4 hours, plating media was removed and cells were transduced with plating media containing R1R2+GFP or GFP adenovirus (~250 viral particles per cardiomyocyte).

PSC maintenance and guided cardiac differentiation. All experiments were approved by the University of Washington Embryonic Stem Cell Research Oversight Committee (ESCRO) and conducted using the H7 (NIHhESC-10-0061) hESC line. PSCs were maintained and differentiated as previously described[72,94]. Briefly, hESCs were cultured on Matrigel-coated plates (BD Biosciences) with mouse embryonic fibroblast-conditioned medium (MEF-CM) containing 4ng/mL basic fibroblast growth factor (bFGF). Cells were passaged using versene-EDTA and cardiogenesis induced with RPMI-B27 (Gibco) containing L-glutamine, Matrigel, and 10μg/mL recombinant human activin A (R&D Systems). After one day the media was switched to RPMI-B27 containing L-glutamine and 100ng/mL recombinant human bone morphogenetic protein-4 (BMP-4, R&D Systems), and four days later the media was aspirated and subsequently replaced every other day with RPMI-B27 containing L-glutamine. Cells typically began beating spontaneously on approximately day 12-15 post-induction. Prior to experimentation, cells were passaged using 0.05% trypsin-EDTA and replated on PEI-gelatin coated fluorodishes as previously described[72].

Dye transfer. Dye transfer experiments were conducted with intracellular microinjection pipettes pulled from 1mm thin walled capillary glass (Sutter Instruments) pulled to a ~1μm final tip diameter using a Sutter P-97. Fluorescein-12-dATP was purchased at >99% purity by HPLC (Perkin Elmer). Pipettes were backloaded with ~1μL of either fluorescein-dATP or control fluorescein (1mM in TE buffer) solution and placed in a Eppendorf Celltram microinjector mounted on a Zeiss AxioObserver microscope with AxioCam imaging hardware. Cells were bathed in Tyrode's buffer at room temperature, and a single cell was injected with dye solution. The resulting dye transfer was imaged every 10 seconds for 5 minutes with minimal excitation to minimize photobleaching.

Image analysis. Images were manually thresholded and quantitatively analyzed in ImageJ using standard analysis plugins. For measurements of dye transfer area, the initial T=0 image was subtracted from the final T=5min image to remove any artifact associated with the injection pipette. To obtain measurements of maximum dye diffusion distance, a minimum of 3 radial measurements to the furthest distance of dye transfer were made, and the largest value was selected.

Optical contraction analysis. Cells were placed in HEPES-buffered Tyrode's solution at 25C and visualized using a Nikon TS100 inverted microscope coupled to an Ionoptix videomicroscopy system (Ionoptix). Traces were collected and analyzed using Ionwizard software, and a minimum of five traces were analyzed and averaged for each cell.

Viral Transduction. HEK293 cells were used to generate adenoviral vectors expressing Rrm1 or Rrm2 under the CMV promotor as previously described[26]. Both vectors contained a green fluorescent protein (GFP) reporter, and as a control we also generated a vector encoding for GFP alone. Cardiomyocytes were transduced for 2-4hrs at 37C with ~250 particles per cell, which yielded >95% transduction efficiency.

Western blot analysis. Cells were harvested using 0.05% trypsin and placed in Laemmli sample buffer at -80 °C, and SDS-PAGE separated proteins were transferred to nitrocellulose membrane, blocked using 5% milk (w/v in Tris-buffered saline) and probed with anti-Rrm1 or anti-Rrm2 antibodies (Santa Cruz Biotechnology, Santa Cruz, Protein bands were quantified using open access software (ImageJ, NIH) and expressed relative to the housekeeping protein GAPDH.

Cell transplantation. All studies were approved by the University of Washington Animal Care and Use Committee and were conducted in accordance with federal guidelines. Using surgical techniques we have previously reported[6,28,31–33], 15 million GFP or R1R2-GFP transduced hESC-derived cardiomyocytes were directly injected into the uninjured left ventricular walls of 200-300g male nude athymic rats (Charles River) in 3-4 spatially distinct injections. Animals were allowed to recover and monitored for signs of discomfort or weight loss.

Histology. Hearts were rapidly excised, grossly sectioned into mm short-axis sections, and fixed overnight in Formalin before being dehydrated and embedded in paraffin. 5

μm thin sections were cut, rehydrated, and stained according to protocols previously published by our group[93,94]. The antibodies used for this study include rabbit polyclonal anti-Rrm1 (Proteintech) and goat anti-GFP (Novus).

*Echocardiography. E*chocardiography was performed as previously described[94] using a GE Vivid7 (GE, Piscataway, NJ). Briefly, we lightly anesthesized the animals using isoflurane and imaged the short axis of the heart using M-mode to measure left ventricular (LV) end systolic dimension (LVESD) and left ventricular end diastolic dimension (LVEDD) to calculate fractional shortening (FS=(LVEDD-LVESD)/LVEDD).

Statistical Analysis. All data is presented as mean ± S.E.M. All data was compiled in Microsoft Excel and normal parameter distributions were confirmed using the Shapiro-Wilk test for normality. All statistical tests were performed using a 2-tailed Student's t-Test with unequal sample variance or Fisher's exact test for proportions.

Results

hESC-CM contractility is increased with R1R2 overexpression

We first verified that overexpression of the enzyme ribonucleotide reductase (R1R2) results in increased contraction magnitude and velocity in hESC-CMs but with no change in relaxation kinetics (**Fig. 3.1C**).

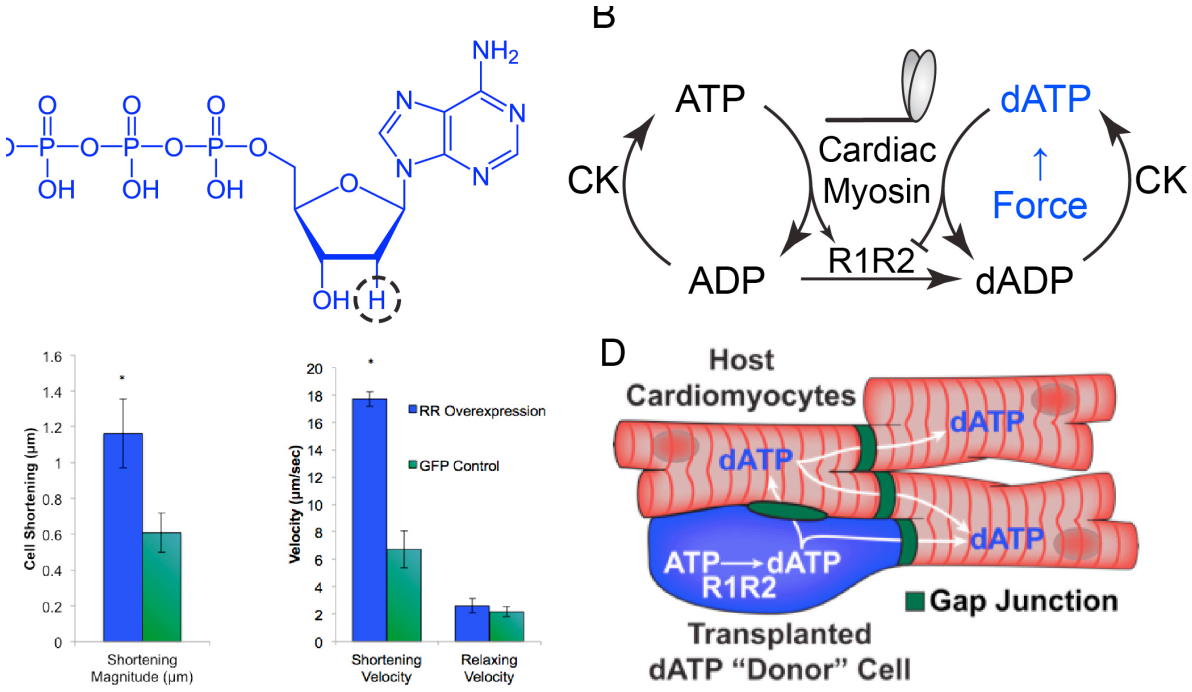

ɟure 3.1 dATP enhances contractility of hESC-CMs and may travel between cells via gap junctions.

Structure of dATP differs from ATP only by the lack of an oxygen at the 2' position (circled). Cardiac myosin produces more force when hydrolyzing dATP as an energy source, and the yme R1R2 catalyzes synthesis of dATP in conjunction with creatine kinase (CK). (**C**) egulation of R1R2 in hESC-CMs increases force and contraction velocity without altering xation velocity. *p<0.05 (**D**) Schematic depicting the gap junction-mediated transfer of P from transplanted donor cells throughout cardiac syncytium.

NRVMs rapidly conduct dATP-fluorescein via gap junctions

We next tested the hypothesis that like ATP[205], dATP is capable of rapidly crossing between coupled cells via gap junctions. To accomplish this, a single NRC within a confluent monolayer was microinjected with either a commercially available dATP-fluorescein conjugate or fluorescein alone using a glass micropipette (**Fig. 3.2**). We restricted our analysis to the 5-minute time point because fluorescein has been shown to leak slowly from certain cultures cell lines with a half-life of 30 mins[217]. 100% of the cells injected in both groups successfully transferred fluorescence to neighboring cells.

5 minutes of diffusion,

ATP-fluorescein signal

hermore, the maximum

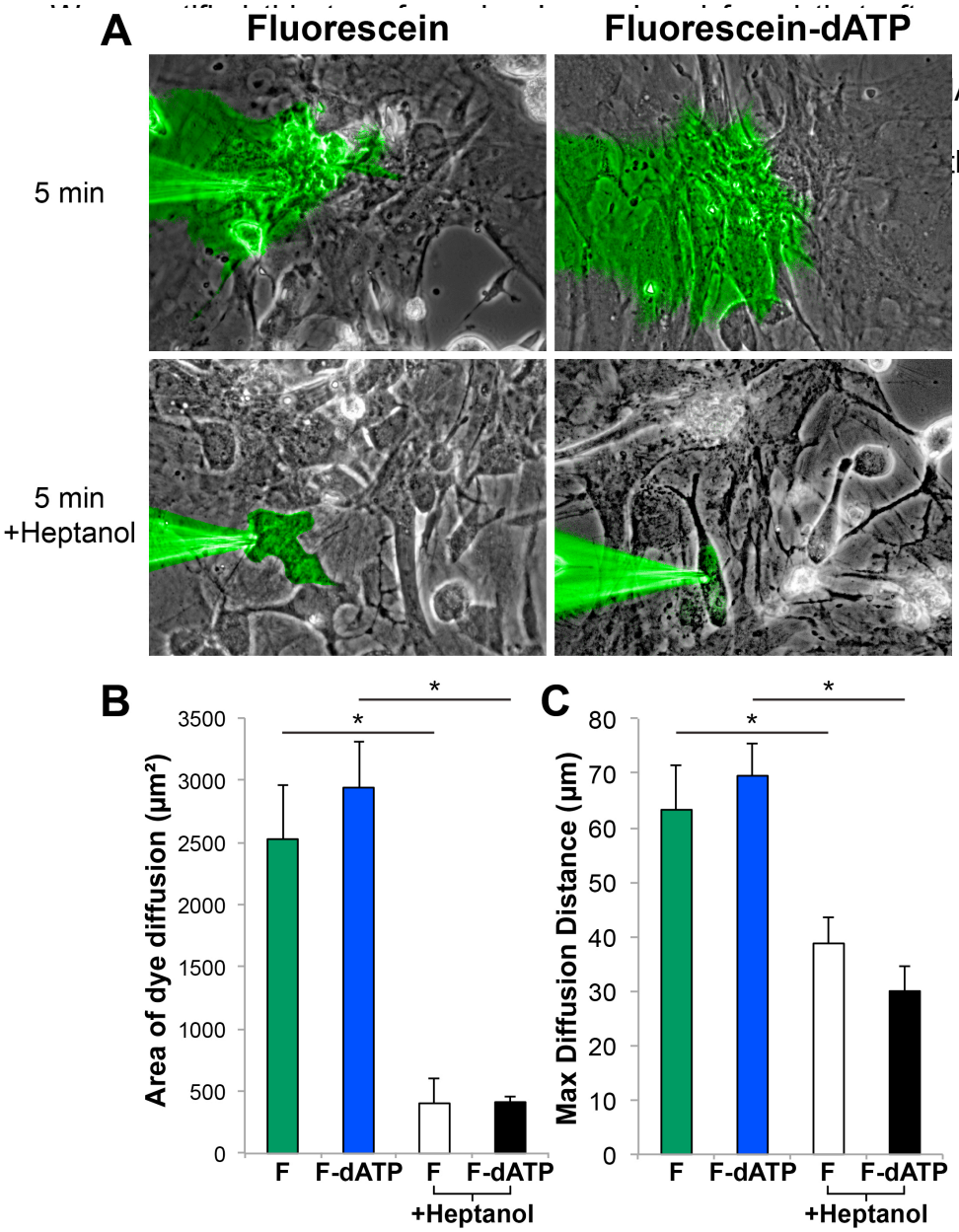

igure 3.2 NRCs rapidly conduct dATP-fluorescein between cells at kinetics similar to fluorescein alone.

RC cultures were microinjected with dATP-fluorescein or fluorescein and serially imaged for minutes. Images were thresholded and quantified for (**B**) maximum area of dye diffusion d (**C**) maximum diffusion distance from the pipette tip. To assess gap junction specificity, also added 2mM heptanol and observed a significant decrease in transfer efficiency. <0.05

distance of dye transfer for fluorescein and dATP-fluorescein was 63.3 ± 8.3 μm and 69.5 ± 5.9 μm, respectively (**Fig. 3.2C**, p=0.54). Pretreatment with 2mM of the gap

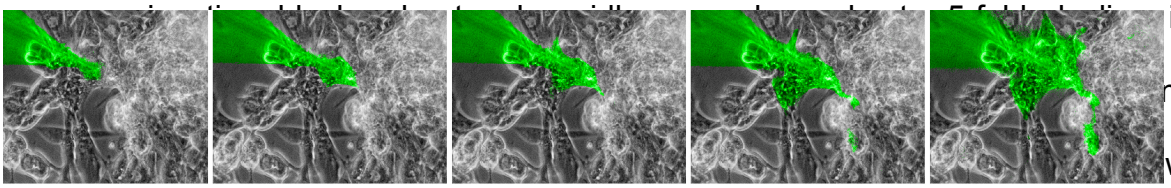

in fluorescence
ne in maximum
we observed is
indeed gap junction-mediated.

gure 3.3 dATP-fluorescein transfers readily in hESC-CMs.

ıltures of hESC-CMs were microninjected with dATP-fluorescein, which rapidly transferred neighboring cells over the course of 5 mins.

hESC-CMs support gap junction-mediated dATP-fluorescein diffusion

To confirm that these results applied to human cardiomyocytes derived from hESCs, we performed a similar experiment in hESC-CM cultures (**Fig. 3.3**). As expected, dATP-fluorescein again rapidly transferred to neighboring cells, and in some cases second and third order transfer occurred.

R1R2-hESC-CMs enhance the contractility of neighboring WT cardiomyocytes

We next sought to demonstrate the functional consequences of dATP overproduction and transfer to neighboring cardiomyocytes. To accomplish this, hESC-CMs were

adenovirally transduced with R1R2+GFP or GFP alone, typsinized 48 hours later, and

cocultures, a number of

ften formed (**Fig. 3.4A**).

f these cells, as well as

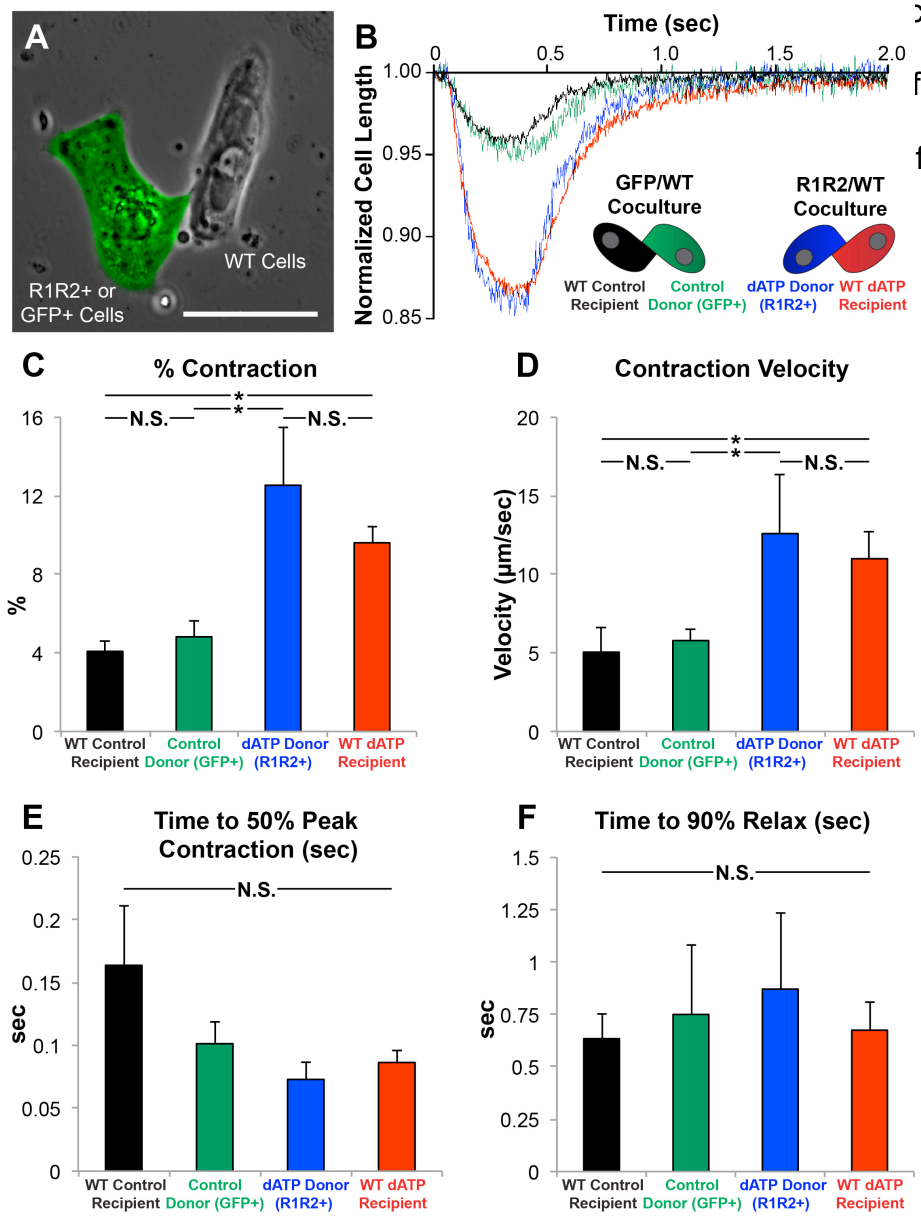

igure 3.4 R1R2-hESC-CMs enhance contractility of neighboring WT cardiomyocytes.

ESC-CMs were transduced with R1R2-GFP or control GFP adenovirus and cocultured with T hESC-CMs. (**A**) The contractile parameters of each cell in a heterogeneous GFP+/GFP- ublet were measured. (**B**) Representative traces show that R1R2-GFP+ cells and coupled T hESC-CMs exhibit greatly increased (**C**) magnitudes and (**D**) velocities of contraction but change in the kinetics of (**E**) contraction or (**F**) relaxation. *p<0.05 N.S. not significant

singlet R1R2+GFP or GFP+ cells and GFP- cells in the same cultures as controls. As expected, GFP+ control hESC-CMs (green trace) and adjacent WT hESC-CMs coupled (black trace) exhibited similar contraction magnitudes to each other (4.8 ± 0.8% and 4.1 ± 0.6%, respectively, p=0.48) and to values previously-published by our group[72] (**Fig. 3.4B**). In start contrast, the R1R2+GFP cells (blue trace) exhibited a substantially larger contraction magnitude (12.5 ± 2.9%). Excitingly, the GFP-negative WT hESC-CM in direct contact (red trace) exhibited a statistically similar contraction magnitude (9.6 ± 0.85%, p=0.42) despite the lack of R1R2 overexpression in these cells. Similarly, both R1R2-GFP hESC-CMs and coupled WT hESC-CMs exhibited increased contraction velocity over respective controls ($p<0.05$). There were no statistically significant differences in the time to peak contraction or the time to 90% relaxation, and uncoupled WT hESC-CMs in both cultures exhibited similar contractile performance across all parameters measured (data not shown). As a control, we also measured the contractile performance of uncoupled singlet GFP+ and GFP- cells and saw no statistical difference in any of the aforementioned parameters (data not shown), suggesting that physical contact between cells is necessary for improvements in contractility.

R1R2-fibroblasts modulate contractility of coupled cardiomyocytes

Based upon literature reports of functional coupling between cardiomyocytes and fibroblasts, we sought to examine whether fibroblasts modified to overexpress R1R2 might modulate the contractility of adjacent coupled hESC-CMs. Human neonatal dermal fibroblasts (HNDFs) were transduced with R1R2-GFP or GFP control virus and allowed to form a confluent monolayer, and hESC-CMs were subsequently plated on

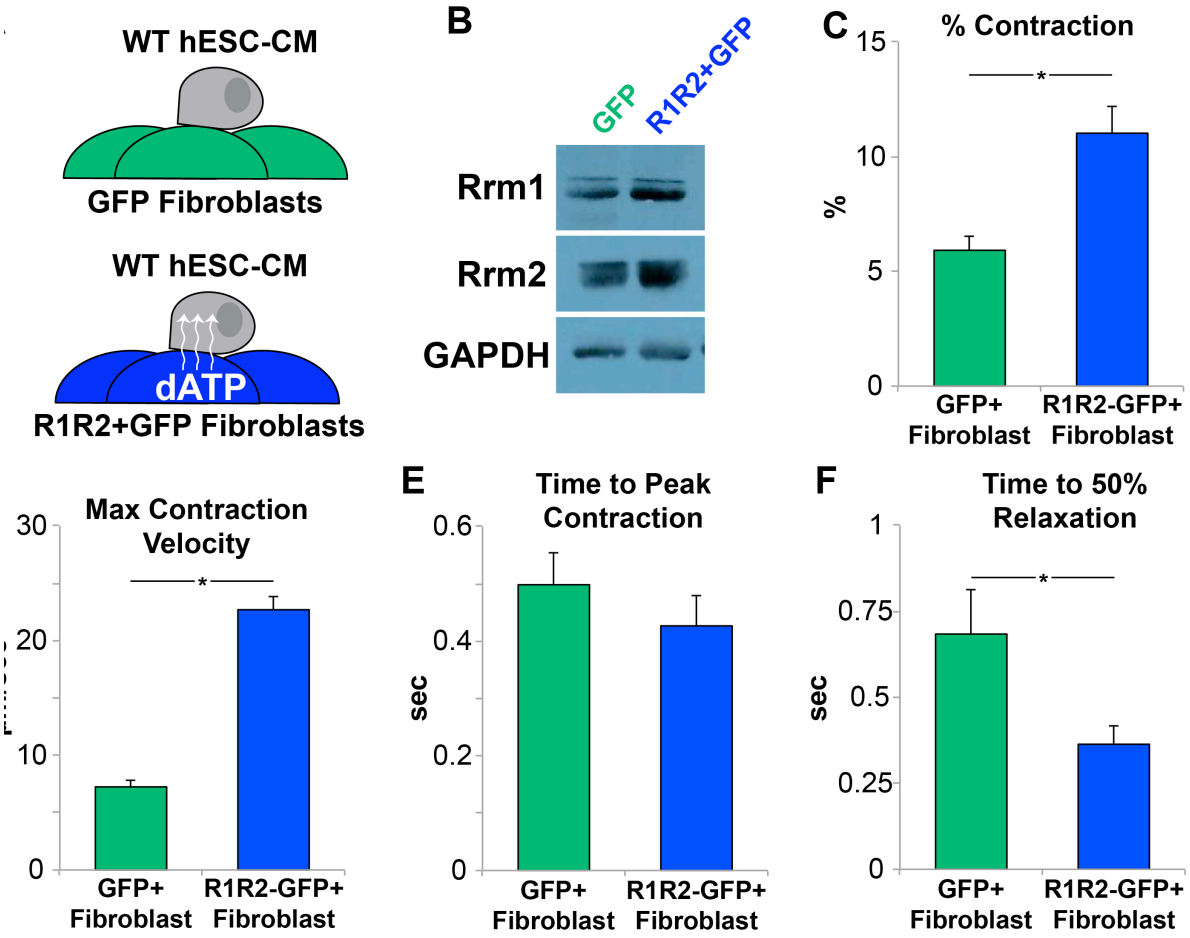

Figure 3.5 R1R2-Fibroblasts modulate contractility of adjacent cardiomyocytes.

.) Fibroblasts were transduced with R1R2-GFP or GFP, and WT hESC-CMs were allowed adhere to the monolayer. (**B**) Western blot analysis of the fibroblast cultures showed gnificantly increased quantities of Rrm1 and Rrm2. Measurement of hESC-CM contractility owed a significant increase in the (**C**) magnitude and (**D**) velocity of contraction in cells on 1R2-GFP feeders. (**E**) While no changes were noted in the time to peak contraction, the (**F**) ne to 50% relaxation was substantially shorter in the hESC-CMs cocultured with R1R2-FP fibroblasts. *p<0.05

top of this monolayer and allowed to adhere for 48hrs (**Fig. 3.5A**). Western blot analysis of the fibroblast feeders showed a >3-fold induction of both Rrm1 and Rrm2 at the protein level (**Fig. 3.5B**). Contractile measurement of the cardiomyocytes on R1R2-transduced fibroblast feeders had roughly a doubling in contractile magnitude compared to those in GFP-control fibroblast cultures (**Fig. 3.5C**, 11.0 ± 1.1% vs 5.9 ± 0.6%, respectively, $p<0.001$). Similarly, maximum contraction velocities were also increased

(**Fig. 3.5D**, 22.7 ± 4.0 vs, 7.2 ± 1.0 μm/sec, P<0.005). No changes in the time to peak contraction were noted (**Fig. 3.5E**), but the time to 50% relaxation was decreased (**Fig. 3.5F**, 87.6 ± 38.1 ms vs. 139.0 ± 20.0 ms, p<0.05) in the R1R2-fibroblast hESC-CMs.

R1R2-hESC-CMs efficiently engraft and survive in healthy rat myocardium

Motivated by the *in vitro* data supporting the hypothesis of gap junction-mediated dATP transfer, we sought to test the ability of R1R2-overproducing cardiomyocytes to elevate global healthy cardiac function. To accomplish this, we transduced hESC-CMs with R1R2+GFP or control GFP virus and two days later transplanted 15e6 cells into the anterior wall of nude rats in a series of 3-4 injections and compared changes in echocardiography 5 days later (**Fig. 3.6A**). Upon excision of the heart and imaging of cross-sectional slices, 100% of hearts displayed positive GFP signal (**Figs. 3.6B-C**). H&E staining demonstrated multiple areas with morphology consistent with surviving engrafted cells (**Figs. 3.6D-E**). Staining for anti-Rrm1 identified large regions of positive staining in hearts from the R1R2+GFP cohort (**Fig. 3.6F**), while hearts receiving control GFP-hESC-CMs showed diffuse low levels of positive staining without clear foci (**Fig. 3.6G**). Further staining for anti-GFP, however, confirmed the presence of graft cells in both groups, and high resolution imaging of these graft regions demonstrated clear regions of direct contact with healthy host myocardium (**Figs. 3.6H-I**), suggesting potential host-graft gap junction formation.

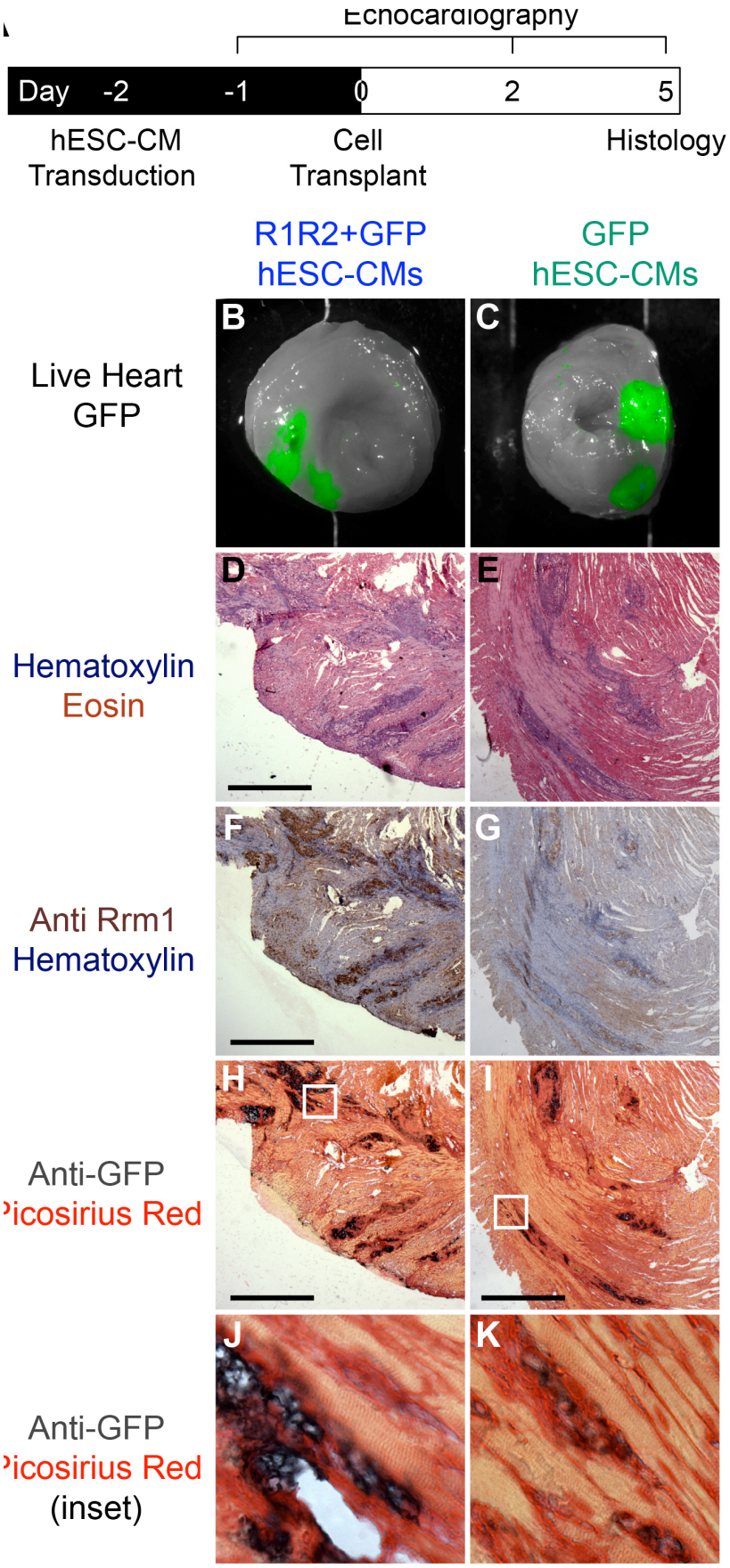

Figure 3.6 In vivo study design and histology.

(**A**) hESC-CMs were transduced with R1R2-GFP or GFP on D-2 and 15e6 cells transplanted into healthy nude rat hearts on D0. Animals were monitored echocardiographically before and after cell transplantation, and on D5 the hearts were explanted and histology performed. (**B,C**) 100% of animals receiving grafts had positive GFP signal upon gross sectioning and imaging. (**D,E**) H&E demonstrated areas of dense nuclei staining consistent with engrafted cells. (**F,G**) Staining for Rrm1 in serial sections revealed strongly positive clusters of cells in R1R2-GFP animals, but only weak signal in GFP-hESC-CM control hearts. (**H,I**) Anti-GFP staining colocalized to the same graft regions identified by H&E. (**J,K**) High magnification inset of these stains show clear regions of GFP+ signal directly adjacent to host myocardium. Scale bar 500 μm

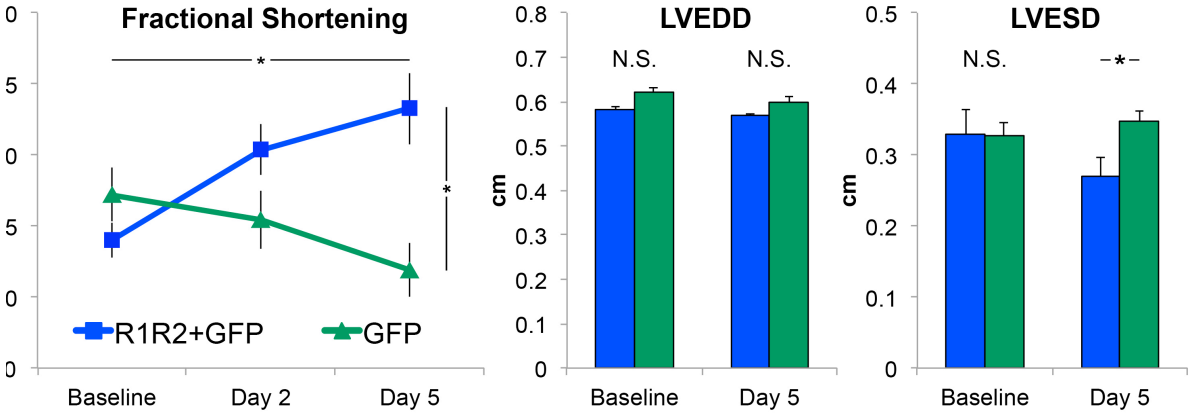

Figure 3.7 Transplanted R1R2-hESC-CMs increase contractility of healthy hearts to above baseline physiological levels.

.) Fractional shortening (FS) of animals receiving R1R2-GFP-hESC-CMs and GFP-hESC-Ms were similar at baseline, but at R1R2-hESC-CM recipient hearts had a significant crease in FS when compared to both GFP-hESC-CM recipients and to baseline pre-nsplantation levels. (**B**) No differences were noted in the left ventricular end diastolic nension (**LVEDD**), but the D5 R1R2-GFP-hESC-CM cohort exhibited a smaller left ntricular end systolic dimension (**LVESD**) than other groups. *p<0.05

R1R2-hESC-CMs Improve Global Healthy Heart Contractility above healthy baseline levels

Finally, using echocardiography we measured the cardiac performance of hearts receiving R1R2-GFP or GFP cells. Both groups exhibited similar (~45%) fractional shortening (FS) at baseline, and the control animals receiving GFP-hESC-CMs had no statistical change in this value over the course of the experiment. In stark contrast, animals receiving R1R2-hESC-CMs had a fractional shortening of 53.2 ± 2.5% at day 5 following transplantation (**Fig. 3.7A**). Not only was this value statistically significantly higher than GFP-hESC-CM recipients at day 5 ($p<0.01$), but it was also significantly higher than baseline values taken before transplantation ($p<0.05$). This increase in FS

was not due to changes in diastolic performance, as both groups had indistinguishable Left Ventricular End Diastolic Dimensions (LVEDD) at both D0 and D5 (**Fig. 3.7B**, $p>0.05$). Only the D5 R1R2-hESC-CM group had a statistical difference in Day 5 Left Ventricular End Systolic Dimension (LVESD) compared GFP-hESC-CM recipient controls ($p<0.05$).

Discussion

Current strategies to restore lost cardiac function using hPSC-CMs as a cell therapy require substantial remuscularization of the infarct with new force-producing units, but most studies to date have suggested that the vast majority of cells fail to survive the initial transplantation[93], and those cells that do are highly immature and produce forces one and two orders of magnitude below adult cardiomyocytes[147,148,172,173]. Rather than fully remuscularizing the hostile scar zone, we hypothesized that cell therapy could be engineered to take advantage the efficient gap junction intercellular communication network in the heart to distribute the novel biological inotropic small molecule dATP. If successful, this approach would eliminate a number of challenges associated with traditional cell therapy, including the necessity to engraft large quantities of cells into the hostile infarct environment, and would instead allow diffuse engraftment of dATP-donor cells throughout the healthy myocardium, where they could easily form gap junctions with host myocardium. While this strategy could also be accomplished using traditional gene therapy to upregulate R1R2, the enzyme responsible for dATP production, using cells as the delivery vehicle offers two primary advantages; first, unlike viral transduction of native myocardium, R1R2-overexpressing cells could be exhaustively characterized

prior to transplantation to remove any possibility of insertional mutagenesis, and second, engraftment of new cardiomyocytes, however immature, may provide additional force-producing units if long-term maturation does indeed occur in the myocardium as suggested by the literature[95].

In order for the proposed strategy to be successful, candidate cells must be (1) capable of overexpressing R1R2, (2) express sufficient quantities of connexin protein to facilitate transfer, and (3) survive transplantation into myocardium. Cells such as skeletal myoblasts robustly engraft, but they fail to express the appropriate connexins[35]. Human mesenchymal stem cells (hMSCs) fulfill some of these requirements[218], but their ability to permanently survive in an infarcted heart remains to be demonstrated[178]. We chose to pursue the use of hESC-CMs as a cell delivery platform because they express high levels of connexins, including Cx-43[72,219,220], they efficiently engraft and survive in healthy and diseased rodent hearts[93,94], and importantly they form functional gap junctions with host myocardium[100].

We first addressed the question of whether dATP is physically capable of crossing between gap junctions by performing dye transfer studies. To accomplish this, we performed dye transfer experiments using either fluorescein dye or dATP-fluorescein conjugates (**Fig. 3.2**). We reasoned that because fluorescein and ATP efficiently transfer individually, the successful transfer of much larger dATP-fluorescein conjugate (~1000kDa) would suggest that dATP sans fluorescein would also transfer. Indeed this occurred in both NRCs and hESC-CMs, and surprisingly there was little difference in the

kinetics of transfer between the conjugates and the dye alone. Addition of heptanol resulted in a precipitous decline in dye transfer efficiency, suggesting that the effect is indeed gap junction-mediated. Indeed, the results of these experiments are not entirely not surprising, given the literature precedent for highly efficient transfer of ATP through cardiac gap junctions[204,205] and the fact that dATP is highly similar in size and charge profile.

We next investigated the ability of dATP-producing cells to modulate the contractility of neighboring coupled cardiomyocytes. We performed a series of experiments involving cocultures of R1R2-overexpressing hESC-CMs with WT cardiomyocytes and saw robust increases in contractile performance in cells directly coupled to R1R2-hESC-CMs (**Fig. 3.4**). Critically, uncoupled single WT cardiomyocytes in the cultures containing R1R2-hESC-CMs were unaffected and demonstrated contraction characteristics identical to the GFP-hESC-CMs and WT hESC-CMs coupled to them; this finding suggests that direct coupling is required for any functional benefit and minimizes the possibility that increases in contractility are due to extracellular signaling or paracrine effects such as purinergic receptor activation.

We then performed a second coculture experiment involving R1R2-fibroblasts as feeder cells to rule out passive mechanical effects associated with the highly contractile R1R2-hESC-CMs, and we saw similar improvements in contractile performance (**Fig. 3.5**). Interestingly, this experiment also demonstrated an increase in the relaxation kinetics of hESC-CMs cocultured with R1R2-fibroblasts; this finding supports previous biochemical

data suggesting that contrary to other myosin activators currently being investigated, dATP is able to increase force while simultaneously also increasing diastolic performance, presumably by speeding the rate-limiting ADP/Pi release step of the crossbridge cycle. Our data from this experiment also supports the notion that fibroblasts functionally couple with cardiomyocytes and may participate in dATP transfer *in vivo*.

Finally, as a proof of principle we tested the hypothesis that R1R2-hESC-CM transplantation and dATP transfer will improve the global function of healthy rodent hearts. We chose this model system first because any elevation of function over baseline is unlikely to occur from transplantation of hESC-CMs alone, and is rather likely due to elevation of host myocardial performance to supraphysiological levels. We chose rats as the model species for this study because of the strong literature precedent for successful graft-host coupling in this species[93,169,221]. Importantly, the ability of graft cells to couple 1:1 to host myocardium is not necessary for GJIC; merely the presence of host-graft gap junction communication is sufficient. Based upon these study requirements, we transplanted R1R2-GFP or GFP-control hESC-CMs and evaluated the results via histological and functional endpoints. Histology revealed positive grafts in 100% of animals, and grafts in R1R2-hESC-CMs were strongly positive for Rrm1 (**Fig, 3.6**). Excitingly, many GFP+ graft cells were in direct opposition to host myocardium, supporting the notion of host-graft coupling.

Echocardiographic data form this study revealed that not only did R1R2-hESC-CM transplantation improve fractional shortening significantly above GFP-hESC-CMs alone, but this increase was equally robust when compared to baseline echo function in the same animals 7 days earlier (**Fig. 3.7**). This increase was directly due to increased systolic function, as no changes in diastolic dimensions were noted.

Taken together, these findings suggest that transplantation of R1R2-overexpressing hESC-CMs improves global cardiac function to a significant degree and suggests that R1R2-based cell therapy may provide a viable therapeutic approach for diseased hearts. Furthermore, the results from this study provide the first direct evidence that gap junctions may be used to deliver a therapeutic molecule of interest within the cardiac syncytium. Such an approach would lend itself well to catheter-based delivery diffusely throughout the myocardium, which would increase the potential for host-graft coupling and dATP transmission. Finally, the present study suggests that hESC-CM cell therapy has the capability to not only remuscularize damaged tissue and contribute new force-generating units, but these cells may also be capable of acting as biological drug delivery devices as well, producing any number of compounds with beneficial effects.

Chapter 4. Conclusions and Implications for Future Studies

In this dissertation, I have attempted to provide both context and data to support the hypothesis that current cardiac cell therapies may be limited in their full therapeutic potential because they lack the ability to contribute meaningful active force generation in relation to host myocardium. In Chapter 1, I discussed the current literature describing techniques to measure force production in single cells and constructs composed of hPSC-CMs, and I noted that even in the best-case scenarios these fall woefully short of the force-generating capacity of adult myocardium.

In chapter 2, I described my work to facilitate and quantify the maturation characteristics of hESC-CMs and hiPSC-CMs. I showed data to suggest that these cells are capable of maturing towards the adult cardiomyocyte phenotype in both structure and function. While these results required over three months of sustained culture to achieve, I believe they represent a proof-of-principle for future work aimed at elucidating the mechanistic basis of this maturation. Previous studies have implicated a number of intracellular pathways involved in hypertrophy[186,222], mechanotransduction[223-225], and maturation[226]. It would be interesting to design experiments to test the role of each of these pathways in early human cardiac differentiation and maturation using the platform I have developed. These experiments could potentially rely on advancements in high throughput screening assays (e.g. high content imaging and/or RNAseq) to identify candidate pathways for further investigation. This data would not only provide valuable

basic science and developmental biology knowledge, but it may also provide insight into strategies to rapidly mature cells for therapeutic applications. Perhaps this may involve a small molecule agonist to stimulate proliferation, or perhaps it will involve the identification of a critical component of myocardial construct design or geometry; only time – and more hard work – will tell.

In chapter 3, I described an innovative approach to use cell therapy as a biological drug delivery system to produce and distribute an inotropic drug throughout the heart via gap junctions. This strategy relies on the overexpression of the enzyme ribonucleotide reductase (R1R2), which catalyzes the formation of dATP. My work primarily focused on testing the hypothesis that dATP can indeed cross gap junctions and improve remote cell/tissue contractility both in cardiomyocyte cultures *in vitro* and in myocardium *in vivo*. The results from this work are clearly translational in nature, and indeed ongoing work is currently testing this approach in disease models, but I find the basic science questions it raises to be equally interesting. For example, nearly any proliferative cell type transplanted into the heart has a transient functional benefit, but the debate over the underlying mechanism of this benefit remains controversial. It is reasonable to suggest that this is due in part to the basal level of R1R2 found in proliferating cells; as long as the transplanted cell is capable of forming gap junctions, then it may provide dATP to the host myocardium. Furthermore, the demonstration of gap junction-mediated dATP transfer offers the possibility that during cardiac development, cardiomyocytes may have added functional benefit due to intrinsic and transient increases in intracellular dATP content during proliferation.

In envisioning the successful development R1R2-based cell therapy, the next hurdle that must be addressed is the development of a stable line of undifferentiated hESCs or hiPSCs overexpressing R1R2 in a consistent and controllable fashion. A recent study by Hockemeyer *et al*[227] applied zinc finger nuclease genome engineering technology[228] to pluripotent stem cells, and our lab has recently published work in using this technology to develop purified preparations of cardiomyocytes expressing the Ca^{2+} indicator GCaMP3[229]. This technology represents a promising strategy to insert a transgene containing Rrm1 and Rrm2 being driven by a cardiac-specific promoter into a known safe harbor locus in the human genome. To avoid any concerns of insertional mutagenesis associated with traditional genome editing (and potentially with R1R2-based gene therapy), the transgenic hPSCs could then be exhaustively characterized and validated *in vitro* prior to transplantation.

In closing, this work represents a small step forward in the development of a viable therapeutic approach to treat heart failure with stem cells, and I have immensely enjoyed contributing it to the ever-expanding body of biomedical knowledge. I can only hope that using the immense knowledge collected by stem cell biologists and engineers alike, one day someone once suffering from heart failure will awake one morning and live their life to the fullest as a person should, with their heart – regenerated with transplanted stem cells – merrily beating away like new.

References

1. Knowlton, F. P. & Starling, E. H. The influence of variations in temperature and blood-pressure on the performance of the isolated mammalian heart. J Physiol (Lond) 44, 206–219 (1912).
2. Patterson, S. W. & Starling, E. H. On the mechanical factors which determine the output of the ventricles. J Physiol (Lond) 48, 357–379 (1914).
3. Markwalder, J. & Starling, E. H. On the constancy of the systolic output under varying conditions. J Physiol (Lond) 48, 348–356 (1914).
4. Laflamme, M. A. & Murry, C. E. Regenerating the heart. Nat Biotechnol 23, 845–856 (2005).
5. Go, A. S. et al. Executive summary: heart disease and stroke statistics--2013 update: a report from the American Heart Association. Circulation 127, 143–152 (2013).
6. Withering, W. An account of the foxglove, and some of its medical uses: with practical remarks on dropsy and other diseases. (1785).
7. Hauptman, P. J. & Kelly, R. A. Digitalis. Circulation 99, 1265–1270 (1999).
8. Farah, A. E. & Frangakis, C. J. Studies on the mechanism of action of the bipyridine milrinone on the heart. Basic Res Cardiol 84 Suppl 1, 85–103 (1989).
9. Tuttle, R. R. & Mills, J. Dobutamine: development of a new catecholamine to selectively increase cardiac contractility. Circulation Research 36, 185–196 (1975).
10. Brixius, K., Reicke, S. & Schwinger, R. H. G. Beneficial effects of the Ca(2+) sensitizer levosimendan in human myocardium. Am J Physiol Heart Circ Physiol 282, H131–7 (2002).
11. Mebazaa, A. et al. Levosimendan vs dobutamine for patients with acute decompensated heart failure: the SURVIVE Randomized Trial. JAMA 297, 1883–1891 (2007).
12. Felker, G. M. et al. Heart failure etiology and response to milrinone in decompensated heart failure: results from the OPTIME-CHF study. J Am Coll Cardiol 41, 997–1003 (2003).
13. Thackray, S., Easthaugh, J., Freemantle, N. & Cleland, J. G. F. The effectiveness and relative effectiveness of intravenous inotropic drugs acting through the adrenergic pathway in patients with heart failure-a meta-regression analysis. Eur. J. Heart Fail. 4, 515–529 (2002).
14. Elkayam, U. et al. Use and impact of inotropes and vasodilator therapy in hospitalized patients with severe heart failure. Am. Heart J. 153, 98–104 (2007).
15. Shen, Y.-T. et al. Improvement of cardiac function by a cardiac Myosin activator in conscious dogs with systolic heart failure. Circ Heart Fail 3, 522–527 (2010).
16. Malik, F. I. et al. Cardiac Myosin Activation: A Potential Therapeutic Approach for Systolic Heart Failure. Science 331, 1439–1443 (2011).

17. Teerlink, J. R. et al. Dose-dependent augmentation of cardiac systolic function with the selective cardiac myosin activator, omecamtiv mecarbil: a first-in-man study. Lancet 378, 667–675 (2011).
18. Cleland, J. G. F. et al. The effects of the cardiac myosin activator, omecamtiv mecarbil, on cardiac function in systolic heart failure: a double-blind, placebo-controlled, crossover, dose-ranging phase 2 trial. Lancet 378, 676–683 (2011).
19. Regnier, M. & Homsher, E. The effect of ATP analogs on posthydrolytic and force development steps in skinned skeletal muscle fibers. Biophysj 74, 3059–3071 (1998).
20. Regnier, M., Martyn, D. A. & Chase, P. B. Calcium regulation of tension redevelopment kinetics with 2-deoxy-ATP or low [ATP] in rabbit skeletal muscle. Biophysj 74, 2005–2015 (1998).
21. Regnier, M., Lee, D. M. & Homsher, E. ATP analogs and muscle contraction: mechanics and kinetics of nucleoside triphosphate binding and hydrolysis. Biophysj 74, 3044–3058 (1998).
22. Regnier, M., Rivera, A. J., Chen, Y. & Chase, P. B. 2-deoxy-ATP enhances contractility of rat cardiac muscle. Circulation Research 86, 1211–1217 (2000).
23. Gordon, A. M., Regnier, M. & Homsher, E. Skeletal and cardiac muscle contractile activation: tropomyosin "rocks and rolls". News Physiol Sci 16, 49–55 (2001).
24. Elledge, S. J., Zhou, Z. & Allen, J. B. Ribonucleotide reductase: regulation, regulation, regulation. Trends Biochem. Sci. 17, 119–123 (1992).
25. Nowakowski, S. G. et al. Transgenic overexpression of ribonucleotide reductase improves cardiac performance. Proc Natl Acad Sci USA 110, 6187–6192 (2013).
26. Steven Korte, F. et al. Upregulation of cardiomyocyte ribonucleotide reductase increases intracellular 2 deoxy-ATP, contractility, and relaxation. J Mol Cell Cardiol (2011). doi:10.1016/j.yjmcc.2011.08.026
27. Isner, J. M. Myocardial gene therapy. Nature 415, 234–239 (2002).
28. Davis, J. et al. Designing heart performance by gene transfer. Physiol Rev 88, 1567–1651 (2008).
29. Vinge, L. E., Raake, P. W. & Koch, W. J. Gene therapy in heart failure. Circulation Research 102, 1458–1470 (2008).
30. Ritterhoff, J. & Most, P. Targeting S100A1 in heart failure. Gene Ther 19, 613–621 (2012).
31. Hoshijima, M. et al. Chronic suppression of heart-failure progression by a pseudophosphorylated mutant of phospholamban via in vivo cardiac rAAV gene delivery. Nat Med 8, 864–871 (2002).
32. Gwathmey, J. K., Yerevanian, A. I. & Hajjar, R. J. Cardiac gene therapy with SERCA2a: from bench to bedside. J Mol Cell Cardiol 50, 803–812 (2011).
33. Jessup, M. et al. Calcium Upregulation by Percutaneous Administration of Gene Therapy in Cardiac Disease (CUPID): a phase 2 trial of intracoronary gene therapy of sarcoplasmic reticulum Ca2+-ATPase in patients with advanced heart failure. Circulation 124, 304–313 (2011).
34. Marelli, D., Desrosiers, C., el-Alfy, M., Kao, R. L. & Chiu, R. C. Cell transplantation for myocardial repair: an experimental approach. Cell Transplant 1, 383–390 (1992).

35. Koh, G. Y., Klug, M. G., Soonpaa, M. H. & Field, L. J. Differentiation and long-term survival of C2C12 myoblast grafts in heart. J Clin Invest 92, 1548–1554 (1993).
36. Murry, C. E., Wiseman, R. W., Schwartz, S. M. & Hauschka, S. D. Skeletal myoblast transplantation for repair of myocardial necrosis. J Clin Invest 98, 2512–2523 (1996).
37. Siminiak, T. et al. Percutaneous trans-coronary-venous transplantation of autologous skeletal myoblasts in the treatment of post-infarction myocardial contractility impairment: the POZNAN trial. Eur Heart J 26, 1188–1195 (2005).
38. Dib, N. et al. Feasibility and safety of autologous myoblast transplantation in patients with ischemic cardiomyopathy. Cell Transplant 14, 11–19 (2005).
39. Menasché, P. et al. Autologous skeletal myoblast transplantation for severe postinfarction left ventricular dysfunction. J Am Coll Cardiol 41, 1078–1083 (2003).
40. Siminiak, T. et al. Autologous skeletal myoblast transplantation for the treatment of postinfarction myocardial injury: phase I clinical study with 12 months of follow-up. Am. Heart J. 148, 531–537 (2004).
41. Hagège, A. A. et al. Skeletal myoblast transplantation in ischemic heart failure: long-term follow-up of the first phase I cohort of patients. Circulation 114, I108–13 (2006).
42. Povsic, T. J. et al. A double-blind, randomized, controlled, multicenter study to assess the safety and cardiovascular effects of skeletal myoblast implantation by catheter delivery in patients with chronic heart failure after myocardial infarction. Am. Heart J. 162, 654–662.e1 (2011).
43. Menasché, P. et al. The Myoblast Autologous Grafting in Ischemic Cardiomyopathy (MAGIC) trial: first randomized placebo-controlled study of myoblast transplantation. Circulation 117, 1189–1200 (2008).
44. Seidel, M., Borczyńska, A., Rozwadowska, N. & Kurpisz, M. Cell-based therapy for heart failure: skeletal myoblasts. Cell Transplant 18, 695–707 (2009).
45. Menasché, P. Skeletal myoblasts and cardiac repair. J Mol Cell Cardiol 45, 545–553 (2008).
46. Orlic, D. et al. Bone marrow cells regenerate infarcted myocardium. Nature 410, 701–705 (2001).
47. Murry, C. E. et al. Haematopoietic stem cells do not transdifferentiate into cardiac myocytes in myocardial infarcts. Nature 428, 664–668 (2004).
48. Menasché, P. Cardiac cell therapy: lessons from clinical trials. J Mol Cell Cardiol 50, 258–265 (2011).
49. Traverse, J. H. et al. Effect of intracoronary delivery of autologous bone marrow mononuclear cells 2 to 3 weeks following acute myocardial infarction on left ventricular function: the LateTIME randomized trial. JAMA 306, 2110–2119 (2011).
50. Traverse, J. H. et al. Effect of the use and timing of bone marrow mononuclear cell delivery on left ventricular function after acute myocardial infarction: the TIME randomized trial. JAMA 308, 2380–2389 (2012).
51. Perin, E. C. et al. Effect of transendocardial delivery of autologous bone marrow mononuclear cells on functional capacity, left ventricular function, and perfusion

in chronic heart failure: the FOCUS-CCTRN trial. JAMA 307, 1717–1726 (2012).
52. Shake, J. G. et al. Mesenchymal stem cell implantation in a swine myocardial infarct model: engraftment and functional effects. Ann Thorac Surg 73, 1919–1926 (2002).
53. Quevedo, H. C. et al. Allogeneic mesenchymal stem cells restore cardiac function in chronic ischemic cardiomyopathy via trilineage differentiating capacity. Proc Natl Acad Sci USA 106, 14022–14027 (2009).
54. Schuleri, K. H. et al. Autologous mesenchymal stem cells produce reverse remodelling in chronic ischaemic cardiomyopathy. European heart … (2009).
55. Yoon, Y.-S. et al. JCI - Clonally expanded novel multipotent stem cells from human bone marrow regenerate myocardium after myocardial infarction. J Clin Invest 115, 326–338 (2005).
56. Hare, J. M. et al. A randomized, double-blind, placebo-controlled, dose-escalation study of intravenous adult human mesenchymal stem cells (prochymal) after acute myocardial infarction. J Am Coll Cardiol 54, 2277–2286 (2009).
57. Hare, J. M. et al. Comparison of allogeneic vs autologous bone marrow–derived mesenchymal stem cells delivered by transendocardial injection in patients with ischemic cardiomyopathy: the POSEIDON randomized trial. JAMA 308, 2369–2379 (2012).
58. Thomson, J. A. et al. Embryonic stem cell lines derived from human blastocysts. Science 282, 1145–1147 (1998).
59. Kim, J., Chu, J., Shen, X., Wang, J. & Orkin, S. H. An extended transcriptional network for pluripotency of embryonic stem cells. Cell 132, 1049–1061 (2008).
60. Takahashi, K. et al. Induction of pluripotent stem cells from adult human fibroblasts by defined factors. Cell 131, 861–872 (2007).
61. Burridge, P. W. et al. A universal system for highly efficient cardiac differentiation of human induced pluripotent stem cells that eliminates interline variability. PLoS ONE 6, e18293 (2011).
62. Sheng, X. et al. Human pluripotent stem cell-derived cardiomyocytes: response to TTX and lidocain reveals strong cell to cell variability. PLoS ONE 7, e45963 (2012).
63. Doetschman, T. C., Eistetter, H., Katz, M., Schmidt, W. & Kemler, R. The in vitro development of blastocyst-derived embryonic stem cell lines: formation of visceral yolk sac, blood islands and myocardium. J Embryol Exp Morphol 87, 27–45 (1985).
64. Xu, C. et al. Efficient generation and cryopreservation of cardiomyocytes derived from human embryonic stem cells. Regen Med 6, 53–66 (2011).
65. Mummery, C. et al. Differentiation of human embryonic stem cells to cardiomyocytes: role of coculture with visceral endoderm-like cells. Circulation 107, 2733–2740 (2003).
66. Yang, L. et al. Human cardiovascular progenitor cells develop from a KDR+ embryonic-stem-cell-derived population. Nature 453, 524–528 (2008).
67. Mummery, C. L. et al. Differentiation of human embryonic stem cells and induced pluripotent stem cells to cardiomyocytes: a methods overview. Circulation Research 111, 344–358 (2012).

68. Zhu, W.-Z., Hauch, K. D., Xu, C. & Laflamme, M. A. Human embryonic stem cells and cardiac repair. Transplant Rev (Orlando) 23, 53–68 (2009).
69. Lian, X., Zhang, J., Zhu, K., Kamp, T. J. & Palecek, S. P. Insulin inhibits cardiac mesoderm, not mesendoderm, formation during cardiac differentiation of human pluripotent stem cells and modulation of canonical wnt signaling can rescue this inhibition. Stem Cells 31, 447–457 (2013).
70. Zhang, J. et al. Extracellular matrix promotes highly efficient cardiac differentiation of human pluripotent stem cells: the matrix sandwich method. Circulation Research 111, 1125–1136 (2012).
71. Lian, X. et al. Robust cardiomyocyte differentiation from human pluripotent stem cells via temporal modulation of canonical Wnt signaling. Proc Natl Acad Sci USA 109, E1848–57 (2012).
72. Lundy, S. D., Zhu, W.-Z., Regnier, M. & Laflamme, M. Structural and Functional Maturation of Cardiomyocytes Derived From Human Pluripotent Stem Cells. Stem Cells Dev (2013). doi:10.1089/scd.2012.0490
73. Kehat, I. et al. Human embryonic stem cells can differentiate into myocytes with structural and functional properties of cardiomyocytes. J Clin Invest 108, 407–414 (2001).
74. Snir, M. et al. Assessment of the ultrastructural and proliferative properties of human embryonic stem cell-derived cardiomyocytes. Am J Physiol Heart Circ Physiol 285, H2355–63 (2003).
75. Xu, C., Police, S., Rao, N. & Carpenter, M. K. Characterization and enrichment of cardiomyocytes derived from human embryonic stem cells. Circulation Research 91, 501–508 (2002).
76. Zhang, J. et al. Functional cardiomyocytes derived from human induced pluripotent stem cells. Circulation Research 104, e30–41 (2009).
77. Kehat, I. et al. Electromechanical integration of cardiomyocytes derived from human embryonic stem cells. Nat Biotechnol 22, 1282–1289 (2004).
78. Lev, S., Kehat, I. & Gepstein, L. Differentiation pathways in human embryonic stem cell-derived cardiomyocytes. Ann N Y Acad Sci 1047, 50–65 (2005).
79. Xu, C. et al. Human embryonic stem cell-derived cardiomyocytes can be maintained in defined medium without serum. Stem Cells Dev 15, 931–941 (2006).
80. He, J.-Q., Ma, Y., Lee, Y., Thomson, J. A. & Kamp, T. J. Human embryonic stem cells develop into multiple types of cardiac myocytes: action potential characterization. Circulation Research 93, 32–39 (2003).
81. Tanaka, T. et al. In vitro pharmacologic testing using human induced pluripotent stem cell-derived cardiomyocytes. Biochem Biophys Res Commun 385, 497–502 (2009).
82. Norström, A. et al. Molecular and pharmacological properties of human embryonic stem cell-derived cardiomyocytes. Exp Biol Med (Maywood) 231, 1753–1762 (2006).
83. Cui, L., Johkura, K., Takei, S., Ogiwara, N. & Sasaki, K. Structural differentiation, proliferation, and association of human embryonic stem cell-derived cardiomyocytes in vitro and in their extracardiac tissues. J. Struct. Biol. 158, 307–317 (2007).

84. McDevitt, T. C., Laflamme, M. A. & Murry, C. E. Proliferation of cardiomyocytes derived from human embryonic stem cells is mediated via the IGF/PI 3-kinase/Akt signaling pathway. J Mol Cell Cardiol 39, 865–873 (2005).
85. White Moyes, K. N. et al. Human Embryonic Stem Cell-Derived Cardiomyocytes Migrate in Response to Gradients of Fibronectin and Wnt5a. Stem Cells Dev (2013). doi:10.1089/scd.2012.0586
86. Sartiani, L. et al. Developmental changes in cardiomyocytes differentiated from human embryonic stem cells: a molecular and electrophysiological approach. Stem Cells 25, 1136–1144 (2007).
87. Zhu, W.-Z., Santana, L. F. & Laflamme, M. A. Local control of excitation-contraction coupling in human embryonic stem cell-derived cardiomyocytes. PLoS ONE 4, e5407 (2009).
88. Satin, J. et al. Mechanism of spontaneous excitability in human embryonic stem cell derived cardiomyocytes. J Physiol (Lond) 559, 479–496 (2004).
89. Liu, J., Fu, J.-D., Siu, C. W. & Li, R. A. Functional sarcoplasmic reticulum for calcium handling of human embryonic stem cell-derived cardiomyocytes: insights for driven maturation. Stem Cells 25, 3038–3044 (2007).
90. Satin, J. et al. Calcium handling in human embryonic stem cell-derived cardiomyocytes. Stem Cells 26, 1961–1972 (2008).
91. Klug, M. G., Soonpaa, M. H., Koh, G. Y. & Field, L. J. Genetically selected cardiomyocytes from differentiating embronic stem cells form stable intracardiac grafts. J Clin Invest 98, 216–224 (1996).
92. Xue, T. et al. Functional integration of electrically active cardiac derivatives from genetically engineered human embryonic stem cells with quiescent recipient ventricular cardiomyocytes: insights into the development of cell-based pacemakers. Circulation 111, 11–20 (2005).
93. Laflamme, M. A. et al. Formation of human myocardium in the rat heart from human embryonic stem cells. Am J Pathol 167, 663–671 (2005).
94. Laflamme, M. A. et al. Cardiomyocytes derived from human embryonic stem cells in pro-survival factors enhance function of infarcted rat hearts. Nat Biotechnol 25, 1015–1024 (2007).
95. Dai, W. et al. Survival and maturation of human embryonic stem cell-derived cardiomyocytes in rat hearts. J Mol Cell Cardiol 43, 504–516 (2007).
96. Leor, J. et al. Human embryonic stem cell transplantation to repair the infarcted myocardium. Heart 93, 1278–1284 (2007).
97. van Laake, L. W. et al. Human embryonic stem cell-derived cardiomyocytes survive and mature in the mouse heart and transiently improve function after myocardial infarction. Stem Cell Res 1, 9–24 (2007).
98. Caspi, O. et al. Transplantation of human embryonic stem cell-derived cardiomyocytes improves myocardial performance in infarcted rat hearts. J Am Coll Cardiol 50, 1884–1893 (2007).
99. van Laake, L. W., Passier, R., Doevendans, P. A. & Mummery, C. L. Human embryonic stem cell-derived cardiomyocytes and cardiac repair in rodents. Circulation Research 102, 1008–1010 (2008).
100. Shiba, Y. et al. Human ES-cell-derived cardiomyocytes electrically couple and suppress arrhythmias in injured hearts. Nature (2012). doi:10.1038/nature11317

101. Kawamura, M. et al. Feasibility, safety, and therapeutic efficacy of human induced pluripotent stem cell-derived cardiomyocyte sheets in a porcine ischemic cardiomyopathy model. Circulation 126, S29–37 (2012).
102. Xiong, Q. et al. Functional Consequences of Human Induced Pluripotent Stem Cells Therapy: Myocardial ATP Turnover Rate in the in vivo Swine Hearts with Post-Infarction Remodeling. Circulation (2013). doi:10.1161/CIRCULATIONAHA.112.000641
103. Moreno-Gonzalez, A. et al. Cell therapy enhances function of remote non-infarcted myocardium. J Mol Cell Cardiol 47, 603–613 (2009).
104. Sugiura, S. et al. Comparison of unitary displacements and forces between 2 cardiac myosin isoforms by the optical trap technique: molecular basis for cardiac adaptation. Circulation Research 82, 1029–1034 (1998).
105. Sata, M., Sugiura, S., Yamashita, H., Momomura, S. & Serizawa, T. Dynamic interaction between cardiac myosin isoforms modifies velocity of actomyosin sliding in vitro. Circulation Research 73, 696–704 (1993).
106. VanBuren, P., Harris, D. E., Alpert, N. R. & Warshaw, D. M. Cardiac V1 and V3 myosins differ in their hydrolytic and mechanical activities in vitro. Circulation Research 77, 439–444 (1995).
107. Iwazumi, T. High-speed ultrasensitive instrumentation for myofibril mechanics measurements. Am J Physiol 252, C253–62 (1987).
108. Colomo, F., Piroddi, N., Poggesi, C., Kronnie, te, G. & Tesi, C. Active and passive forces of isolated myofibrils from cardiac and fast skeletal muscle of the frog. J Physiol (Lond) 500 (Pt 2), 535–548 (1997).
109. Colomo, F., Poggesi, C. & Tesi, C. Force responses to rapid length changes in single intact cells from frog heart. J Physiol (Lond) 475, 347–350 (1994).
110. Tesi, C., Piroddi, N., Colomo, F. & Poggesi, C. Relaxation kinetics following sudden Ca(2+) reduction in single myofibrils from skeletal muscle. Biophysj 83, 2142–2151 (2002).
111. Piroddi, N. et al. Tension generation and relaxation in single myofibrils from human atrial and ventricular myocardium. Pflugers Arch 454, 63–73 (2007).
112. Delbridge, L. M. & Roos, K. P. Optical methods to evaluate the contractile function of unloaded isolated cardiac myocytes. J Mol Cell Cardiol 29, 11–25 (1997).
113. Herron, T. J., Korte, F. S. & McDonald, K. S. Loaded shortening and power output in cardiac myocytes are dependent on myosin heavy chain isoform expression. Am J Physiol Heart Circ Physiol 281, H1217–22 (2001).
114. Hanft, L. M., Korte, F. S. & McDonald, K. S. Cardiac function and modulation of sarcomeric function by length. Cardiovasc Res 77, 627–636 (2008).
115. Iribe, G., Helmes, M. & Kohl, P. Force-length relations in isolated intact cardiomyocytes subjected to dynamic changes in mechanical load. Am J Physiol Heart Circ Physiol 292, H1487–97 (2007).
116. King, N. M. P. et al. Mouse intact cardiac myocyte mechanics: cross-bridge and titin-based stress in unactivated cells. J Gen Physiol 137, 81–91 (2011).
117. Kentish, J. C., Keurs, ter, H. E., Ricciardi, L., Bucx, J. J. & Noble, M. I. Comparison between the sarcomere length-force relations of intact and skinned trabeculae from rat right ventricle. Influence of calcium concentrations on these

relations. Circulation Research 58, 755–768 (1986).
118. Backx, P. H., Gao, W. D., Azan-Backx, M. D. & Marban, E. The relationship between contractile force and intracellular [Ca2+] in intact rat cardiac trabeculae. J Gen Physiol 105, 1–19 (1995).
119. Hancock, W. O., Martyn, D. A., Huntsman, L. L. & Gordon, A. M. Influence of Ca2+ on force redevelopment kinetics in skinned rat myocardium. Biophysj 70, 2819–2829 (1996).
120. Neely, J. R., Liebermeister, H., Battersby, E. J. & Morgan, H. E. Effect of pressure development on oxygen consumption by isolated rat heart. Am J Physiol 212, 804–814 (1967).
121. Rovetto, M. J., Whitmer, J. T. & Neely, J. R. Comparison of the effects of anoxia and whole heart ischemia on carbohydrate utilization in isolated working rat hearts. Circulation Research 32, 699–711 (1973).
122. Liedtke, A. J., Hughes, H. C. & Neely, J. R. An experimental model for studying myocardial ischemia. Correlation of hemodynamic performance and metabolism in the working swine heart. J. Thorac. Cardiovasc. Surg. 69, 203–211 (1975).
123. Dolnikov, K. et al. Functional properties of human embryonic stem cell-derived cardiomyocytes. Ann N Y Acad Sci 1047, 66–75 (2005).
124. Dolnikov, K. et al. Functional properties of human embryonic stem cell-derived cardiomyocytes: intracellular Ca2+ handling and the role of sarcoplasmic reticulum in the contraction. Stem Cells 24, 236–245 (2006).
125. Binah, O. et al. Functional and developmental properties of human embryonic stem cells-derived cardiomyocytes. Journal of electrocardiology 40, S192–6 (2007).
126. Germanguz, I. et al. Molecular characterization and functional properties of cardiomyocytes derived from human inducible pluripotent stem cells. J Cell Mol Med 15, 38–51 (2011).
127. Shinozawa, T., Imahashi, K., Sawada, H., Furukawa, H. & Takami, K. Determination of Appropriate Stage of Human-Induced Pluripotent Stem Cell-Derived Cardiomyocytes for Drug Screening and Pharmacological Evaluation In Vitro. J Biomol Screen (2012). doi:10.1177/1087057112449864
128. Hansma, P. K., Drake, B., Marti, O., Gould, S. A. & Prater, C. B. The scanning ion-conductance microscope. Science 243, 641–643 (1989).
129. Gorelik, J. et al. Functional characterization of embryonic stem cell-derived cardiomyocytes using scanning ion conductance microscopy. Tissue Eng 12, 657–664 (2006).
130. Abdul Kadir, S. H. S. et al. Embryonic stem cell-derived cardiomyocytes as a model to study fetal arrhythmia related to maternal disease. J Cell Mol Med 13, 3730–3741 (2009).
131. Kita-Matsuo, H. et al. Lentiviral vectors and protocols for creation of stable hESC lines for fluorescent tracking and drug resistance selection of cardiomyocytes. PLoS ONE 4, e5046 (2009).
132. Jacot, J. G., McCulloch, A. D. & Omens, J. H. Substrate stiffness affects the functional maturation of neonatal rat ventricular myocytes. Biophys J 95, 3479–3487 (2008).
133. Bhana, B. et al. Influence of substrate stiffness on the phenotype of heart cells.

Biotechnol Bioeng 105, 1148–1160 (2010).
134. Serena, E. et al. Micro-arrayed human embryonic stem cells-derived cardiomyocytes for in vitro functional assay. PLoS ONE 7, e48483 (2012).
135. Sniadecki, N. J. & Chen, C. S. Microfabricated silicone elastomeric post arrays for measuring traction forces of adherent cells. Methods Cell Biol. 83, 313–328 (2007).
136. Liu, Z. et al. Mechanical tugging force regulates the size of cell-cell junctions. Proc Natl Acad Sci USA 107, 9944–9949 (2010).
137. Rodriguez, A. G., Han, S. J., Regnier, M. & Sniadecki, N. J. Substrate stiffness increases twitch power of neonatal cardiomyocytes in correlation with changes in myofibril structure and intracellular calcium. Biophys J 101, 2455–2464 (2011).
138. Taylor, R. E. et al. Sacrificial layer technique for axial force post assay of immature cardiomyocytes. Biomed Microdevices (2012). doi:10.1007/s10544-012-9710-3
139. Tan, Y. et al. Probing the mechanobiological properties of human embryonic stem cells in cardiac differentiation by optical tweezers. Journal of biomechanics 45, 123–128 (2012).
140. Saenz Cogollo, J. F., Tedesco, M., Martinoia, S. & Raiteri, R. A new integrated system combining atomic force microscopy and micro-electrode array for measuring the mechanical properties of living cardiac myocytes. Biomed Microdevices 13, 613–621 (2011).
141. Sumita Yoshikawa, W. et al. Increased passive stiffness of cardiomyocytes in the transverse direction and residual actin and myosin cross-bridge formation in hypertrophied rat hearts induced by chronic β-adrenergic stimulation. Circ J 77, 741–748 (2013).
142. Lieber, S. C. et al. Aging increases stiffness of cardiac myocytes measured by atomic force microscopy nanoindentation. Am J Physiol Heart Circ Physiol 287, H645–51 (2004).
143. Lieu, D. K. et al. Absence of transverse tubules contributes to non-uniform Ca(2+) wavefronts in mouse and human embryonic stem cell-derived cardiomyocytes. Stem Cells Dev 18, 1493–1500 (2009).
144. Davis, J. J., Hill, H. A. & Powell, T. High resolution scanning force microscopy of cardiac myocytes. Cell Biol. Int. 25, 1271–1277 (2001).
145. Domke, J., Parak, W. J., George, M., Gaub, H. E. & Radmacher, M. Mapping the mechanical pulse of single cardiomyocytes with the atomic force microscope. Eur. Biophys. J. 28, 179–186 (1999).
146. Wang, I.-N. E. et al. Apelin enhances directed cardiac differentiation of mouse and human embryonic stem cells. PLoS ONE 7, e38328 (2012).
147. Sun, N. et al. Patient-specific induced pluripotent stem cells as a model for familial dilated cardiomyopathy. Sci Transl Med 4, 130ra47 (2012).
148. Pillekamp, F. et al. Force measurements of human embryonic stem cell-derived cardiomyocytes in an in vitro transplantation model. Stem Cells 25, 174–180 (2007).
149. Pillekamp, F. et al. Neonatal murine heart slices. A robust model to study ventricular isometric contractions. Cell Physiol Biochem 20, 837–846 (2007).

150. Pfannkuche, K. et al. Cardiac myocytes derived from murine reprogrammed fibroblasts: intact hormonal regulation, cardiac ion channel expression and development of contractility. Cell Physiol Biochem 24, 73–86 (2009).
151. Pillekamp, F. et al. Contractile properties of early human embryonic stem cell-derived cardiomyocytes: beta-adrenergic stimulation induces positive chronotropy and lusitropy but not inotropy. Stem Cells Dev 21, 2111–2121 (2012).
152. Korte, F. S., Herron, T. J., Rovetto, M. J. & McDonald, K. S. Power output is linearly related to MyHC content in rat skinned myocytes and isolated working hearts. Am J Physiol Heart Circ Physiol 289, H801–12 (2005).
153. Xi, J. et al. Comparison of contractile behavior of native murine ventricular tissue and cardiomyocytes derived from embryonic or induced pluripotent stem cells. FASEB J 24, 2739–2751 (2010).
154. Eschenhagen, T. et al. Three-dimensional reconstitution of embryonic cardiomyocytes in a collagen matrix: a new heart muscle model system. FASEB J 11, 683–694 (1997).
155. Fink, C. et al. Chronic stretch of engineered heart tissue induces hypertrophy and functional improvement. FASEB J 14, 669–679 (2000).
156. Zimmermann, W.-H. et al. Three-dimensional engineered heart tissue from neonatal rat cardiac myocytes. Biotechnol Bioeng 68, 106–114 (2000).
157. Zimmermann, W.-H. et al. Cardiac grafting of engineered heart tissue in syngenic rats. Circulation 106, I151–7 (2002).
158. Naito, H. et al. Optimizing engineered heart tissue for therapeutic applications as surrogate heart muscle. Circulation 114, I72–8 (2006).
159. Yildirim, Y. et al. Development of a biological ventricular assist device: preliminary data from a small animal model. Circulation 116, I16–23 (2007).
160. Schaaf, S. et al. Human engineered heart tissue as a versatile tool in basic research and preclinical toxicology. PLoS ONE 6, e26397 (2011).
161. Shimko, V. F. & Claycomb, W. C. Effect of mechanical loading on three-dimensional cultures of embryonic stem cell-derived cardiomyocytes. Tissue engineering Part A 14, 49–58 (2008).
162. Stevens, K. R. et al. Physiological function and transplantation of scaffold-free and vascularized human cardiac muscle tissue. Proc Natl Acad Sci USA 106, 16568–16573 (2009).
163. Tulloch, N. L. et al. Growth of engineered human myocardium with mechanical loading and vascular coculture. Circulation Research 109, 47–59 (2011).
164. Liau, B., Christoforou, N., Leong, K. W. & Bursac, N. Pluripotent stem cell-derived cardiac tissue patch with advanced structure and function. Biomaterials 32, 9180–9187 (2011).
165. Kensah, G. et al. Murine and human pluripotent stem cell-derived cardiac bodies form contractile myocardial tissue in vitro. Eur Heart J (2012). doi:10.1093/eurheartj/ehs349
166. Didié, M. et al. Parthenogenetic stem cells for tissue-engineered heart repair. J Clin Invest (2013). doi:10.1172/JCI66854
167. Streckfuss-Bömeke, K. et al. Comparative study of human-induced pluripotent stem cells derived from bone marrow cells, hair keratinocytes, and skin

fibroblasts. Eur Heart J (2012). doi:10.1093/eurheartj/ehs203
168. Soong, P. L., Tiburcy, M. & Zimmermann, W.-H. Cardiac differentiation of human embryonic stem cells and their assembly into engineered heart muscle. Curr Protoc Cell Biol Chapter 23, Unit23.8 (2012).
169. Pillekamp, F. et al. Physiological differences between transplanted and host tissue cause functional decoupling after in vitro transplantation of human embryonic stem cell-derived cardiomyocytes. Cell Physiol Biochem 23, 65–74 (2009).
170. Gai, H. et al. Generation and characterization of functional cardiomyocytes using induced pluripotent stem cells derived from human fibroblasts. Cell Biol. Int. 33, 1184–1193 (2009).
171. Ren, Y. et al. Small molecule Wnt inhibitors enhance the efficiency of BMP-4-directed cardiac differentiation of human pluripotent stem cells. J Mol Cell Cardiol 51, 280–287 (2011).
172. Liu, J., Sun, N., Bruce, M. A., Wu, J. C. & Butte, M. J. Atomic force mechanobiology of pluripotent stem cell-derived cardiomyocytes. PLoS ONE 7, e37559 (2012).
173. Hazeltine, L. B. et al. Effects of substrate mechanics on contractility of cardiomyocytes generated from human pluripotent stem cells. Int J Cell Biol 2012, 508294 (2012).
174. Sedan, O. et al. 1,4,5-Inositol trisphosphate-operated intracellular Ca(2+) stores and angiotensin-II/endothelin-1 signaling pathway are functional in human embryonic stem cell-derived cardiomyocytes. Stem Cells 26, 3130–3138 (2008).
175. Sato, M. et al. Functional and morphological maturation of implanted neonatal cardiomyocytes as a comparator for cell therapy. Stem Cells Dev 19, 1025–1034 (2010).
176. Szokodi, I. et al. Apelin, the novel endogenous ligand of the orphan receptor APJ, regulates cardiac contractility. Circulation Research 91, 434–440 (2002).
177. Iwai, S. & Uyeda, T. Q. P. Visualizing myosin-actin interaction with a genetically-encoded fluorescent strain sensor. Proc Natl Acad Sci USA 105, 16882–16887 (2008).
178. Laflamme, M. A. & Murry, C. E. Heart regeneration. Nature 473, 326–335 (2011).
179. Segers, V. F. M. & Lee, R. T. Stem-cell therapy for cardiac disease. Nature 451, 937–942 (2008).
180. Bernstein, H. S. & Srivastava, D. Stem cell therapy for cardiac disease. Pediatr. Res. 71, 491–499 (2012).
181. Boyle, A. J., Schulman, S. P., Hare, J. M. & Oettgen, P. Is stem cell therapy ready for patients? Stem Cell Therapy for Cardiac Repair. Ready for the Next Step . Circulation 114, 339–352 (2006).
182. Cao, F. et al. Transcriptional and functional profiling of human embryonic stem cell-derived cardiomyocytes. PLoS ONE 3, e3474 (2008).
183. Fernandes, S. et al. Human embryonic stem cell-derived cardiomyocytes engraft but do not alter cardiac remodeling after chronic infarction in rats. J Mol Cell Cardiol 49, 941–949 (2010).
184. Liu, J. et al. Facilitated maturation of Ca2+ handling properties of human

embryonic stem cell-derived cardiomyocytes by calsequestrin expression. Am J Physiol, Cell Physiol 297, C152–9 (2009).
185. Kim, C. et al. Non-cardiomyocytes influence the electrophysiological maturation of human embryonic stem cell-derived cardiomyocytes during differentiation. Stem Cells Dev 19, 783–795 (2010).
186. Földes, G. et al. Modulation of human embryonic stem cell-derived cardiomyocyte growth: a testbed for studying human cardiac hypertrophy? J Mol Cell Cardiol 50, 367–376 (2011).
187. Zhu, W.-Z. et al. Neuregulin/ErbB signaling regulates cardiac subtype specification in differentiating human embryonic stem cells. Circulation Research 107, 776–786 (2010).
188. Olivetti, G. et al. Aging, cardiac hypertrophy and ischemic cardiomyopathy do not affect the proportion of mononucleated and multinucleated myocytes in the human heart. J Mol Cell Cardiol 28, 1463–1477 (1996).
189. Schmid, G. & Pfitzer, P. Mitoses and binucleated cells in perinatal human hearts. Virchows Arch., B, Cell Pathol. 48, 59–67 (1985).
190. Dabiri, G. A., Turnacioglu, K. K., Sanger, J. M. & Sanger, J. W. Myofibrillogenesis visualized in living embryonic cardiomyocytes. Proc Natl Acad Sci USA 94, 9493–9498 (1997).
191. Stout, A. L., Wang, J., Sanger, J. M. & Sanger, J. W. Tracking changes in Z-band organization during myofibrillogenesis with FRET imaging. Cell Motil Cytoskeleton 65, 353–367 (2008).
192. Korte, F. S. & McDonald, K. S. Sarcomere length dependence of rat skinned cardiac myocyte mechanical properties: dependence on myosin heavy chain. J Physiol (Lond) 581, 725–739 (2007).
193. New, R. B. et al. Isolated left ventricular myocyte contractility in patients undergoing cardiac operations. J. Thorac. Cardiovasc. Surg. 116, 495–502 (1998).
194. Ou, D.-B. et al. Three-dimensional co-culture facilitates the differentiation of embryonic stem cells into mature cardiomyocytes. J. Cell. Biochem. (2011). doi:10.1002/jcb.23283
195. Baharvand, H., Azarnia, M., Parivar, K. & Ashtiani, S. K. The effect of extracellular matrix on embryonic stem cell-derived cardiomyocytes. J Mol Cell Cardiol 38, 495–503 (2005).
196. McDevitt, T. C. et al. In vitro generation of differentiated cardiac myofibers on micropatterned laminin surfaces. J. Biomed. Mater. Res. 60, 472–479 (2002).
197. McDevitt, T. C., Woodhouse, K. A., Hauschka, S. D., Murry, C. E. & Stayton, P. S. Spatially organized layers of cardiomyocytes on biodegradable polyurethane films for myocardial repair. J Biomed Mater Res A 66, 586–595 (2003).
198. Bursac, N., Parker, K. K., Iravanian, S. & Tung, L. Cardiomyocyte cultures with controlled macroscopic anisotropy: a model for functional electrophysiological studies of cardiac muscle. Circulation Research 91, e45–54 (2002).
199. Kim, D.-H. et al. Nanoscale cues regulate the structure and function of macroscopic cardiac tissue constructs. Proc Natl Acad Sci USA 107, 565–570 (2010).
200. Kim, D.-H. et al. Nanopatterned cardiac cell patches promote stem cell niche

formation and myocardial regeneration. Integr Biol (Camb) 4, 1019–1033 (2012).
201. Engler, A. J. et al. Embryonic cardiomyocytes beat best on a matrix with heart-like elasticity: scar-like rigidity inhibits beating. J Cell Sci 121, 3794–3802 (2008).
202. Jacot, J. G. et al. Cardiac myocyte force development during differentiation and maturation. Ann N Y Acad Sci 1188, 121–127 (2010).
203. Sparrow, J. C. & Schöck, F. The initial steps of myofibril assembly: integrins pave the way. Nat Rev Mol Cell Biol 10, 293–298 (2009).
204. Goldberg, G. S., Lampe, P. D. & Nicholson, B. J. Selective transfer of endogenous metabolites through gap junctions composed of different connexins. Nat Cell Biol 1, 457–459 (1999).
205. Goldberg, G. S., Moreno, A. P. & Lampe, P. D. Gap junctions between cells expressing connexin 43 or 32 show inverse permselectivity to adenosine and ATP. J Biol Chem 277, 36725–36730 (2002).
206. World Health Organization. Global Status Report on Noncommunicable Diseases 2010. 1–176 (2011).
207. Sesti, C. & Kloner, R. A. Gene therapy in congestive heart failure. Circulation 110, 242–243 (2004).
208. Regnier, M. et al. Cross-bridge versus thin filament contributions to the level and rate of force development in cardiac muscle. Biophysj 87, 1815–1824 (2004).
209. Adhikari, B. B., Regnier, M., Rivera, A. J., Kreutziger, K. L. & Martyn, D. A. Cardiac length dependence of force and force redevelopment kinetics with altered cross-bridge cycling. Biophysj 87, 1784–1794 (2004).
210. Moreno-Gonzalez, A. et al. Thin-filament regulation of force redevelopment kinetics in rabbit skeletal muscle fibres. J Physiol (Lond) 579, 313–326 (2007).
211. Schoffstall, B., Clark, A. & Chase, P. B. Positive inotropic effects of low dATP/ATP ratios on mechanics and kinetics of porcine cardiac muscle. Biophysj 91, 2216–2226 (2006).
212. Schoffstall, B. & Chase, P. B. Increased intracellular [dATP] enhances cardiac contraction in embryonic chick cardiomyocytes. J. Cell. Biochem. 104, 2217–2227 (2008).
213. O'Sullivan, W. J. & Cohn, M. Nucleotide specificity and conformation of the active site of creatine kinase. Magnetic resonance and sulfhydryl reactivity studies. J Biol Chem 241, 3116–3125 (1966).
214. Chien, S. Intracellular ATP delivery using highly fusogenic liposomes. Methods Mol Biol 605, 377–391 (2010).
215. Valiunas, V. et al. Connexin-specific cell-to-cell transfer of short interfering RNA by gap junctions. J Physiol (Lond) 568, 459–468 (2005).
216. Reinecke, H., Zhang, M., Bartosek, T. & Murry, C. E. Survival, integration, and differentiation of cardiomyocyte grafts: a study in normal and injured rat hearts. Circulation 100, 193–202 (1999).
217. Stewart, W. W. Functional connections between cells as revealed by dye-coupling with a highly fluorescent naphthalimide tracer. Cell 14, 741–759 (1978).
218. Valiunas, V. et al. Human mesenchymal stem cells make cardiac connexins and form functional gap junctions. J Physiol (Lond) 555, 617–626 (2004).
219. Kehat, I., Gepstein, A., Spira, A., Itskovitz-Eldor, J. & Gepstein, L. High-

resolution electrophysiological assessment of human embryonic stem cell-derived cardiomyocytes: a novel in vitro model for the study of conduction. Circulation Research 91, 659–661 (2002).
220. Goh, G. et al. Molecular and phenotypic analyses of human embryonic stem cell-derived cardiomyocytes: opportunities and challenges for clinical translation. Thromb Haemost 94, 728–737 (2005).
221. Rubart, M. et al. Physiological coupling of donor and host cardiomyocytes after cellular transplantation. Circulation Research 92, 1217–1224 (2003).
222. Molkentin, J. D. Calcineurin-NFAT signaling regulates the cardiac hypertrophic response in coordination with the MAPKs. Cardiovasc Res 63, 467–475 (2004).
223. Lammerding, J., Kamm, R. D. & Lee, R. T. Mechanotransduction in cardiac myocytes. Ann N Y Acad Sci 1015, 53–70 (2004).
224. Wang, N., Tytell, J. D. & Ingber, D. E. Mechanotransduction at a distance: mechanically coupling the extracellular matrix with the nucleus. Nat Rev Mol Cell Biol 10, 75–82 (2009).
225. Sugden, P. H. Mechanotransduction in cardiomyocyte hypertrophy. Circulation 103, 1375–1377 (2001).
226. Lee, Y.-K. et al. Triiodothyronine promotes cardiac differentiation and maturation of embryonic stem cells via the classical genomic pathway. Mol. Endocrinol. 24, 1728–1736 (2010).
227. Hockemeyer, D. et al. Efficient targeting of expressed and silent genes in human ESCs and iPSCs using zinc-finger nucleases. Nat Biotechnol 27, 851–857 (2009).
228. Urnov, F. D. et al. Highly efficient endogenous human gene correction using designed zinc-finger nucleases. Nature 435, 646–651 (2005).
229. Gantz, J. A., Palpant, N. J., Welikson, R. E. & Hauschka, S. D. Targeted Genomic Integration of a Selectable Floxed Dual Fluorescence Reporter in Human Embryonic Stem Cells. PLoS ONE (2012).